Norges miljø- og
biovitenskapelige
universitet

Master's Thesis 2019 60 ECTS

Faculty of Chemistry, Biotechnology and Food Science (KBM)

Systematic evaluation of RT-qPCR kits and protocols for detection and quantitation of microRNAs

Sofie Strøm Andersen

Biotechnology - Genetics

Acknowledgments

This thesis represents the completion of my master's degree in Biotechnology at the Norwegian University of Life Sciences (NMBU). It was written in collaboration with the Department for Medical Genetics at Oslo University Hospital (OUS), Ullevål over the period August 2018 to May 2019.

First and foremost, I would like to thank my inspiring supervisor at OUS, professor Benedicte Alexandra Lie for her valuable comments, guidance and support throughout the thesis. I would also like to thank Siri Tennebø Flåm and Fatima Heinicke for important and helpful comments, incredible support and for always having time to answer questions. All three have been of invaluable help throughout the whole process.

I would also like to thank the whole IMMGEN research group for good feedback on presentations, making me feel like a part of the group and huge inspiration within the field.

My family and friends have also been a great support throughout the period of my thesis. I would especially like to thank my friend, Kristine, for interesting discussions, help and support throughout the entire education.

Additionally, I would like to thank my supervisor at NMBU, professor Harald Carlsen for his counseling and support with the work of this thesis.

Oslo, May 2019

Sofie Strøm Andersen

Abstract

MicroRNAs (miRNAs) are small single-stranded non-coding RNAs with an average length of ~ 22 nucleotides. The main function of miRNA is post-transcriptional regulation of gene expression by targeting specific mRNAs. The value of miRNA regulation and expression has become an interesting focus in diagnostics. Extracellular miRNAs have been found in a variety of body fluids, making miRNAs suitable as noninvasive biomarkers. For the understanding of miRNAs biological roles and for identifying potential biomarkers, reliable technologies are required for detection and quantitation. Reverse transcription of miRNA to cDNA template followed by quantitative PCR (RT-qPCR) are often the method of choice, however different RT-qPCR technologies have been observed to give varying results.

In this thesis, a systematic evaluation has been conducted for three kits and protocols to perform RT-qPCR for detection and quantitation of miRNA. The three different methods evaluated was miRCURY RT-qPCR setup (Qiagen), TaqMan Advanced RT-qPCR setup (Thermo Fisher Scientific) with and without preamplification, and TaqMan MicroRNA RT-qPCR setup (Thermo Fisher Scientific) with and without uracil-N glycosylase (UNG) included in the master mix. All setups included assays for six miRNAs represented by synthetic material. The miRNAs were analyzed once with added synthetical noise and once with added biological noise.

The objective of the evaluation was to find a preferred RT-qPCR setup that later can be used for verifying miRNA-findings from RNA sequencing. It was indicated that miRCURY RT-qPCR setup gave best result for verifying lowly expressed miRNAs. This was based on least deviation in the reaction efficiency, low indication of false positives and unspecific amplification and a wide range of input of total RNA. This study indicated that TaqMan Advanced RT-qPCR setup without the preamplification reaction, should not be used for detection and quantitation of lowly expressed miRNA. This was based on the setup's poor reaction efficiency, observed detection range and precision. TaqMan MicroRNA RT-qPCR setup indicated being advantageous when few miRNA-targets and replicates are required due to the lowest price per reaction for one target and the feasibility. By including UNG in the master mix the deviation of the reaction efficiency decreased.

Sammendrag

MicroRNA (miRNA) er korte, ikke-kodene, enkeltrådige RNA med en gjennomsnittlig størrelse på ~ 22 nukleotider. Hovedfunksjonen til miRNA er regulering av genuttrykk etter transkripsjonen. Dette gjøres ved at miRNA bindes til komplementære sekvenser på mål-mRNA. Genregulering av miRNA har fått økende fokus i sykdomssammenheng. MicroRNA har blitt funnet i ulike kroppsvæsker, blant annet i plasma, og dette gjør miRNA egnet som ikke-invasive biomarkører. For å identifisere potensielle biomarkører er det nødvendig med nøyaktige metoder til deteksjon og kvantifisering. Reversert transkripsjon av miRNA til cDNA, etterfulgt av kvantitativ PCR (RT-qPCR) er ofte den foretrukne metoden, men ulike RT-qPCR fremgangsmåter har vist varierende resultat.

I denne studien ble det utført en systematisk evaluering av tre ulike fremgangsmåter for å utføre RT-qPCR til deteksjon og kvantifisering av miRNA. De tre ulike fremgangsmåtene som ble vurdert var miRCURY RT-qPCR oppsett (Qiagen), TaqMan Advanced RT-qPCR oppsett (Thermo Fisher Scientific) med og uten pre-amplifisering og TaqMan MicroRNA RT-qPCR oppsett (Thermo Fisher Scientific) med og uten uracil-N glycosylase (UNG) inkludet i reaksjonsmiksen. Vurderingen ble utført med assay for seks miRNA representert av syntetisk materiale. MiRNAene ble analysert både med inkludert syntetisk og biologisk bakgrunnsstøy i to ulike oppsett.

Målet av evalueringen var å finne en foretrukken RT-qPCR fremgangsmåte som videre kunne bli brukt til verifisering av miRNA-funn fra RNA-sekvensering. Resultatene indikerte at ved verifisering av lavt uttrykte miRNA er miRCURY RT-qPCR oppsettet det foretrukne. Dette er basert på minst avvik fra optimal reaksjonseffektivitet, lav indikasjon på amplifisering av falske positive, og lavest startkonsentrasjon av total-RNA inn i cDNA syntesen. Studien indikerte også at TaqMan Advanced RT-qPCR uten pre-amplifisering ikke er å foretrekke ved deteksjon og kvantifisering av lavt uttrykte miRNA. Dette skyldes at oppsettet viste dårligst reaksjonseffektivitet, observert deteksjonsgrense og presisjon. TaqMan MicroRNA RT-qPCR oppsettet indikerte å være fordelaktig ved identifisering av få miRNA, og ved å inkludere UNG i reaksjonsmiksen minsket avviket fra optimal reaksjonseffektivitet.

Abbreviations

AGO	Argonaute protein
cDNA	Complementary DNA
DGCR8	DiGeorge syndrome critical region 8
isomiR	MicroRNA isoforms
LNA	Locked nucleic acids
MGB	Minor groove binding
miRNA	MicroRNA
MRE	MicroRNA response elements
NGS	Next generation sequencing
Nt	Nucleotides
Oligos	Oligonucleotides
Pre-miRNAs	Precursor transcripts of miRNA
Pri-miRNA	Primary transcripts of miRNA
qPCR	Quantitative polymerase chain reaction
RA	Rheumatoid arthritis
RISC	RNA-induced silencing complex
RNA-seq	Sequencing of RNA
RT	Reverse transcription
RT-qPCR	Reverse transcription - quantitative polymerase chain reaction
SD	Standard deviation
ShRNA	Short hairpin RNA
UNG	Uracil-N glycosylase
UTR	Untranslated region

Table of Contents

1 Introduction

1.1 MicroRNA

MicroRNA (miRNA) are small single-stranded non-coding RNA with an average length of ~22 nucleotides (nt) (Bartel, 2018). The first miRNA that was discovered in 1993 was lin-4 in *C. elegans* (Lee, Feinbaum, & Ambros, 1993; Wightman, Ha, & Ruvkun, 1993). The lin-4 was found to be complementary to conserved elements in 3´untranslated region (UTR) of the lin-14 gene. The extent of these findings was not understood until let-7 was discovered in 2000 (Pasquinelli et al., 2000). Unlike lin-4, the let-7 was found across species. After these findings, this class of non-coding RNA was studied more frequently, and the term microRNA (miRNA) was established. Today, we know that miRNAs are involved in a variety of biological processes and are important for normal development (Fu, Brkić, Hayder, & Peng, 2013).

The main function of miRNAs are post-transcriptional regulation of gene expression by targeting specific mRNAs (O'Brien, Hayder, Zayed, & Peng, 2018). Each miRNA can regulate hundreds to thousands of target genes and interacts mostly with the 3´UTR of target mRNAs to suppress expression. The miRNAs only constitute a small part of the human genome but can regulate at least one third of the human transcriptome (Long et al., 2018).

1.1.1 Genomic organization of miRNAs

MiRNAs can be monocistronic or polycistronic transcribed. When miRNAs are transcribed polycistronic as long primary transcript, they are called clusters (Tanzer & Stadler, 2004). Different genomic organizations of single miRNAs and clusters have been described (Figure 1), but the characterization of the miRNA gene structure and organization is still ongoing (Olena & Patton, 2010).

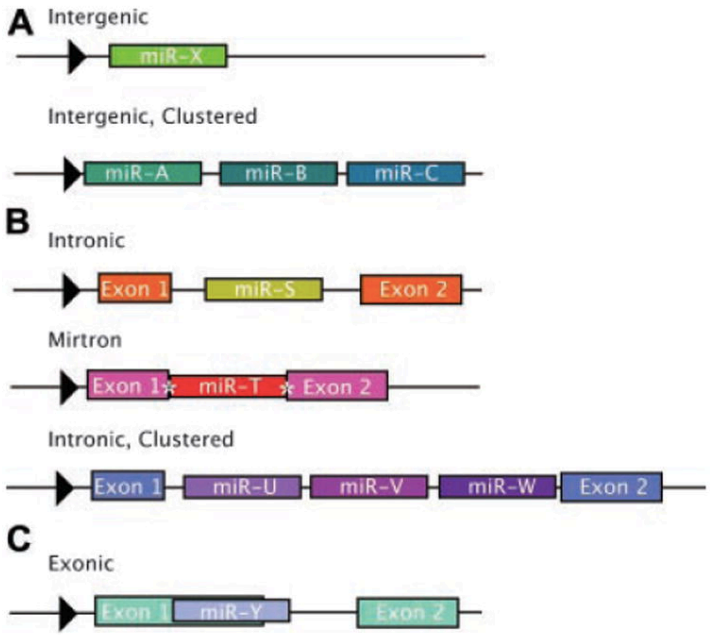

Figure 1: *Genomic organizations of miRNAs. MiRNAs could be located intergenic and regulated by their own promoters (A), or miRNAs could be found in introns, where they are regulated by the promoters of the host gene (B). Exonic miRNAs are regulated by the promoters of the host gene, which is usually non-coding (C). The figure is retrieved from Olena and Patton (2010).*

Intergenic miRNAs are found in genomic regions distinct from known transcription units (De Rie et al., 2017). Transcription of these miRNAs are independently regulated by their own promoters, and can be monocistronic (Figure 1A, top) or polycistronic (Figure 1A, bottom). There are also identified miRNAs in the introns. Transcription of these are regulated by the same promoters as the host gene (De Rie et al., 2017). These miRNAs can also be monocistronic (Figure 1B, top) or polycistronic (Figure 1B, bottom). The intronic transcription of miRNAs includes mirtrons. However, mirtrons are found in introns of the exact sequence of the precursor transcripts of the miRNA (Figure 1B, middle). Additionally, exonic miRNAs have also been reported (Rodriguez, Griffiths-Jones, Ashurst, & Bradley, 2004). Transcription of these miRNAs are regulated by their host gene promoters, but maturation of the exonic miRNAs often excludes the function of the host gene and renders it non-functional (Figure 1C).

1.1.2 Biogenesis of human miRNA

The biogenesis of human miRNA is classified into canonical and non-canonical pathways (Figure 2). The canonical pathway is the dominant pathway miRNAs are processed.

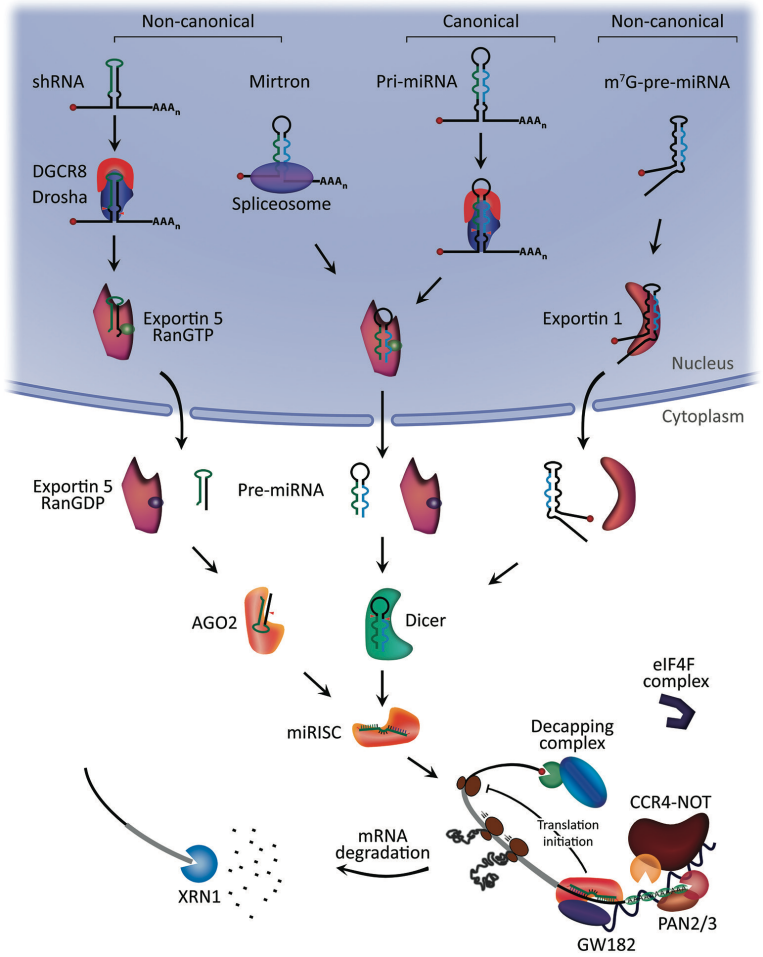

Figure 2: *The biogenesis of miRNAs in human, classified into canonical and non-canonical pathways. The non-canonical biogenesis pathways are grouped into Drosha/DGCR8-independent and Dicer-independent. The figure is retrieved from O'Brien et al. (2018).*

Canonical biogenesis of miRNA

Transcription of miRNA is initiated by RNA polymerase II (Lee et al., 2004). RNA polymerase II generates primary transcripts of the miRNAs (pri-miRNAs). The pri-miRNAs can be monocistronic or polycistronic transcripts from 200 nt to several kilobases, folded in hairpin structures. Pri-miRNAs are transcribed and then processed into precursor miRNAs (pre-miRNAs) by a microprocessor complex. The complex consists of RNA binding protein DiGeorge Syndrome Critical Region 8 (DGCR8) and ribonuclease III enzyme, Drosha (Denli, Tops, Plasterk, Ketting, & Hannon, 2004). The DGCR8 recognizes motifs within the pri-miRNA, while Drosha cleaves the pri-miRNA duplex at the base of the hairpin structure. This results in smaller pre-miRNAs with a length of 70-100 nt. The pre-miRNAs are exported into the cytoplasm by an Exportin 5/RanGTP complex and then processed by the RNase III endonuclease Dicer (Hutvágner et al., 2001; Lund, Güttinger, Calado, Dahlberg, & Kutay, 2004). The Dicer cleaves the terminal loop, and this results in a miRNA duplex. The miRNA

duplex includes both the 3p- and 5p-strand of the pre-miRNAs. Both strands can be loaded into Argonaute protein family (AGO) but only one of the strands is further processed by AGO, depending on tissue type and cellular environment. The processed miRNA-strand loaded into the AGO is considered the guide strand, and the unloaded strand is considered the passenger strand. The passenger strand will be unwound from the guide strand by RNA helicase in the cytoplasm. AGO loaded with the mature miRNA are dissociate from Dicer and forms an RNA-induced silencing complex (RISC) (Figure 2).

Non-canonical biogenesis pathway of miRNA

There have been described multiple non-canonical biogenesis pathways. These pathways can be grouped into Drosha/DGCR8-independent and Dicer-independent (Ruby, Jan, & Bartel, 2007; Yang et al., 2010). One examples of pre-miRNAs produced by the Drosha/DGCR8-independent pathway are mirtrons (Figure 2) (O'Brien et al., 2018). These are not cleaved by the microprocessor complex, consisting of Drosha and DGCR8, but are exported directly to cytoplasm via Exportin 5/RanGTP. From the Dicer-independent pathway, miRNAs are processed by the microprocessor complex from endogenous short hairpin RNA (shRNA) transcripts and the pre-miRNAs are exported to cytoplasm by Exportin 5/RanGTP (Figure 2). However, these pre-miRNAs are of insufficient length to be cleaved and processed by Dicer and require AGO 2 to complete their maturation. The entire pre-miRNA is therefore loaded into AGO 2 and promotes AGO 2-dependent slicing.

1.1.3 Nomenclature

Thousands of miRNAs have been discovered, and new ones are still being detected. The most recent version of the miRNA database, miRbase (v22.1) lists over 2600 human miRNAs (Kozomara & Griffiths-Jones, 2013). This gives the need of a consistent naming scheme. The nomenclature has the format of “hsa-miR-30c-2-3p” as an example. The miRNAs are given an abbreviation to identify the species in which they were found, for instance “hsa” for humans or “mmu” for mouse. The mature miRNA sequences are labelled “miR”, whereas the pre-miRNAs are labelled “mir” (Griffiths-Jones, Grocock, van Dongen, Bateman, & Enright, 2006). The miRNAs were continuously numbered according to their time point of discovery. The miRNA sequences that differ at only one or two positions are given suffixes of letters, for example hsa-miR-30a, hsa-miR-30b and hsa-miR-30c (Griffiths-Jones et al., 2006). Identical mature miRNAs that have derived from distinct hairpin loci are given numbered suffixes, for

example hsa-miR-30c-1 and hsa-miR-30c-2. The name of the mature miRNA is also determined by the direction of the miRNA strand. Earlier the two mature miRNA products were called “mature strand” and “star strand” (Desvignes et al., 2015). The mature strand was more highly expressed while the star strand was less expressed. The nomenclature was for example, hsa-miR-30c-2 for the mature strand and hsa-miR-30c-2* for the star strand. However, this caused bias as the two miRNA stands can be differentially expressed depending on species or/and tissues. Now, the strand that arises from the 5´end of the pre-miRNA hairpin gets the name “5p” and the strand that arises from the 3´end gets the name “3p”. For instance, this mean that hsa-miR-30c-2-3p is generated from the 3´end of the pre-miRNA hairpin.

1.1.4 Functions and mechanisms

Gene silencing by RISC

The RISC consists of the guide strand from the mature miRNA and the Argonaut protein (AGO). MiRNAs have a seed sequence consisting of 6-8 nucleotides located at the 5`end of the guide strand (O'Brien et al., 2018). The seed sequence is a conserved sequence which is complementary to the target mRNA (Figure 3). If several miRNAs have similar seed regions, they are considered a family. The sequence where the seed sequence binds to target mRNA is called miRNA recognition elements (MRE). The target MRE is usually at the 3´UTR of the mRNA, and target mRNA can have several conserved MRE sites for different RISC interactions.

Figure 3*: Binding between seed sequence in the miRNA and the miRNA response elements (MRE) at the 3´UTR of the target mRNA. The figure is retrieved from miRmap (Available from: http://mirmap.ezlab.org/).*

Gene silencing by RISC starts by recruiting GW182 family proteins which leads to recruitment of other effector proteins, such as poly(A)-deadenylase complexes, PAN2-PAN3 and CCR4-NOT (Figure 2) (Behm-Ansmant et al., 2006). The poly(A)-deadenylase complexes catalyze deadenylation of the mRNA which leads to decapping of the 5´cap. Exoribonuclease XRN1 may then conduct 5´-3´ degradation of the mRNA (Figure 2) (O'Brien et al., 2018). The degradation of target mRNA by RISC will lead to inhibition of gene expression.

Other functions of miRNAs

Other regulatory functions of miRNAs have also been studied and reported. For instance, miRNA gene regulation within the nucleus for direct interference with DNA (Benhamed, Herbig, Ye, Dejean, & Bischof, 2012; Miao et al., 2016). Miao et al. (2016) reported that miR-552 also was present in the nucleus and inhibits the CYP2E1 gene at transcriptional level. This shows that some miRNA might have the ability to inhibit target-genes both transcriptional and post-transcriptional.

1.2 MicroRNAs role in diagnostics

There has become an increasing interest in miRNAs, and the value of miRNA regulation and expression has become an interesting focus for diagnostic, prognostic and therapeutic uses. Studies have revealed several associations between miRNA expression and various diseases like cancer, cardiovascular and autoimmune disease (D'alessandra et al., 2010; Jin et al., 2018; youn Cha, ho Choi, Hwang, Jeong, & An, 2017). This thesis will focus on miRNA expression associated with the autoimmune disease rheumatoid arthritis, as the motivation for testing assays for quantification of miRNA is to lay the ground for selecting an assay for this setting later.

1.2.1 MicroRNAs role in autoimmune diseases

MiRNAs are reported to have a function of maintaining the immune homeostasis, and insufficient biogenesis of miRNAs in either T cells or B cells can lead to the development of autoimmunity (Long et al., 2018). The Dicer enzyme is an important factor for completing the biogenesis of mature miRNAs, and deficient expression will give deficient expression of miRNAs and may lead to critical alterations of the cell functions (Belver, de Yébenes, & Ramiro, 2010; Liston, Lu, O'Carroll, Tarakhovsky, & Rudensky, 2008; Zhou et al., 2008). Deficient Dicer expression in regulatory T cells have been observed to render development of systemic autoimmune diseases (Liston et al., 2008; Zhou et al., 2008). It has also been shown that Dicer-deficiency in B cells lead to skewed repertoire of B cell antigen receptors, which results in higher amounts of autoreactive antibodies (Belver et al., 2010).

MicroRNAs in Rheumatoid arthritis

Rheumatoid arthritis (RA) is a chronic, systemic autoimmune disease. The disease causes inflammation of joint and destruction of cartilage due to loss of immunological tolerance to self-antigens (National Rheumatoid Arthritis Society, 2001). The etiology of RA still remains elucidated, but it is suggested that both genetic and environmental factors play a role in the development of the disease. More than 100 genes have been associated with RA susceptibility (Okada et al., 2014). It is not clearly known how these genetic factors affect the development of the disease, however several recent studies have reported that miRNA dysregulation of the associated genes may play a crucial role (Long et al., 2018).

By comparing synoviocytes from joints of patients with RA to those from patient with osteoarthritis (a presumed non-autoimmune disease), it has been reported that the expression of miR-124a is significantly downregulated and functional studies suggested that miR-124a is a key in the posttranscriptional regulatory mechanisms of cells in the joints of RA-patients (Nakamachi et al., 2009). Several other miRNAs have also been reported to be downregulated in synoviocytes from the joints of RA-patients compared to controls, like miR-10a-5p. The downregulation of the miR-10a-5p will lead to higher expression of the target gene TBX5 causing increased expression of various inflammatory cytokines (Hussain et al., 2018). Studies have also suggested that miRNA expression levels can be used as predictive biomarker for treatment response (Duroux-Richard et al., 2014). Duroux-Richard et al. (2014) observed that increased levels of miR-125b measured at the point of disease flare for RA-patients, were associated with good clinical response to the treatment, rituximab, three months later. Overall, numerous miRNAs have been found at increased or decreased levels in various cell types, also immune cells, like CD4+ and CD8+ T cells, as well as in serum and plasma of RA patients (Moran-Moguel, Petarra-Del Rio, Mayorquin-Galvan, & Zavala-Cerna, 2018).

1.2.2 MicroRNAs as biomarkers

MiRNAs are present in our cells, however, miRNAs are also present in body fluids (Weber et al., 2010). These extracellular miRNAs have been found in a variety of body fluids, including plasma, urine, breast milk, amniotic fluid and saliva. The functions of these miRNAs are still being unraveled, but it is believed that they play a role in cell-to-cell communication (Montecalvo et al., 2012).

Body fluids are material that are easy to collect. This makes miRNAs tested in such material suitable as noninvasive biomarkers. However, miRNAs vary in presence and expression in different type of tissue and fluids (Ludwig et al., 2016). Establishment of a wide range of miRNAs expression profiles are therefore important for identifying potential biomarkers.

Murata et al. (2013) evaluated the expression of 768 miRNAs in peripheral blood of RA-patients and controls, and found 26 miRNAs with significant differences in expression patterns (Murata et al., 2013). Of these, miR-24, miR-26a and miR-125a-5p were proposed to be used as potential biomarkers for the identification of RA patients. This shows a large potential as for future biomarkers for RA. However, more studies are required before miRNA biomarkers can be used in diagnostics.

1.3 Detection and quantitation of microRNAs

For understanding the biological roles of miRNAs and for the establishment of miRNA expression profiles, reliable technologies and methods are required for detection and quantitation of miRNA. However, designing primers and probes for detection of miRNAs can be challenging. This is caused by the small size of mature miRNAs, the high degree of similarity, possibility of multiple isomers (isomiRs) and varying GC-content. Another challenge for detection and quantitation, is that miRNA only comprise a small part of the total RNA from biological material.

Initially, Northern blotting was used to detect miRNA. This was done by separating total RNA by gel electrophoresis and then transferring small RNA components to a membrane for visualizing the miRNA by using radioactively labeled probes complementary to the target miRNA sequence (de Planell-Saguer & Rodicio, 2011). However, this method is laborious and cannot be used for discovering new miRNAs or for absolute quantitation, which is craved by the increasing interest of miRNA expression in diagnostic.

This chapter will give a brief overview of different high-throughput platforms and technologies for miRNA detection and quantification, yet focus on different technologies based on reverse transcription and quantitative PCR (RT-qPCR).

1.3.1 Next generation sequencing

The discovery of miRNAs has been greatly enhanced by using high-throughput next-generation sequencing (NGS). The principle of NGS for small RNA-sequencing (RNA-seq) begins with library preparation where adaptors are ligated to the miRNA followed by reverse transcription. Almost all NGS library preparations also uses size-selective purification to remove unwanted fragments that can interfere with the analysis. Then, a massively parallel sequencing of millions of individual cDNA molecules from the library is conducted (Pritchard, Cheng, & Tewari, 2012).

Through small RNA-seq both known and novel miRNA can be discovered. Furthermore, RNA-seq can provide relative quantification by using the ratio of sequence reads for a given miRNA and overall reads from the sample (Pritchard et al., 2012). NGS is the only technique suitable for accurate detection of miRNA sequences with high similarity, even for miRNAs that differs by as little as one nucleotide like for instance seen in isomiRs. This gives the NGS approach a huge advantage. However, NGS is often limited as the analysis is expensive and time consuming due to labor intensive downstream data analysis and interpretation. This makes the technology disfavored for detection of few miRNAs. Additionally, NGS suffer from biases introduced in the library preparation process. This might lead to an incorrect representation of the miRNAs which complicates absolute quantification of miRNAs (Hafner et al., 2011).

1.3.2 MicroRNA specific hybridization

Several methods for detection and quantification of miRNAs by using hybridization specific to target miRNA have been developed (Pritchard et al., 2012). The methods are based on labeling the target miRNA in a sample with fluorescence before hybridization to oligonucleotide probes on microarrays.

The biogenesis of mature miRNA does not include poly(A) tailing at the 3´end of the miRNA strands. One common method for enzymatic labelling is therefore based on 3′end tailing, for instant by polyadenylation of poly(A) polymerase. Another widely used method for labeling the target, include the use of T4 RNA ligase for enzymatic ligation of a fluorescent nucleotide or oligonucleotide to the 3´end.

A challenge for the microarray approach is the lack of specificity caused by labelling of other cellular RNA. This can provide high background signals and cross-hybridization with specific miRNA probes (Pritchard et al., 2012). This problem can be reduced by including gel electrophoresis for fraction separation of the RNAs, however, this will not avoid the detection challenges of miRNAs with high sequence similarity. Microarrays can neither be used for absolute quantification nor for detection of novel miRNAs. On the other hand, advantages by use of miRNA microarrays are the low cost, compared to NGS and RT-qPCR, and the multiple possibility of enzymatic- and chemical labelling of target. The microarrays are also advantageous for detection of many miRNAs.

1.3.3 Reverse transcription and quantitative PCR

Reverse transcription of miRNA to cDNA template followed by quantitative PCR (RT-qPCR) (Figure 4) used to be the main approach for miRNA detection and quantitation (Heid, Stevens, Livak, & Williams, 1996). Quantitative PCR is highly used for gene expression studies, therefore, the adoption of the technique for miRNA expression profiling is often preferred by laboratories. The technique is often the method of choice if only a few miRNAs are to be tested, for instant for replication studies or for verification of miRNA sequencing results.

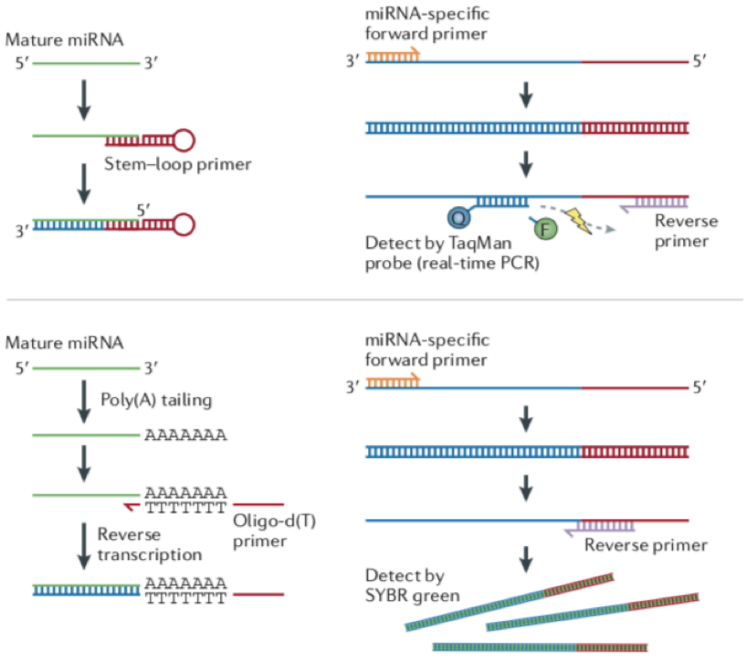

Figure 4: *The most common approaches for RT-qPCR for miRNA detection and quantitation. For the RT-reaction, stem–loop primers that are specific to the 3′ end of the microRNA (top left) or polyadenylation by poly(A) polymerase and reverse transcription by oligo-dT primers (bottom left), are the most used methods. For the qPCR-reaction miRNA specific primer are mostly used, and detection can be performed by TaqMan probes (top right) or SYBR green fluorescent dye (bottom right). The figure is modified from Pritchard et al. (2012).*

Reverse transcription (RT)

The reverse transcription is conducted by reverse transcriptase synthesis of single stranded target miRNA to double stranded complementary DNA (cDNA). Different techniques for priming the target miRNA are used. One common method is the use of stem-loop structures specific to the miRNA sequence (Chen et al., 2005). The primer consists of a short single stranded sequence that anneals to the complementary sequence at the 3′end of the target miRNA (Chen et al., 2005). The primer also includes a double stranded part (the stem) and a loop, resulting in a small stem-loop structure (Figure 4, top left). Another widely used method is based on poly(A) polymerase to lengthen the mature miRNA by adding an adenosine tail, poly(A) tail, to the 3´end. The poly(A) tail makes it possible for oligo-dT primers to reverse transcribe the miRNA into cDNA (Figure 4, bottom left). Unlike the stem-loop primer, this reaction is universal to all miRNAs in the sample.

Quantitative PCR (qPCR)

The qPCR method is based on the knowledge of the process where the cDNA template is amplified to multiple copies. The amplification is generally repeated for 40 cycles and is composed of different phases (Figure 5). When the amplification reaches the exponential phase, the template will increase exponentially as the reagents in the reaction are unlimited (Yuan, Reed, Chen, & Stewart, 2006). The exponential increase of template is only reached by optimal reaction efficiency of 100 %. Then, when the linear phase is reached, the template will increase linear as the reagents have become limited. The plateau is reached when the reagents are consumed, in this phase the template amount will not increase.

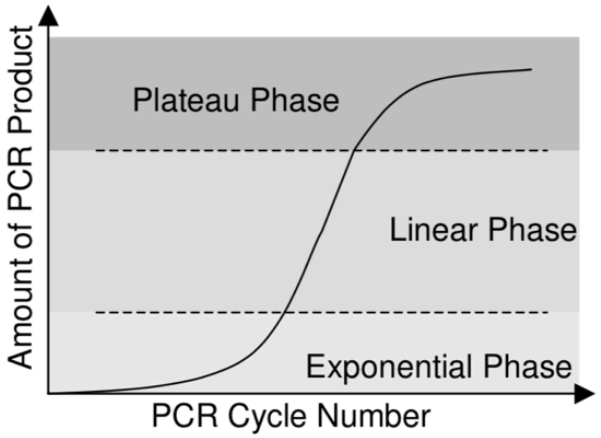

Figure 5: *The different phases of the qPCR amplification. The figure is modified from Yuan et al. (2006).*

In the phase where the template increases exponentially, a threshold cycle is set based on which level the template reaches a defined threshold. The threshold can be determined by two methods (Figure 6). The baseline threshold method considers all amplification curves in the reaction setup collectively to determine the threshold (Applied Biosystems, 2016). The cycle where a selected curve hits the baseline threshold is called the C_t (Figure 6A). The relative threshold method determines a threshold for each amplification curve individually. This second method uses the reaction efficiency to estimate the threshold based on the shape of each separate amplification curve, and uses this to determine the relative threshold (Applied Biosystems, 2016). The cycle where a selected curve hits relative threshold is called the C_{rt} (Figure 6B).

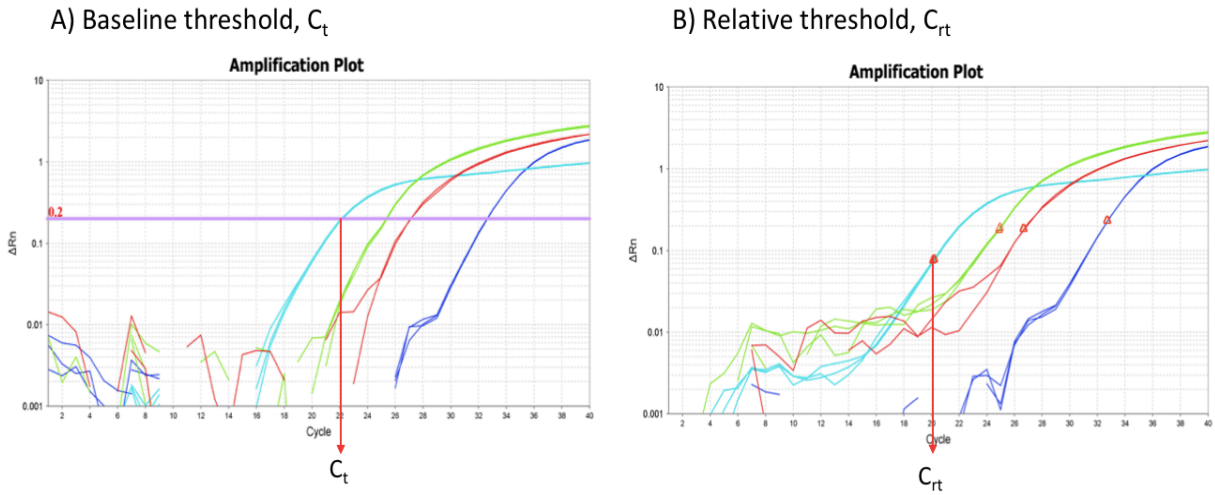

Figure 6: *The different methods to determine the threshold, baseline threshold (C_t) and relative threshold (C_{rt}).*

Specific primers, complementary to the target cDNA sequences, are used for the amplification, but the quantitative detection can be performed by several different methods. There are especially two common methods for detecting the amounts of template. One method is based on non-specific fluorescent dye that intercalate with all double-stranded DNA. The fluorescent dye SYBR green is the most popular (Figure 4, bottom right). The other method is based on sequence-specific probes. The probes consist of oligonucleotides that are labelled with a fluorescent reporter that hybridizes to a complementary sequence of the target. The most common used are the TaqMan probes (Figure 4, top right). The TaqMan probes consist of a reporter dye at the 5´end and a quencher at the 3´end. The quencher suppresses the fluorescence of the reporter dye when the probe is intact, but when annealed to

target the encounter with the DNA polymerase results in cleavage of the probe. The cleavage separates the reporter and the quencher, and the fluorescence of the reporter is emitted. The sequence-specific probes have greater specificity than the non-specific fluorescent dye, as they hybridize to target-specific sequences.

Challenges for RT-qPCR technology

Challenges for the RT-qPCR technologies for miRNA detection include the difficulty of creating stable primers and sequence-specific probes, as miRNAs are a small in size and have varying GC-content. As a solution to overcome this, some primers are incorporated with locked nucleic acids (LNA). For LNA the ribose ring is locked in the ideal conformation for base pairing (Singh, Koshkin, Wengel, & Nielsen, 1998). This makes the primers more stable and increases the melting temperature (T_m) (Kauppinen, Vester, & Wengel, 2005). The increased T_m will increase the binding strength of the primers, which again will increase the sensitivity of the reaction. This also makes it possible to reduce the minimum requirements for template (Ballantyne, Van Oorschot, & Mitchell, 2008). The increased T_m make it possible to create the LNA oligonucleotides shorter than RNA oligonucleotides which is beneficial for detection of short miRNAs with varying GC content. It has also been seen that secondary structure of RNA can introduce bias in cDNA synthesis (Ståhlberg, Kubista, & Pfaffl, 2004). When using universal annealing temperatures, primer efficiency and qPCR cycling conditions, the varying GC-content and the secondary structures of miRNAs can cause challenges (Chugh & Dittmer, 2012). The challenges are introduced by the varying T_m different CG-content and secondary structures leads to.

The RT-qPCR technology does not make it possible to discover novel miRNAs, as design of primers and probes are limited to known sequences of the target. However, RT-qPCR is advantageous as it allows absolute quantification, also of small amounts of target. This makes the technology suitable for discovery and validation of biomarkers. However, different RT-qPCR technologies have been observed to give variable results (Mestdagh et al., 2014; Redshaw et al., 2013). Mestdagh et al. (2014) evaluated different vendors for miRNA profiling technologies for three different platforms, hybridization, sequencing and RT-qPCR. The study demonstrated differences in performance for platforms based on the same technology, and reported the most varying results for reproducibility and specificity for qPCR platforms (Mestdagh et al., 2014).

2 Aim of the study

The aim of this study was to conduct a systematic evaluation of various kits and protocols to perform reverse transcription and quantitative PCR (RT-qPCR) for detection and quantitation of microRNA.

To evaluate the performance, the output from the RT-qPCR-reactions was compared by specificity, efficiency, precision, costs and feasibility.

The objective of the evaluation was to find a preferred RT-qPCR setup that later will be used in an ongoing research project for verifying miRNA-findings from next-generation sequencing (NGS) of lymphocytes from patients with rheumatoid arthritis (RA).

3 Method theory

3.1 Comparison of technologies for quantitative miRNA detection

First an overview of the different RT-qPCR technologies that are available was generated. Some of the technologies were commercially available through Thermo Fisher Scientific, Qiagen and Quantabio (Table 1).

Table 1: *Comparison of different commercially available technologies for conducting reverse transcription (RT) and quantitative detection of miRNAs.*

	Provider	**Input total RNA**	**Reverse transcription**	**qPCR primers**	**Detection**
TaqMan Advanced miRNA	Thermo Fisher Scientific	1 ng - 10 ng	Polyadenylation by poly(A) polymerase at the 3´end, ligase and universal RT primers, miR-Amp reaction	miRNA specific primers	TaqMan MGB probes
TaqMan MicroRNA	Thermo Fisher Scientific	1 ng - 10 ng	miRNA specific stem-loop primer transcription	miRNA specific primers	TaqMan MGB probes
miRCURY	Qiagen	10 pg - 200 ng	Polyadenylation by poly(A) polymerase at the 3´end universal RT primers	LNA optimized miRNA specific primers	SYBR Green I fluorescent dye
miScript	Qiagen	10 pg - 2 µg	Polyadenylation by poly(A) polymerase at the 3´end and transcription by oligo-dT primers and hexamers	miRNA specific forward primer and universal reverse primer	SYBR Green I fluorescent dye
qScript microRNA	Quantabio	10 pg -1 µg	Polyadenylation by poly(A) polymerase at the 3´end and transcription by oligo-dT primers and hexamers	miRNA specific forward primer and universal reverse primer	SYBR Green I fluorescent dye

In addition, some novel methods were also found through literature searches (Table 2).

Table 2: *Comparison of different technologies found by literature search for conducting reverse transcription (RT) and quantitative detection of miRNAs.*

	Provider	**Input total RNA**	**Reverse transcription**	**qPCR primers**	**Detection**
SplintR Ligase (1)	None	40 pg -1 ng	Probe ligation to the miRNA by SplintR Ligase	miRNA specific primers	Double-quenched DNA probe with fluorescent dye at the 5′end
Two-tailed RT-qPCR (2)	None	10 ng	Target specific primer that contain two hemiprobes complementary to the miRNA connected by a hairpin sequence	Forward primer specific to the predesigned region in the 5′-end of the RT primer and miRNA specific reverse primer	SYBR Green I fluorescent dye
Dumbbell-PCR (3)	None	Unknown	Stem–loop adapters, hybridized and ligated by Rnl2 to the 5′- and 3′-ends	miRNA specific primers	TaqMan MGB probes
Double Molecular Beacon Approach (4)	None	1 - 3 µg	Hybridization of specific LNA optimized molecular beacons with target nucleic acid		Molecular beacons probes labeled with a fluorescent dye in 5’end and quencher at the 3’end
miQPCR (5)	None	10 ng	Universal elongation of ssRNA at 3’end ligated to the 5’ end of synthetic miLINKER by truncated RNA T4ligase2	miRNA specific forward primer and universal reverse primer	SYBR Green I fluorescent dye

References of the technologies are (1) J. Jin, Vaud, Zhelkovsky, Posfai, and McReynolds (2016), (2) Androvic, Valihrach, Elling, Sjoback, and Kubista (2017), (3) Honda and Kirino (2015), (4) James, Baker, Bao, and Searles (2017) and (5) Benes et al. (2015)

On account of limited time and economic aspects, all of the listed technologies could not be evaluated in this study. The technologies that were not commercially available were excluded, as it was preferred to focus on thoroughly developed methods and protocols that can be purchased off the shelf for the evaluation. The TaqMan MicroRNA kit is often used in literature, and sometimes referred to as the *gold standard* RT-qPCR method. The TaqMan Advanced miRNA is quite similar to the TaqMan MicroRNA but harbours a different RT-method. It was therefore interesting to compare these two protocols. Another main detection method includes SYBR Green I dye, and as the TaqMan MicroRNA and TaqMan Advanced use TaqMan probes for detection, it was also of interest to compare technologies having these two detection methods. Another aspect was the LNA optimized primers, the miRCURY technology, was therefore selected, instead of miScript and qScript microRNA.

The three selected kits for conducting the systematic evaluation of RT-qPCR for miRNA detection and quantitation were therefore: TaqMan Advanced miRNA, TaqMan MicroRNA and miRCURY. The chemical and theoretical details for the selected methods are further described below.

3.2 miRCURY RT-qPCR

The miRCURY technology is provided by Qiagen, and the chemical and theoretical details were found in *miRCURY® LNA® miRNA PCR Handbook* from October 2017.

3.2.1 miRCURY Reverse Transcription (RT)

The miRCURY RT are based on polyadenylation by poly(A) polymerase at the 3´end of the miRNA, creating a poly(A) tail. The poly(A) tail makes it possible for oligo-dT primers to reverse transcribe the miRNA into cDNA. The primers also include a 3´degenerate anchor and a 5′ universal tag that allows amplification of the miRNA in the qPCR-reaction (Figure 7). This RT-reaction is universal for all miRNAs in the sample.

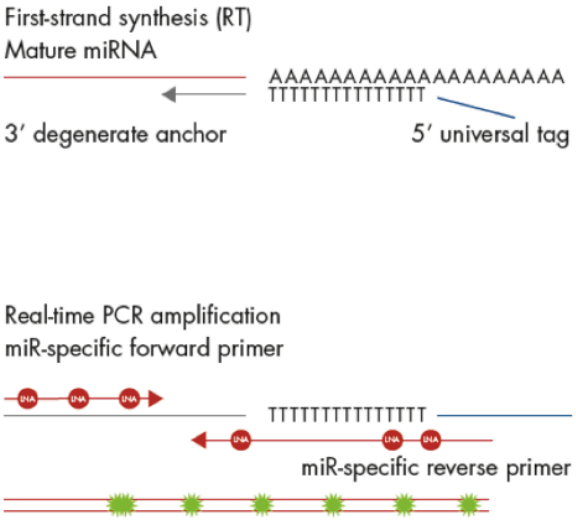

***Figure** 7: The RT-qPCR method using miRCURY technology. This figure is modified from miRCURY® LNA® miRNA PCR Handbook from October 2017.*

3.2.2 miRCURY quantitative PCR (qPCR)

After the RT the cDNA-strands is used as template for the qPCR-reaction. The forward and reverse primers are miRNA specific and binds to the complementary sequence of target miRNA. The primers are optimized with LNA. According to the provider (Qiagen), the melting temperature of the assays increases with about 2-8 ºC for each incorporated LNA.

The fluorescent dye, SYBR green I, is used to detect the miRNAs. SYBR green I emits a fluorescent signal when intercalating between the bases of all double-stranded nucleic acids (Figure 7). Detection by SYBR green I also makes it possible to create a melting curve. The melting curve is generated by increasing the temperature to 95 ℃ causing denaturation of the double-stranded DNA. The fluorescent signal of SYBR green I will increase with decreasing temperature. The change in fluorescent signal for different temperature is registered and this makes it possible to evaluate the melting temperature (T_m) of all detected template in the sample. The T_m gives an important indicator of the detected template and makes it possible to discover unspecific amplification. This is seen by divergent T_m in the reactions. The melting curve is therefore an important control of the specificity of the qPCR-reaction.

3.3 TaqMan Advanced RT-qPCR

The TaqMan Advanced technology is provided by Thermo Fisher Scientific, and the chemical and theoretical details were found in *TaqMan® Advanced miRNA Assays User guide* from September 2016.

3.3.1 TaqMan Advanced Reverse Transcription (RT)

The TaqMan Advanced RT is based on, similar as the miRCURY RT, polyadenylation to the 3´end of the miRNA by poly(A) polymerase which creates a poly(A) tail. Further, the miRNA undergoes adaptor ligation at the 5'end. After adaptor ligation, the miRNA is reverse transcribed into cDNA by adding a universal RT primer to the 3´poly(A) tail. The polyadenylation, adaptor ligation and reverse transcription happens in separate reactions and are universal for all miRNAs in the sample (Figure 8). For the TaqMan Advanced RT, there is also included a preamplification reaction to increase the amount of cDNA, called miR-Amp. In the miR-Amp reaction, the adaptor from the adaptor ligation step function as forward primer binding site. The miR-Amp reaction is conducted for 14 amplification cycles.

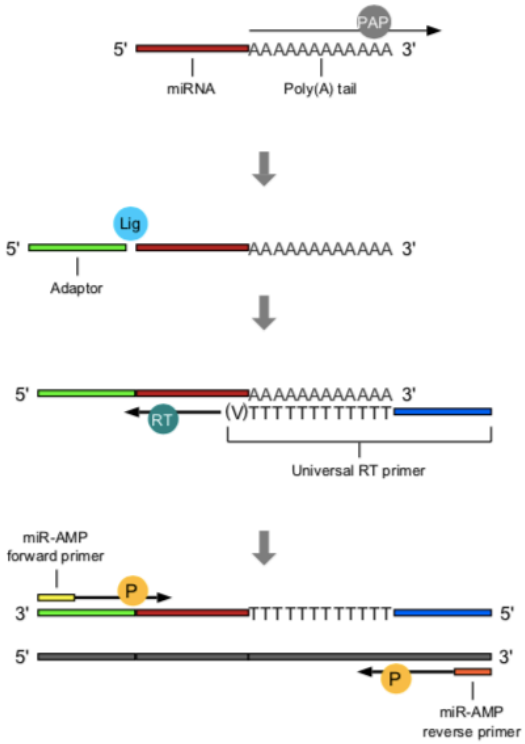

Figure 8: *The TaqMan Advanced RT-reactions. The figure is modified from TaqMan® Advanced miRNA Assays User guide from September 2016.*

3.3.2 TaqMan Advanced quantitative PCR (qPCR)

The cDNA-strands, created by the TaqMan Advanced RT, are used as template for the qPCR-reaction. The miRNA specific forward and reverse primers binds to the complementary sequences along the denatured template strands. TaqMan MGB probe (Figure 9) anneals to a complementary sequence between the forward and reverse primer. The probe has a reporter, FAM dye, at the 5´end and a quencher at the 3´end. The 3´end of the probe also include a minder-groove binding (MGB) molecule which increase the binding of the probe to the target. When the DNA polymerase cleaves the TaqMan MGB probe fluorescence of the FAM dye increases. The increased fluorescence is detected, and the polymerization of the strand continues. Because the 3' end of the probe is blocked, extension of the probe will not continue.

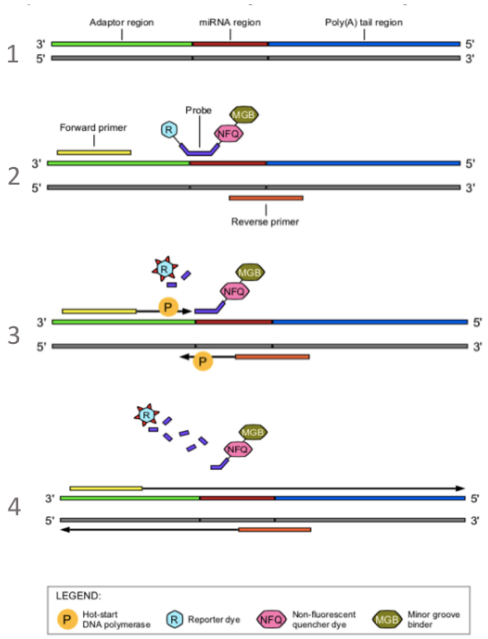

Figure 9: *The qPCR detection by using TaqMan MGB probes. The figure is modified from TaqMan® Advanced miRNA Assays User guide from September 2016.*

3.4 TaqMan MicroRNA RT-qPCR

The TaqMan MicroRNA technology is provided by Thermo Fisher Scientific, and the chemical and theoretical details were found in *TaqMan® Small RNA Assays Protocol* from January 2011.

3.4.1 TaqMan MicroRNA Reverse Transcription (RT)

The TaqMan MicroRNA RT differs from the miRCURY RT and TaqMan Advanced RT, as it is based on a miRNA specific, stem-loop primers. The primers consist of a short single stranded sequence at the 3′end that anneals to the complementary sequence at the 3′end of target miRNA (Figure 10). This reaction is thereby specific to target-miRNAs, and not universal for all miRNAs in a samples.

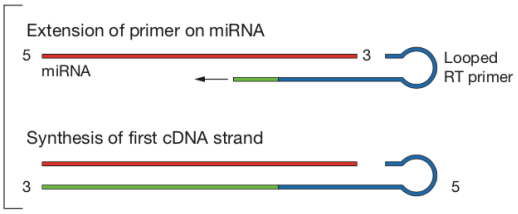

Figure 10: *The TaqMan MicroRNA RT based on miRNA specific, stem-loop RT primers. This figure is modified from TaqMan® Small RNA Assays Protocol from January 2011.*

3.4.2 TaqMan MicroRNA quantitative PCR (qPCR)

The cDNA-strands, created by the TaqMan MicroRNA RT, are used as template for the qPCR-reaction. Forward and reverse primers specific to target miRNA binds to the complementary sequences of the denatured cDNA. Similar to the TaqMan Advanced qPCR-reaction, TaqMan MGB probe are used for detection (Figure 9), as described in chapter 3.3.2 TaqMan Advanced quantitative PCR (qPCR).

4 Materials and methods

4.1 The MicroRNA (miRNA) selection and material

There were chosen six miRNAs to conduct the study. All six miRNAs were detected in sequencing data of lymphocytes from patients with rheumatoid arthritis, and the three providers had available assays for all of them. The miRNA-assays were named differently for each provider, but it was checked that they were based on the same sequences and miRBase ID. The miRNAs miRBase ID, their sequences and assay names are listed in Table 3. TaqMan MicroRNA assays do not specifies the 3p- or 5p-strand but uses the old nomenclature (chapter 1.1.3 Nomenclature).

Table 3: *An overview of the six different microRNAs and the names of the assays used to conduct this study.*

miRbase ID	Sequence	miRCURY LNA miRNA PCR assay	TaqMan Advanced miRNA Assays	TaqMan MicroRNA Assays
Hsa-miR-30c-2-3p	5′CUGGGAGAAGGCUGUUUACUCU′3	Hsa-miR-30c-2-3p	Hsa-miR-30c-2-3p	Hsa-miR-30c-2*
Hsa-miR-125b-1-3p	5′ACGGGUUAGGCUCUUGGGAGCU′3	Hsa-miR-125b-1-3p	Hsa-miR-125b-1-3p	Hsa-miR-125b-1*
Hsa-miR-136-3p	5′CAUCAUCGUCUCAAAUGAGUCU′3	Hsa-miR-136-3p	Hsa-miR-136-3p	Hsa-miR-136*
Hsa-miR-379-5p	5′UGGUAGACUAUGGAACGUAGG′3	Hsa-miR-379-5p	Hsa-miR-379-5p	Mmu-miR-379
Hsa-miR-493-5p	5′UUGUACAUGGUAGGCUUUCAUU′3	Hsa-miR-493-5p	Hsa-miR-493-5p	Hsa-miR-493
Hsa-miR-495-3p	5′AAACAAACAUGGUGCACUUCUU′3	Hsa-miR-495-3p	Hsa-miR-495-3p	Mmu-miR-495

In order to test the different setups, synthetic template material for the six miRNAs were used. Hsa-miR-379-5p, hsa-miR-493-5p and hsa-miR-495-3p were represented by a synthetic miRNA pool. The three other miRNAs, hsa-miR-30c-2-3p, hsa-miR-125b-1-3p and hsa-miR-136-3p, were represented by single oligonucleotides (oligos). The material is further described below.

4.1.1 Single oligos

The single oligos represented hsa-miR-30c-2-3p, hsa-miR-125b-1-3 and hsa-miR-136-3p and were HPLC purified, 5'phosphorylated, synthetic oligonucleotides. They were purchased from Eurofins MWG Synthesis GmbH, and had a stock concentration of 100 pmol/µl. The three single oligos consisted of pure synthetic miRNAs but the input ranges given in the providers protocols were based on total RNA. Several dilutions were therefore tested, and a previous in-house validation had shown that 1:600 dilutions of each single oligo would result in a reliable range for conducting RT-qPCR (data not shown).

4.1.2 Synthetic miRNA pool

The synthetic miRNA pool consisted of the miRXplore Universal Reference purchased from MACS, Miltenyi Biotec. The pool comprised 962 HPLC purified, 5' phosphorylated, synthetic RNA oligonucleotides matching mature miRNA-sequences. Among the 962 miRNAs, hsa-miR-379-5p, hsa-miR-493-5p and hsa-miR-495-3p were included. The synthetic miRNA pool was equimolar which means that the pool contained equal amounts of all the 962 miRNAs. The concentration of the pool was 31.4 ng/µl. The synthetic miRNA pool was also used as synthetical noise by mixing a diluted amount with each single oligo representing hsa-miR-30c-2-3p, hsa-miR-125b-1-3 and hsa-miR-136-3p. This was done to include competitive noise for all analysis of the six chosen miRNAs.

4.1.3 Biological noise

To create samples that somewhat mimic normal biological samples, all dilution of the synthetic miRNAs was repeated with added biological noise in the qPCR reaction. The biological noise was established from available material, which was CD8+ lymphocytes from peripheral blood from three healthy individuals. To ensure sufficient amounts of total RNA input for the cDNA synthesis and qPCR of all setups, the three healthy samples were mixed together to make a pool of biological noise. The total RNA integrity values were above 8.5 (data not shown) for all three samples pooled. The pool had a concentration of 300 ng. Due to earlier NGS data of total RNA from the lymphocytes, it was known that the material contained all six miRNAs: hsa-miR-30c-2-3p, hsa-miR-125b-1-3, hsa-miR-136-3p, hsa-miR-495-3p, hsa-miR-493-5p and hsa-miR-379-5p. It was therefore expected some quantitative differences in the results for the template mixtures with added biological noise compared to the template mixtures without.

4.2 Evaluation of dilution and noise of the synthetic miRNA pool

Since the target material used in this study was synthetic miRNAs, it was necessary to examine which dilutions and amount that could be used as template for the systematic evaluations of the different RT-qPCR methods.

For the synthetic miRNA pool containing 962 synthetic miRNAs including hsa-miR-379-5p, hsa-miR-493-5p and hsa-miR-495-3p, different dilutions of template were tested using miRCURY LNA RT kit, miRCURY LNA SYBR Green PCR kit and miRCURY LNA miRNA PCR assay. The material details can be found in appendix (Appendix A). The miRCURY components were chosen due to economic aspects (limitations of reagents) as the protocol listed the highest dilution step after reverse transcription. Further, it was created a 10-fold dilution series comprising six points, and qPCR was conducted with quintuplicates of the six dilutions.

Furthermore, the amount of the synthetic miRNA pool that could be used as synthetical noise added together with the single oligos, was evaluated using TaqMan MicroRNA Reverse Transcription kit, TaqMan Universal PCR Master Mix II, No UNG and TaqMan MicroRNA Assays for hsa-miR-125b-1*, hsa-miR-136* and hsa-miR-30c-2*. The material details can be found in the appendix (Appendix A). The TaqMan MicroRNA components were chosen due to economic aspects and as the protocol did not include any dilution step after reverse transcription. If the added synthetic noise would create interfering background noise for the tested components, the same added amount of synthetic noise would result in less interfering background noise for the miRCURY and TaqMan Advanced setups as their protocols listed different dilutions steps after reverse transcription. Three different amounts of synthetic miRNA pool were tested. For this 0.133 ng, 0.066 ng or 0.033 ng was added as noise together with each single oligos. Next, qPCR was conducted with quintuplicates of the three different amounts of synthetical noise.

The tests were conducted by using 2720 Thermal Cycler PCR System by Applied Biosystems (Thermo Fisher Scientific) to perform the RT-reactions, and QuantStudio 12K Flex Real-Time PCR System by Applied Biosystems (Thermo Fisher Scientific) to perform qPCR. One negative control for each assay which contained RNase free water as template (no template

control) was included both for the RT- and the qPCR-reactions.

4.3 Systematic evaluation of RT-qPCR for miRNA detection

Figure 11 shows the general setup with the materials and different mixtures of template.

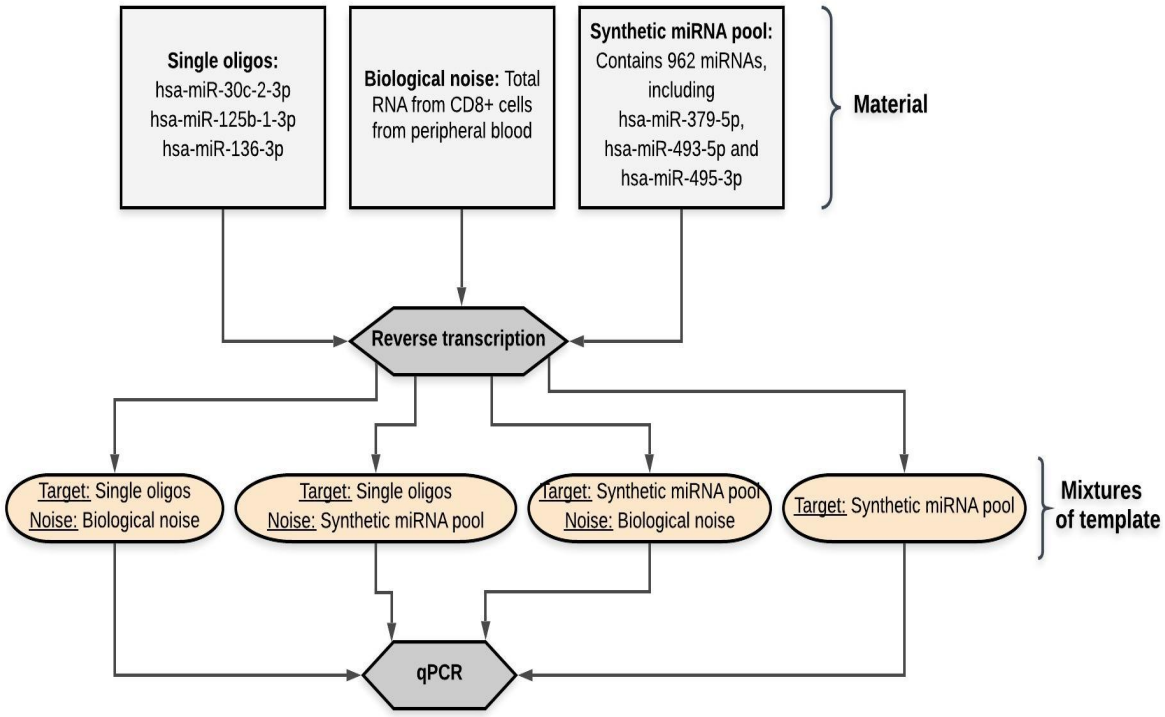

Figure 11: *The material used in the reverse transcriptase reaction and template mixtures used in the systematic evaluation of RT-qPCR miRNA setup.*

The 2720 Thermal Cycler PCR System by Applied Biosystems (Thermo Fisher Scientific) was used to perform the RT-reactions. To perform the qPCR-reactions the QuantStudio 12K Flex Real-Time PCR System by Applied Biosystems (Thermo Fisher Scientific) was used. To retrieve a reliable standard curve, a six point 10-fold dilutions series of the different mixtures of template were created. The qPCR for the different setups was conducted with quintuplicates for all dilution points.

Two different negative controls were including as triplicates in all runs. This was necessary to test if the reagents from the RT- and qPCR-reactions would create false positive results. One of the negative controls consisted of the reagents from the RT-reaction without any target template (RT-reagents template control). The other negative control consisted only of the

reagents from the qPCR-reaction with RNase free water as template (no template control). For both controls, it was expected no amplification.

4.3.1 miRCURY RT-qPCR setup

The components used for the RT and qPCR were miRCURY LNA RT kit, miRCURY LNA SYBR Green PCR kit and miRCURY LNA miRNA PCR assay for hsa-miR-495-3p, hsa-miR-125b-1-3p, hsa-miR-493-5p, hsa-miR-136-3p, hsa-miR-30c-2-3p and hsa-miR-379-5p. All components were provided by Qiagen. The details can be found in appendix (Appendix A). These components will hereafter be called *miRCURY RT-qPCR setup*.

The different steps of the miRCURY RT-qPCR setup are shown in Figure 12.

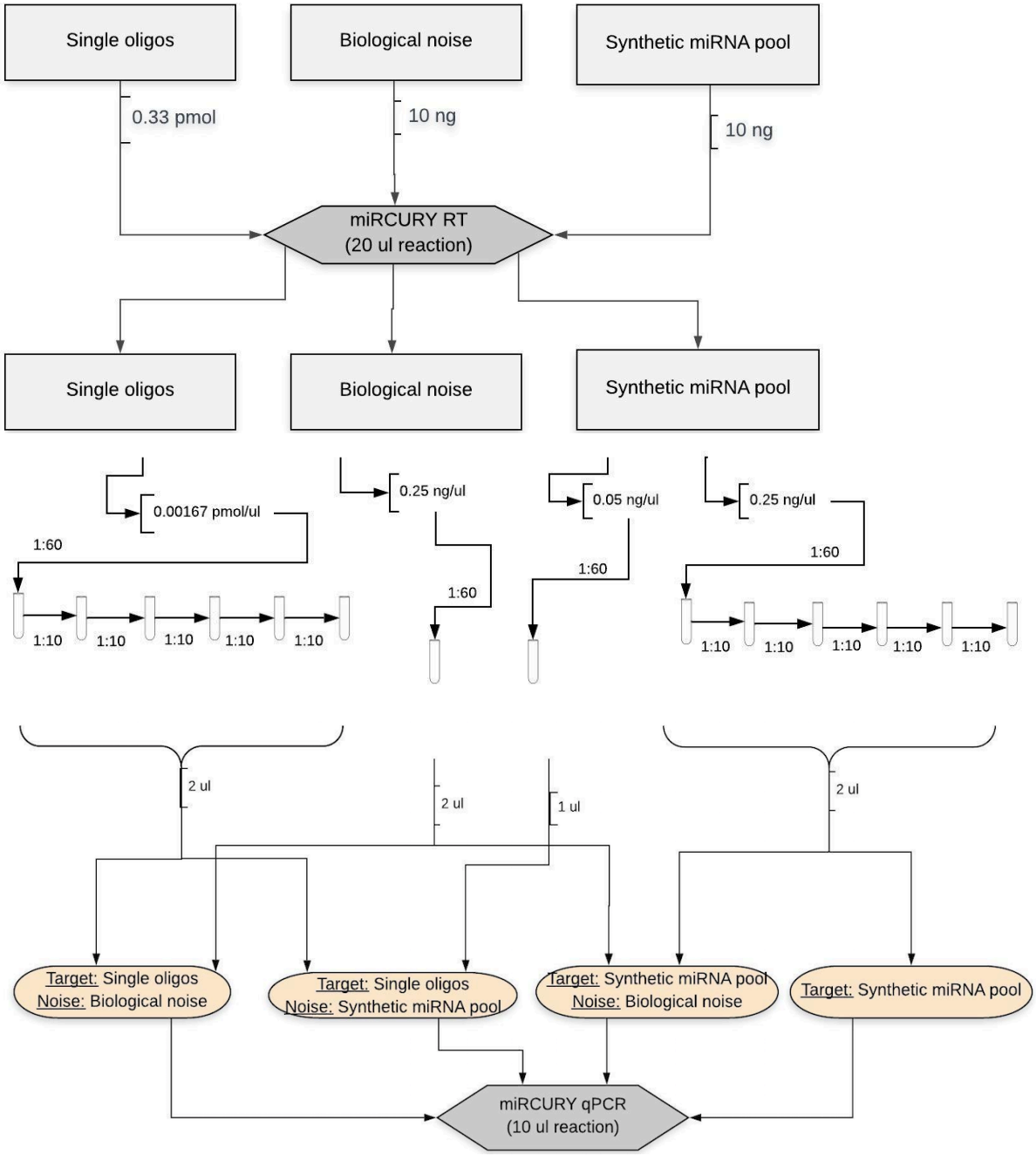

Figure 12: *The dilutions and input for the different steps of miRCURY RT-qPCR setup*

As input for the RT-reaction, 10 ng of the synthetic miRNA pool, 0.33 pmol of each single oligos and 10 ng of the biological noise were added. The RT-reaction was conducted by following the protocol and the temperature conditions are listed in Table 4.

Table 4: *The temperature conditions for the cDNA synthesis for miRCURY RT-setup.*

Step	Time	Temperature
Reverse transcriptions step	60 min	42℃
Inactivation of reaction	5 min	95℃
Storage	∞	4℃

After RT, the cDNA of the single oligos was diluted 1:10, giving a concentration of 0.00167 pmol/µl. The cDNA was further diluted 1:60 by following the protocol and a 10-fold dilution series of six steps were created. Then, these six concentrations were added together with biological noise and together with synthetical noise from the synthetic miRNA pool as input for the qPCR reactions.

The cDNA of the biological noise was diluted 1:2 after RT, giving a concentration of 0.25 ng/µl. Further, the cDNA was diluted 1:60 by following the protocol and added as noise together with each single oligos and the synthetic miRNA pool for the qPCR reactions.

For the synthetic miRNA pool, half of the cDNA was diluted 1:10, giving a concentration of 0.05 ng/µl, and further a 1:60 dilution was created by following the protocol. This dilution was added as synthetical noise to each single oligos. The other half of the cDNA was diluted 1:2, giving a concentration of 0.25 ng/µl, before it was diluted 1:60 by following the protocol. This gave the concentration of the first dilution point in the 10-fold dilution series of six steps. Further, these six concentrations were used as input for qPCR-reaction alone or together with added biological noise.

The qPCR analysis was conducted by following protocol, and the thermal cycling conditions are listed in Table 5.

Table 5: *The qPCR thermal cycling conditions of the miRCURY qPCR-setup.*

Step	Time	Temperature	Ramp rate	Cycles
Enzyme activation	2 min	95℃	Fast	1
Denaturation	10 sec	95℃	Fast	40
Annealing/Extension	60 sec	56℃	Fast	
Melting curve analysis		60 - 95℃		1

4.3.2 TaqMan Advanced RT-qPCR setup

The components used for the RT and qPCR were TaqMan Advanced miRNA cDNA Synthesis kit, TaqMan Fast Advanced Master Mix and TaqMan Advanced miRNA Assays for hsa-miR-495-3p, hsa-miR-125b-1-3p, hsa-miR-493-5p, hsa-miR-136-3p, hsa-miR-30c-2-3p and hsa-miR-379-5p. All components were provided by Thermo Fisher Scientific. The details can be found in appendix (Appendix A). These components will hereafter be called *TaqMan Advanced RT-qPCR setup*.

The different steps of the TaqMan Advanced RT-qPCR setup are shown in Figure 13. For the TaqMan Advanced RT-qPCR setup, it was also tested the if the preamplification of cDNA by the miR-Amp reaction described in the protocol, was necessary to achieve reliable qPCR-results. The miR-Amp reaction is represented in the figure by the red lines.

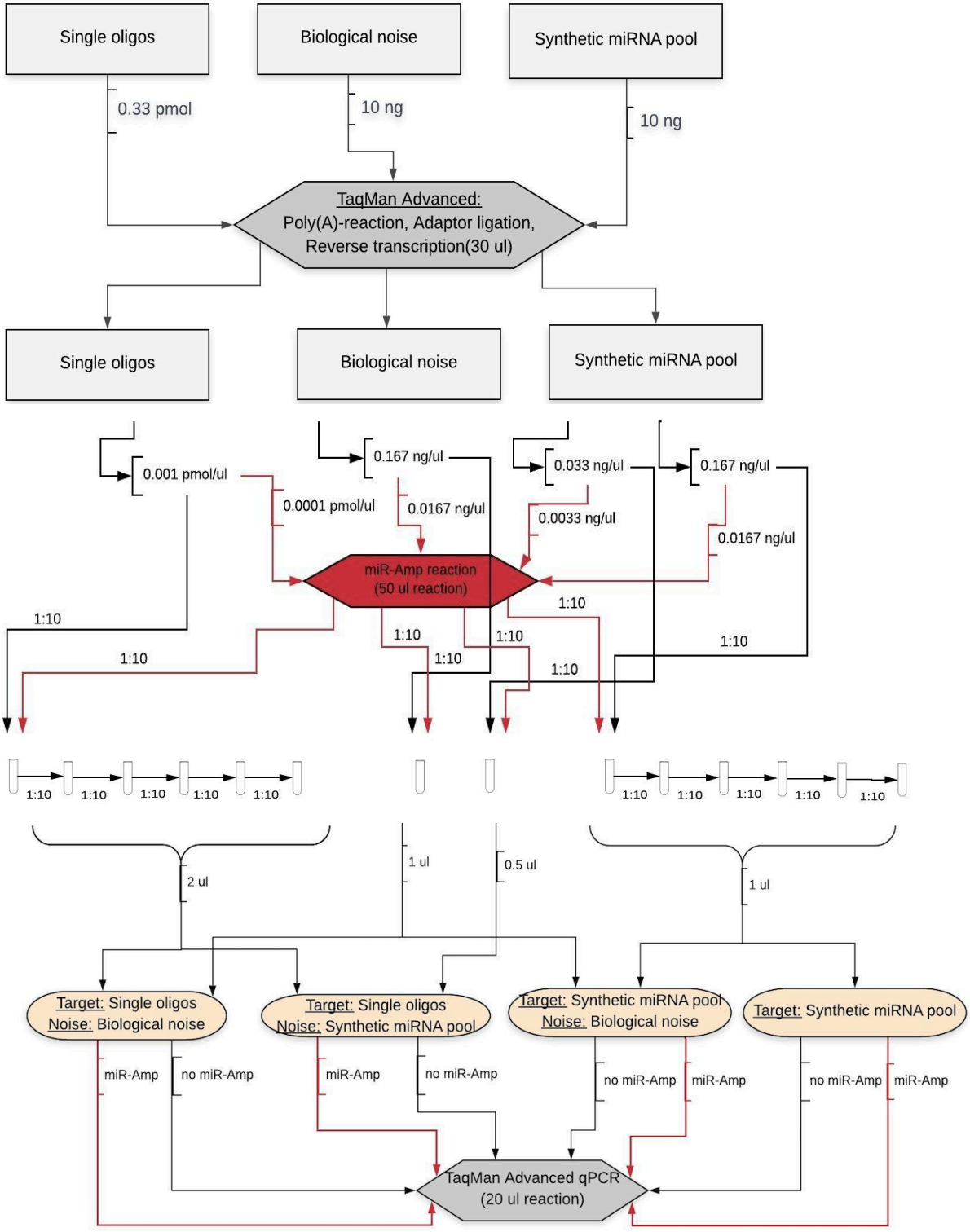

Figure 13: *The dilutions and input of the different steps for TaqMan Advanced RT-qPCR setup. The red lines show the steps for conducting RT-qPCR with miR-Amp reaction.*

As input for the poly(A)-reaction, adaptor ligation and RT-reaction, 10 ng of the synthetic miRNA pool to create the dilution series, 10 ng of the synthetic miRNA pool to create synthetical noise, 0.33 pmol of each single oligo and 10 ng of the biological noise was added.

The poly(A)-reaction, adaptor ligation and RT-reaction were conducted by following the protocol.

After the RT-reaction, the cDNA of the single oligos was diluted 1:10, giving a concentration of 0.001 pmol/µl. The cDNA of the biological noise was diluted 1:2, giving a concentration of 0.167 ng/µl. The cDNA of the synthetic miRNA pool for the dilution series was diluted 1:2 giving a concentration of 0.167 ng/µl, and the cDNA of the synthetic miRNA pool used for synthetical noise was diluted 1:10, giving a concentration of 0.033 ng/µl. For conducting the miR-Amp reactions, 5 µl of these dilutions were added as input by following the protocol.

The temperature conditions for the poly(A) tailing reaction, adaptor ligation, RT and the PCR conditions for the miR-Amp reaction are listed in Table 6.

Table 6: *The temperature conditions for the cDNA synthesis for TaqMan Advanced RT-setup.*

	Step	Time	Temperature	Cycles
Poly(A) tailing reaction	Polyadenylation	45 min	37℃	
	Stop reaction	10 min	65℃	
	Hold	∞	4℃	
Adaptor ligation reaction	Ligation	60 min	16℃	
	Hold	∞	4℃	
Reverse transcription reaction	Reverse transcription	15 min	42℃	
	Stop reaction	5 min	85℃	
	Hold	∞	4℃	
miR-Amp reaction	Enzyme activation	5 min	95℃	1
	Denature	3 sec	95℃	
	Anneal/Extend	30 sec	60℃	14
	Stop reaction	10 min	99℃	1
	Hold	∞	4℃	1

The rest of the cDNA for the single oligos that did not include the miR-Amp reaction, was diluted 1:10 by following the protocol. Further, it was created a 10-fold dilution series of six steps, and the six concentrations were added as input for qPCR added together with biological noise and added together with synthetical noise from the synthetic miRNA pool.

The rest of the cDNA for the biological noise was diluted 1:10 by following the protocol and added together with each single oligo and the synthetic miRNA pool as input for qPCR. The rest of the cDNA from the synthetic miRNA pool used for synthetical noise, was also diluted 1:10 by following the protocol and added together with each single oligo as input for qPCR.

For the rest of the cDNA of the synthetic miRNA pool to make the dilution series, a dilution of 1:10 was conducted by following the protocol. It was then created a 10-fold dilution series of six steps, and the six concentrations were used as input for qPCR either alone or together with added biological noise.

After the miR-Amp reactions, the same dilutions and dilution series were generated for the cDNA that went through the preamplification of the miR-Amp.

The qPCR analysis was conducted by following the protocol, and the thermal cycling conditions are listed in Table 7.

Table 7: *The qPCR thermal cycling conditions for the TaqMan Advanced qPCR-setup.*

Step	Time	Temperature	Ramp rate	Cycles
Enzyme activation	20 sec	95℃	Standard	1
Denature	1 sec	95℃	Standard	40
Anneal/Extend	20 sec	60℃	Standard	

4.3.3 TaqMan MicroRNA RT-qPCR setup

The components used for the RT and qPCR were TaqMan MicroRNA Reverse Transcription kit, TaqMan Universal PCR Master Mix II, No UNG, TaqMan Universal PCR Master Mix II, With UNG and TaqMan MicroRNA Assays for mmu-miR-495, hsa-miR-125b-1*, hsa-miR-493, hsa-miR-136*, hsa-miR-30c-2* and mmu-miR-379. All components were provided by Thermo Fisher Scientific. The details can be found in appendix (Appendix A). These components will hereafter be called *TaqMan MicroRNA RT-qPCR setup*.

The different steps of the TaqMan MicroRNA RT-qPCR setup are shown in Figure 14. For the TaqMan MicroRNA RT-qPCR setup it was also tested two different master mixes, one with and one without uracil-N glycosylase (UNG). The UNG-enzyme prevents contamination by carryover in the qPCR-reaction by removing uracil by catalyzing hydrolysis in the N-

glycosylic bond between uracil and sugar. Both master mixes were suggested by the provider, and they were compared to evaluate how UNG effected the result. The master mix containing UNG is represented in the figure by the red lines.

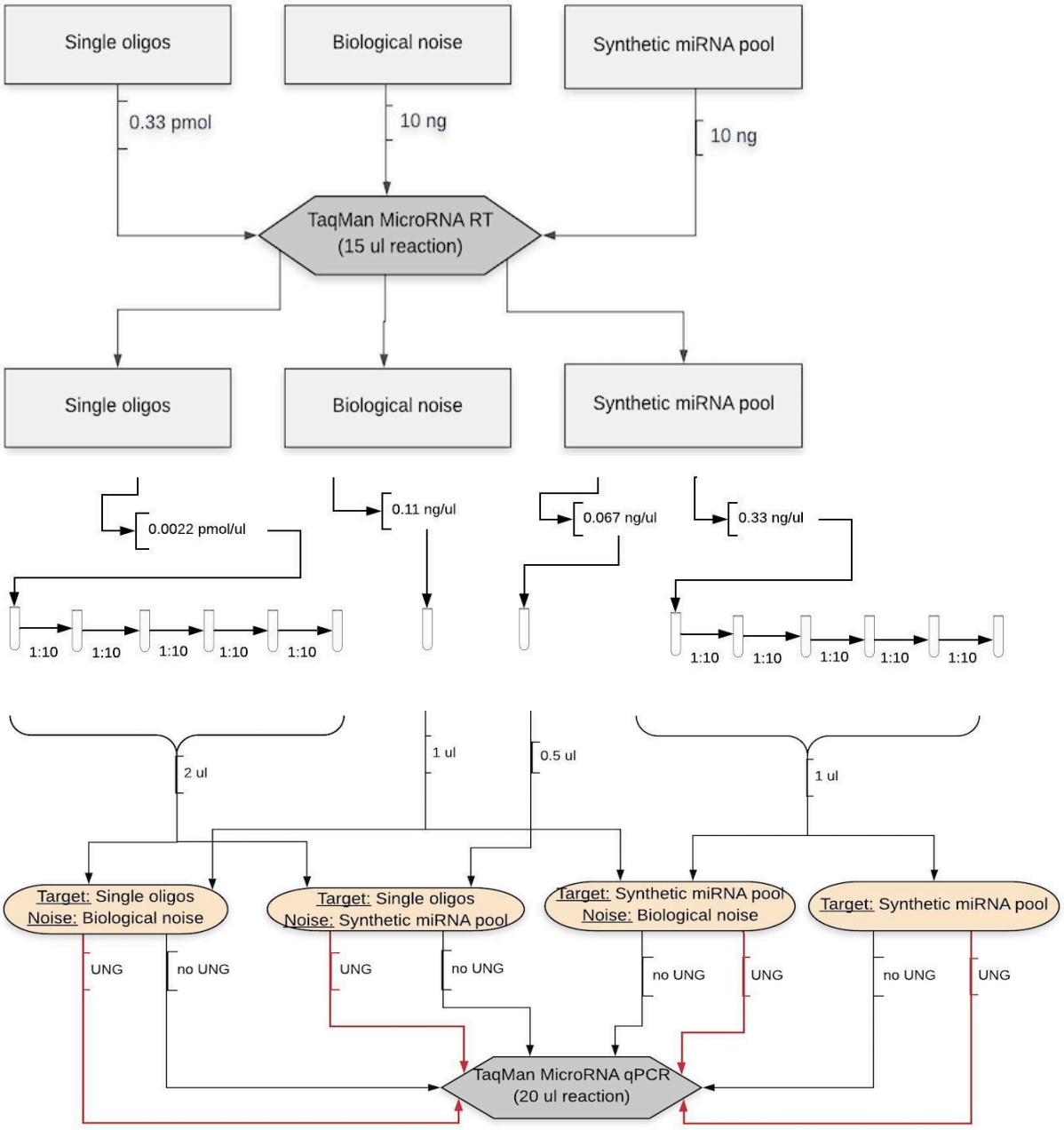

Figure 14: *The dilutions and input of the different steps for TaqMan MicroRNA RT-qPCR setup. The red lines show reactions containing master mix with UNG*

As input for the RT-reactions, 10 ng of the synthetic miRNA pool to create the dilution series, 10 ng of the synthetic miRNA pool to create synthetical noise, 0.33 pmol of each single oligo and 10 ng of the biological noise was added.

The RT was conducted by following the protocol and the temperature conditions are listed in Table 8.

Table 8: *The temperature conditions for cDNA synthesis for TaqMan MicroRNA RT-setup.*

Step	Time	Temperature
Start	30 min	16℃
Reverse transcriptions	30 min	42℃
Stop reaction	5 min	85℃
Storage	∞	4℃

After RT, the cDNA for the single oligos were diluted 1:10 and used to create the 10-fold dilution series of six points. The first point of the dilution series had a concentration of 0.0022 pmol/µl. Then these six concentrations were mixed together with either added biological noise or added synthetical noise from the synthetic miRNA pool as input for qPCR.

The cDNA for the biological noise was diluted 1:2 after RT, giving a concentration of 0.11 ng/µl. This dilution was added-together with each single oligos and the synthetic miRNA pool as input for qPCR. Further, the cDNA for the synthetic miRNA pool used for synthetical noise was diluted 1:10. This gave a concentration of 0.067 ng/µl, and this dilution was added together with each single oligos as input for qPCR.

The cDNA for the synthetic miRNA pool to create the dilution series was diluted 1:2, giving a concentration of 0.33 ng/µl. Then a 10-fold dilution series of six points were created, and the six concentrations were added as input for qPCR either alone or together with added biological noise.

The qPCR analysis was conducted by following protocol and the thermal cycling conditions are listed in Table 9. For the template mixtures containing UNG, activation of the UNG-enzyme occurs as the first qPCR step by 50°C incubation for 2 minutes.

Table 9: *The qPCR thermal cycling conditions for the TaqMan MicroRNA qPCR-setup.*

Step	Time	Temperature	Ramp rate	Cycles
UNG activation* *** Only needed when the master mix contain UNG**	2 min	50℃	Standard	1
Enzyme activation	10 min	95℃	Standard	1
Denature	15 sec	95℃	Standard	40
Anneal/Extend	60 sec	60℃	Standard	

4.4 Data analysis and statistics

As a result of the analysis, standard curves from all miRNAs from the different template mixtures were retrieved. For miRCURY RT-qPCR setup the melting curves for all template mixtures were also retrieved. This was done through QuantStudio 12K Flex System Software version 1.2.2 by Applied Biosystems (Thermo Fisher Scientific). This software gave a threshold cycle for the qPCR reaction, the standard deviation and the efficiency measure.

The threshold method used in this study was relative threshold, C_{rt}. The C_{rt} method sets a threshold in the exponential phase for each curve individually based on the shape of the amplification curve (Applied Biosystems, 2016). The C_{rt} method accounts for low reactions volumes and associated differences in fluorescence levels. The cycle where the amplification curve crossed the relative threshold (C_{rt}) is called the C_{rt} -value. C_{rt}-values at early cycles mean high amounts of detected signal. However, for detection at the earliest cycles this can lead to false positives as it makes it hard to distinguish the different signals. Therefore, the lowest accepted range for this study was chosen to start at the 10^{th} thermal cycle.

The standard deviation (SD) is the square root of the variance, and was calculated by this formula:

$$SD = \sqrt{\frac{\sum(x - \bar{x})^2}{n - 1}}$$

The x is the C_{rt} -value for the replicate, $\bar{x}$ is the mean C_{rt} -value for all replicates and n is the number of replicates. The SD that was chosen as acceptable between the five technical

replicates was 0.3. This is the same SD that will be further used to verify miRNA-findings from sequencing. For the five technical replicates at least three out of five replicates with SD ≤ 0.3 was acceptable.

The reaction efficiency was calculated by this formula (Bustin et al., 2009):

$$E = 10^{(-1/slope)} - 1$$

E is the amplification factor. If the standard curve has a slope of -3.32, this will give an amplification factor of 2. An amplification factor of 2 gives an optimal reaction efficiency of 100 %. If the reaction efficiency is 100 %, the template doubles after each thermal cycle during exponential amplification. An efficiency range of 90-110 % will give a slope lower than -3.5 and higher than -3.1 (Nolan, Hands, & Bustin, 2006). This is used as an acceptable range for practical purposes.

The data from QuantStudio 12K Flex System Software was downloaded to Microsoft Excel for Mac version 16.20 (181208). In Microsoft Excel the data from all runs were merged and sorted by different setups. The results were thereby loaded to R version 3.5.1 for data visualization and analysis. The miRNA secondary structure predictions were performed using the Vienna RNA cofold package (Lorenz et al., 2011).

5 Results

5.1 Determination of dilution series and amount of synthetical noise

To determine the range for the 10-fold dilution series for miRNAs represented by the synthetic miRNA pool for further use in the systematic evaluation of the RT-qPCR setups, the C_{rt}-values were evaluated (Figure 15).

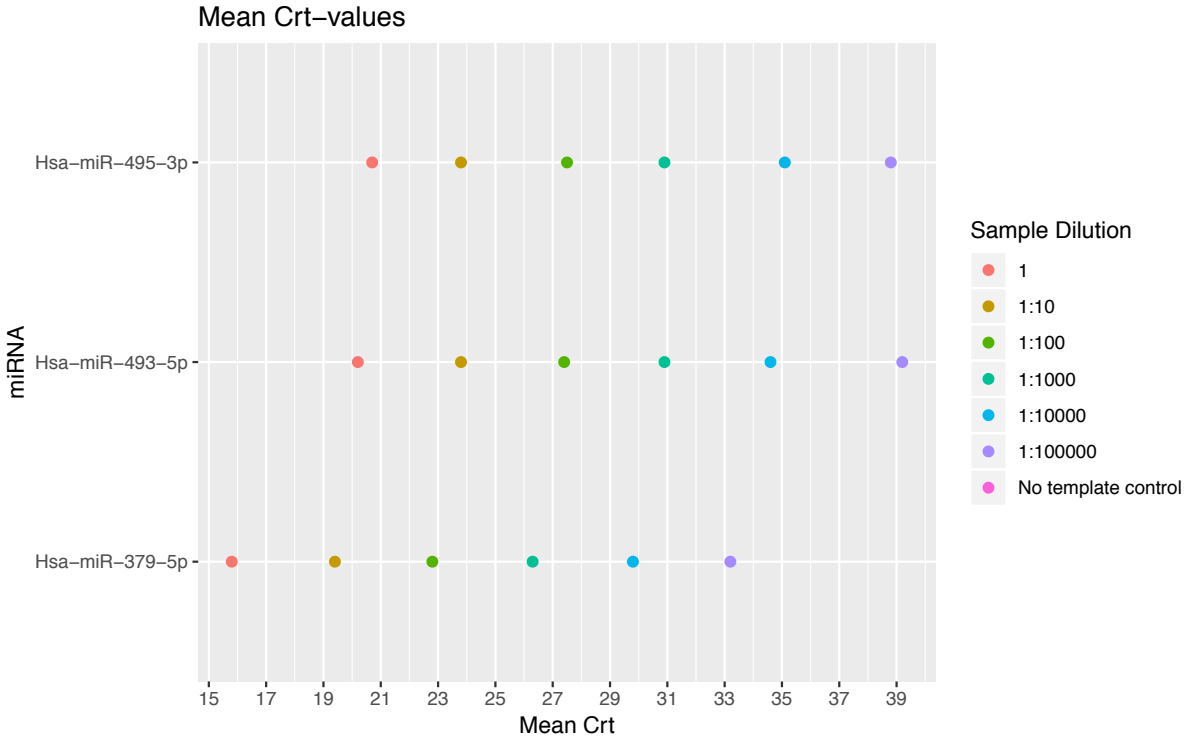

Figure 15: *The mean C_{rt}-value of the 10-fold dilution series for the miRNAs tested with miRCURY LNA RT-qPCR to determine the dilutions of the synthetic miRNA pool.*

All C_{rt}-values fell within the range of 10^{th} – 40^{th} thermal cycle and none of the no template controls showed any indications of detection of false positives. The standard curves also showed high linearity and correlation between the points of the dilution series, and no outliers were observed. Results showed that the range could be used to conduct the systematic evaluation of RT-qPCR setup.

To determine the amount of synthetic miRNA pool added as synthetical noise for further use in the systematic evaluation of the RT-qPCR setup, the efficiency measures for three tested amounts of synthetical noise were evaluated (Figure 16).

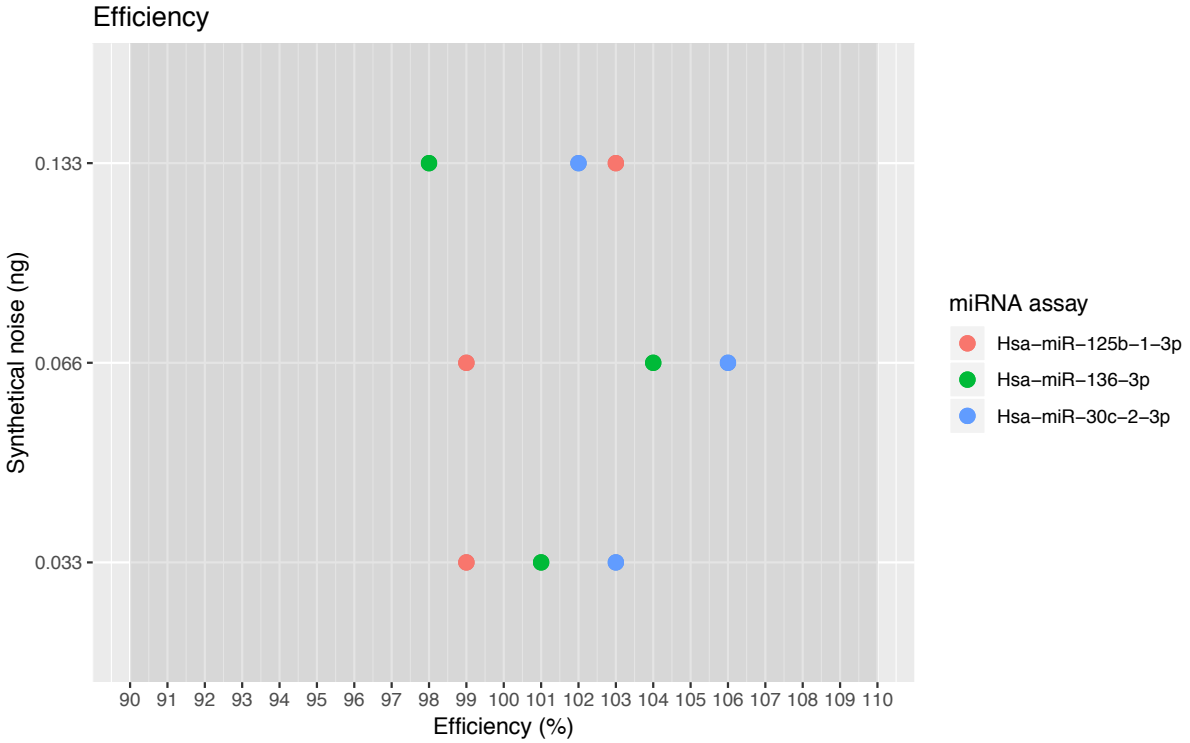

Figure 16: *The efficiency measures for the miRNAs and three different amounts of added synthetic miRNA pool tested with TaqMan MicroRNA RT-qPCR to determine the amount of synthetical noise.*

All efficiency measures were within the acceptable range 100 % ± 10 %. The efficiency measures only showed slight variation with different amounts of added synthetical noise. To reduce material costs, 0.033 ng of the synthetic miRNA pool was added as synthetical noise for further use in the systematic evaluation of RT-qPCR setup.

5.2 Results of the systematic evaluation of RT-qPCR setup

To determine the performance of miRCURY RT-qPCR setup, TaqMan Advanced RT-qPCR setup and MicroRNA RT-qPCR setup, the following parameters were evaluated and compared: (i) input of total RNA, (ii) detection range, (iii) efficiency, (iv) indication of false positives, (v) repeatability and (vi) C_{rt}-values. For the miRCURY RT-qPCR setup, the melting curves were also evaluated. Additionally, the laboratory procedure and price were compared.

5.2.1 Comparison of input and detection range

The input of total RNA for RT and the detection range of total RNA for the RT-reactions were compared for the three different setups (Table 10). The detection range were calculated

by using highest and lowest input of total RNA for the RT-reaction recommended by the provider, the dilutions listed in the protocols, and the maximum and minimum input of cDNA template for the qPCR-reactions.

The maximum input was listed in the providers protocols, while 0.5 µl was selected as minimum input. The minimum input of 0.5 µl was selected due to high pipetting variance for lower volume. The detection range for TaqMan Advanced RT-qPCR setup was only calculated for the reactions without miR-Amp, as the copy-number of cDNA in the material is unknown.

Table 10: *The recommended input of total RNA for the three different reverse transcription (RT) kit, the dilution after RT listed by protocols and the calculated detection range for each setup.*

	Input of total RNA for RT	**Dilution after RT**	**Minimum and maximum input for qPCR**	**Detection range for qPCR**
miRCURY RT-qPCR setup	10 pg – 200 ng	1:60	0.5 µl – 4 µl	0.0042 pg – 0.67 ng
TaqMan Advanced RT-qPCR setup, without miR-Amp	1 ng – 10 ng	1:10	0.5 µl – 9 µl	0.0017 ng – 3 ng
TaqMan MicroRNA RT-qPCR setup	1 ng – 10 ng	None	0.5 µl – 1.3 µl	0.033 ng – 0.89 ng

The detection range were calculated by using highest and lowest input of total RNA for the RT-reaction, the dilutions listed in the protocols, and the maximum input and selected minimum input of cDNA template for the qPCR-reactions.

Only the miRCURY RT-qPCR setup allowed input of total RNA < 1 ng and >10 ng. Calculated detection range showed that TaqMan Advanced RT-qPCR setup without miR-Amp, could detect the highest amount of total RNA (3 ng), while miRCURY RT-qPCR setup could detect the lowest amount of total RNA (0.0042 pg). The widest detection range was noted for TaqMan Advanced RT-qPCR setup without miR-Amp.

5.2.2 Efficiency

The efficiency measures were evaluated based on the standard curves (chapter 4.4 Data analysis and statistics) for all miRNAs assays both with synthetical or biological noise added from the different setups (Figure 17). The standard curves used for calculations can be found

in appendix (Appendix B). An efficiency of 100 % ± 10 % was the acceptable range and represented in the figure by the dark grey area.

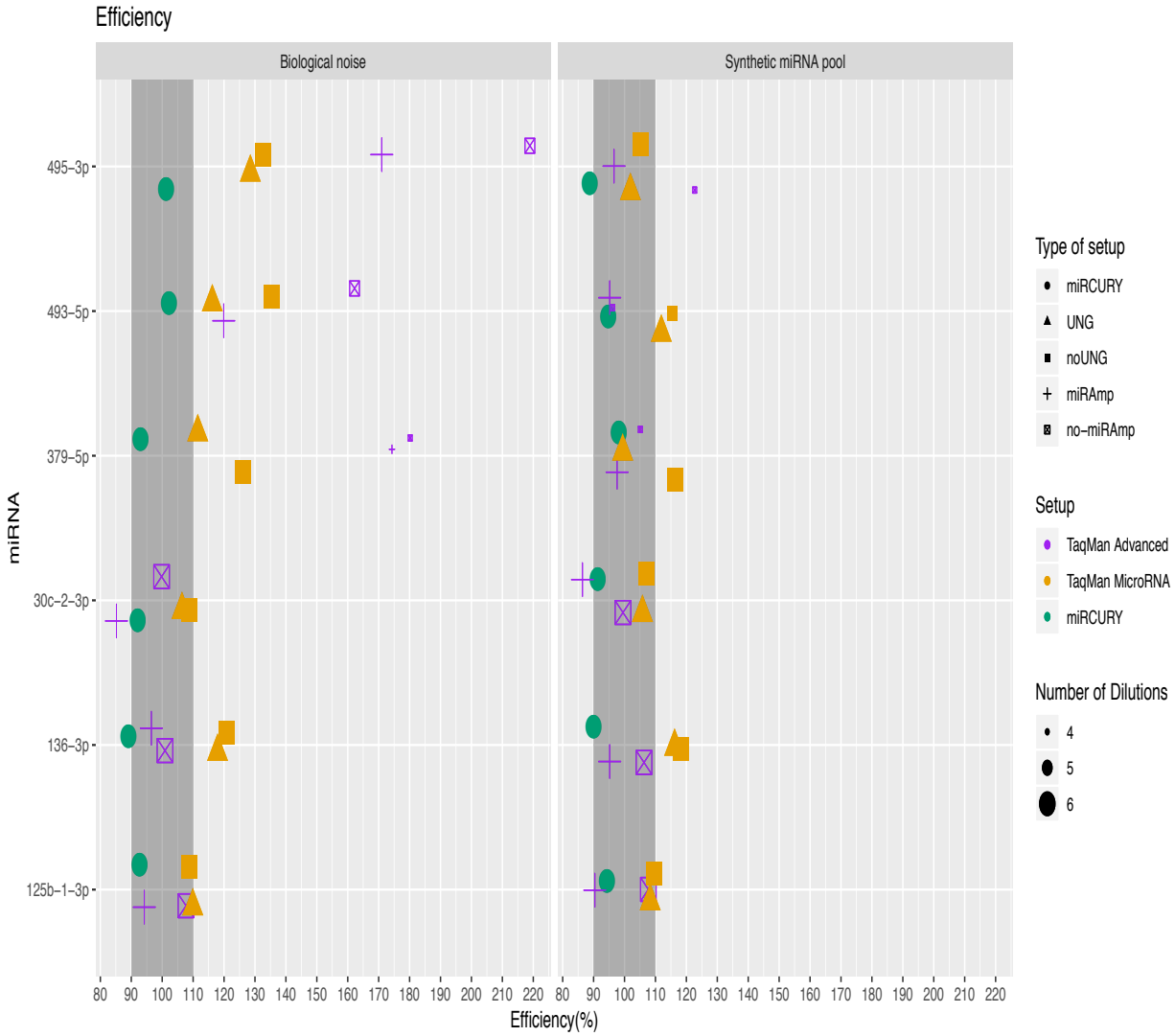

Figure 17: *The efficiency measures for all miRNAs with synthetic and biological noise from the three setups. The number of dilutions represent the number of dilutions points with at least one replicate with C_T-value between 10^{th}-40^{th} thermal cycle. The dark grey area represented the acceptable range efficiency.*

All calculated efficiency measures, the R^2 and the slope for the standard curves are listed in Table 11.

Table 11: *The measured efficiency (E), R^2 and slope for the standard curves of each template mixture for the five different type of setups.*

		With Biological noise			With Synthetic miRNA pool		
	Hsa-miR	**E (%)**	**R^2**	**Slope**	**E (%)**	**R^2**	**Slope**
miRCURY RT-qPCR Setup	**125b-1-3p**	93	1.00	-3.51	94	1.00	-3.47
	136-3p	89	1.00	-3.61	90	1.00	-3.59
	30c-2-3p	92	1.00	-3.53	91	1.00	-3.55
	379-5p	93	1.00	-3.52	98	1.00	-3.37
	493-5p	102	0.98	-3.27	95	0.99	-3.45
	495-3p	101	0.98	-3.29	89	0.99	-3.62
TaqMan Advanced RT-qPCR Setup, without miR-Amp	**125b-1-3p**	108	1.00	-3.15	108	1.00	-3.15
	136-3p	101	1.00	-3.30	106	0.99	-3.18
	30c-2-3p	100	1.00	-3.33	99	1.00	-3.34
	379-5p	180	0.88	-2.23	105	1.00	-3.21
	493-5p	162	0.87	-2.39	96	0.99	-3.42
	495-3p	219	0.88	-1.99	123	0.99	-2.88
TaqMan Advanced RT-qPCR Setup, with miR-Amp	**125b-1-3p**	94	1.00	-3.47	90	1.00	-3.58
	136-3p	96	1.00	-3.41	95	1.00	-3.44
	30c-2-3p	85	1.00	-3.74	86	1.00	-3.70
	379-5p	174	0.96	-2.28	98	1.00	-3.38
	493-5p	120	0.97	-2.92	95	1.00	-3.44
	495-3p	171	0.92	-2.31	97	1.00	-3.41
TaqMan MicroRNA RT-qPCR Setup, without UNG	**125b-1-3p**	109	1.00	-3.13	110	1.00	-3.11
	136-3p	121	0.98	-2.91	118	0.98	-2.95
	30c-2-3p	109	1.00	-3.13	107	1.00	-3.16
	379-5p	126	0.98	-2.82	116	0.99	-2.98
	493-5p	135	0.96	-2.69	116	0.94	-3.00
	495-3p	133	0.94	-2.73	105	0.96	-3.20
TaqMan MicroRNA RT-qPCR Setup, with UNG	**125b-1-3p**	110	1.00	-3.11	108	1.00	-3.14
	136-3p	118	0.98	-2.96	116	0.98	-2.99
	30c-2-3p	106	1.00	-3.18	106	1.00	-3.19
	379-5p	112	0.99	-3.07	99	0.98	-3.34
	493-5p	116	0.95	-2.99	112	0.95	-3.07
	495-3p	128	0.95	-2.79	102	0.96	-3.29

Samples with added biological noise showed more efficiency measures outside the acceptable range. Most of the samples with efficiency outside the acceptable range, both with biological- and synthetical noise, showed efficiency higher than 110 %. The setups for the miRNAs represented by the synthetic miRNA pool, hsa-miR-495-3p, hsa-miR-493-5p and hsa-miR-379-5p, with added biological noise showed the highest efficiency measures. The miRNAs

represented by the single oligos, hsa-miR-125b-1-3p, hsa-miR-136-3p and hsa-miR-30c-2-3p, did not show any notable difference in the efficiency measures for the setups with biological and synthetical noise added. All samples with an efficiency higher than 110 % were from the TaqMan Advanced RT-qPCR setup or the TaqMan MicroRNA RT-qPCR setups. The TaqMan Advanced RT-qPCR setup showed the most deviating and highest efficiency results, with measures over 150 %. However, TaqMan MicroRNA RT-qPCR setup had an increased number of efficiency measures outside the acceptable range. The miRCURY RT-qPCR setup generally showed lower efficiency as most of the samples were below 100 %.

The standard curves for the miRNAs represented by the synthetic miRNA pool, hsa-miR-495-3p, hsa-miR-493-5p and hsa-miR-379-5p, with added biological noise also showed the poorest linearity and correlation between the dilution points for all setups. In accordance, the poorest correlation between the dilution points was observed for the TaqMan Advanced RT-qPCR setup with the lowest R^2 values and slope.

The mean differences from 100 % efficiency of all miRNAs, with synthetical and biological noise, from the various setups were calculated as a comparison of the efficiency measures (Table 12).

Table 12: *The mean difference from 100 % for the efficiency measures for all miRNAs from the three different RT-qPCR setups.*

		Mean diff. from 100 %
miRCURY RT-qPCR Setup		
Biological noise		-5.0
Synthetic miRNA pool		-7.2
TaqMan Advanced RT-qPCR Setup		
Biological noise	no miR-Amp	45.0
Synthetic miRNA pool		6.2
Biological noise	miR-Amp	23.3
Synthetic miRNA pool		-6.5
TaqMan MicroRNA RT-qPCR Setup		
Biological noise	no UNG	22.2
Synthetic miRNA pool		12.0
Biological noise	with UNG	15.0
Synthetic miRNA pool		7.2

The mean difference from 100 % efficiency was higher for the miRNAs with added biological noise compared to synthetical noise, particularly for TaqMan Advanced RT-qPCR setup, but

also for TaqMan MicroRNA RT-qPCR setup. For the miRCURY RT-qPCR setup, the mean differences from 100 % efficiency was almost similar between miRNAs with synthetical noise and biological noise.

Including the miR-Amp reaction in the TaqMan Advanced RT-qPCR setup, somewhat lowered the mean differences from 100 % efficiency. The mean difference from 100 % efficiency for TaqMan Advanced RT-qPCR setup with miR-Amp reaction for samples with added synthetical noise, resulted in efficiency measures lower than 100 % for all miRNAs. Likewise, adding UNG in the master mix for the TaqMan MicroRNA RT-qPCR setup also resulted in a lower mean difference from 100 % efficiency than without UNG included in the master mix.

5.2.3 Secondary structure

The secondary structures and CG-content of the six miRNAs were compared (Figure 18). This was done to observe if similarities and dissimilarities in the secondary structures could possibly explain differences in specificity and reaction efficiency measures.

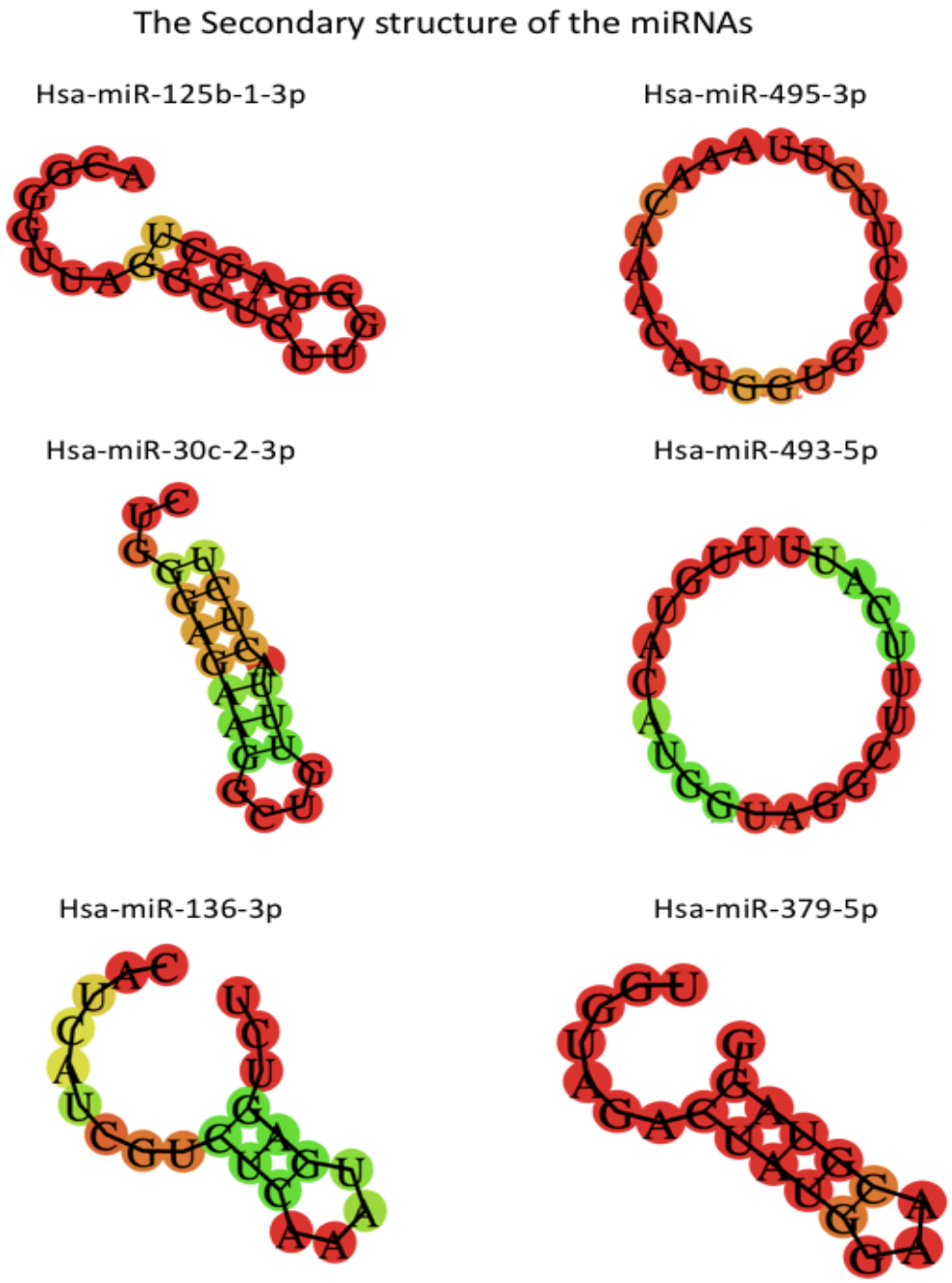

Figure 18: *The secondary structure for the miRNAs. The color represents the probability for base pairing, where red is the highest probability and green is the lowest. When the bases are not paired, the color represents the probability of being unpaired. The secondary structures are retrieved from Lorenz et al. (2011).*

The secondary structure showed that hsa-miR-136-3p, hsa-miR-125-1-3p, hsa-miR-30c-2-3p and hsa-miR-379-5p were folded in hairpin structures. The structures of hsa-miR-125-1-3p and hsa-miR-30c-3-3p revealed inaccessible 3'ends as they were predicted to complementary base pair with other regions of the miRNA. The predicted hairpin structure had the highest probability of occurring for hsa-miR-379-5p and hsa-miR-125-1-3p. The CG-content was highest for hsa-miR-125-1-3p, and lowest for hsa-miR-495-3p and hsa-miR-493-5p.

5.2.4 Indication of false positives in the negative controls

Two different types of negatives controls (without adding cDNA template or noise) were evaluated to see if the reagents in the RT-qPCR reactions could cause false positive results (Figure 19). The first type of control was used to evaluate the RT-reactions, and the second control was used to evaluate the qPCR-reactions. For both controls, triplicates of all assays were analyzed together with the different type of setups.

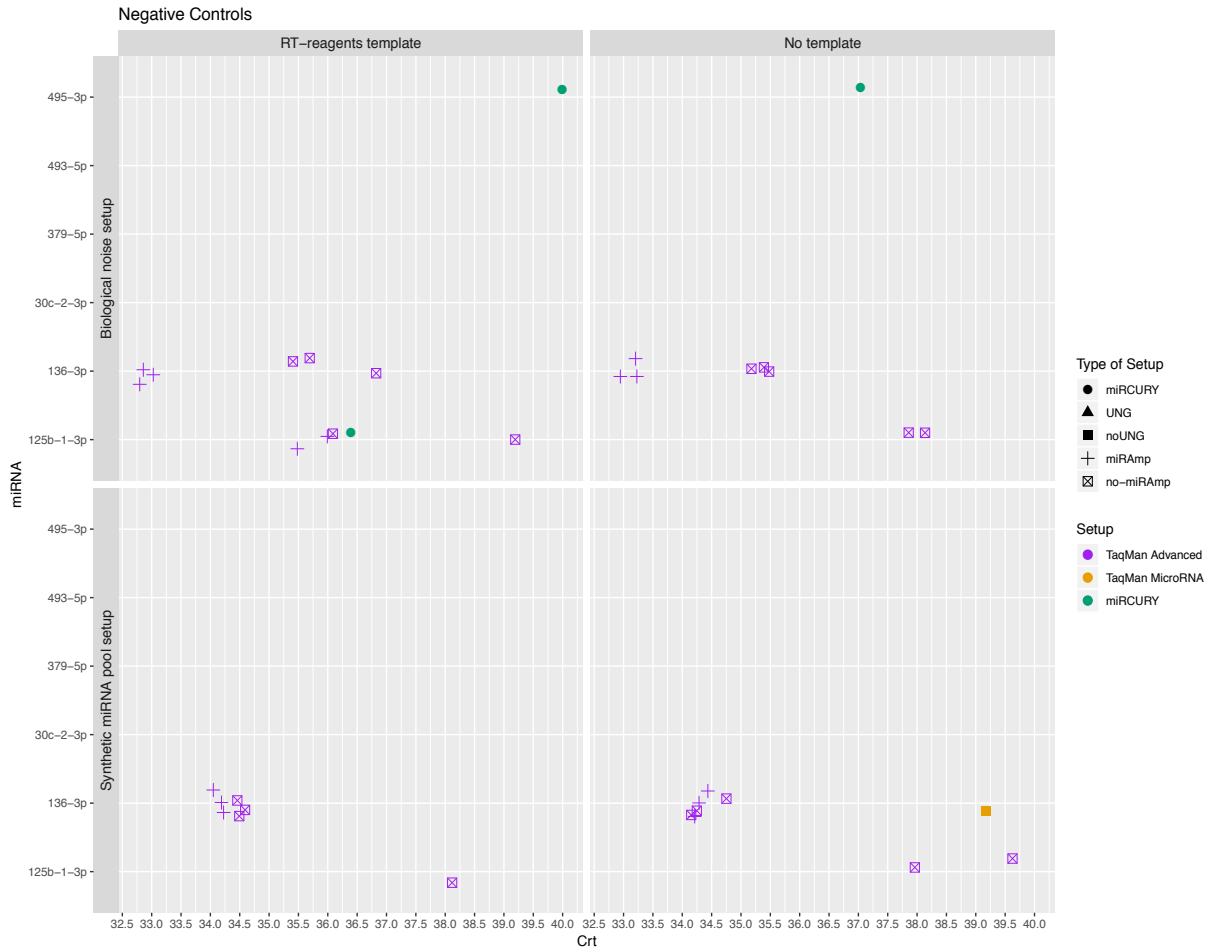

Figure 19: *The triplicates of negative controls consisting of RT-reagents as template and negative controls consisting of RNase free water as template (no template) for the different type of setups.*

For the negative controls where amplification had occurred, all C_{rt}-values were detected above cycle 32. The two assays, hsa-miR-136-3p and hsa-miR-125-1-3p, accounted for almost all negative controls with signs of false positive amplification. For the assay hsa-miR-495-3p from the miRCURY RT-qPCR setup, one replicate for each of the negative controls also had detectable C_{rt}-values. The negative controls for TaqMan Advanced RT-qPCR setup showed most signs of false positive amplification, with detected signals both for RT-reagents

template controls and no template controls for both setups. These controls also showed signs of amplification at the earliest cycle. The TaqMan Advanced RT-qPCR setup was also the only setup with more than one replicate showing signs of false positive for the controls. The standard curves (Appendix B) for TaqMan Advanced RT-qPCR setup for hsa-miR-136-3p and hsa-miR-125-1-3p both with biological and synthetical noise also showed an extra sample dilution point in the curves for the highest C_{rt}-values. This was most distinct for the samples with the miR-Amp reaction included, where the extra point in the standard curves was observed several C_{rt}-values higher than the last dilution point from the 10-fold dilution series. The extra point for the samples with the miR-Amp included also showed high linearity and correlation to the other points in the standard curves. This was not shown in the standard curves for any other assay or type of setups.

5.2.5 Melting curves for miRCURY RT-qPCR setup

For the miRCURY RT-qPCR setup, it was also generated a melting curve for each mixture of template, registering the meting temperature (T_m) for the template detected (Figure 20 and Figure 21). A melting curve gives an indication of any unspecific amplification in the qPCR-reaction.

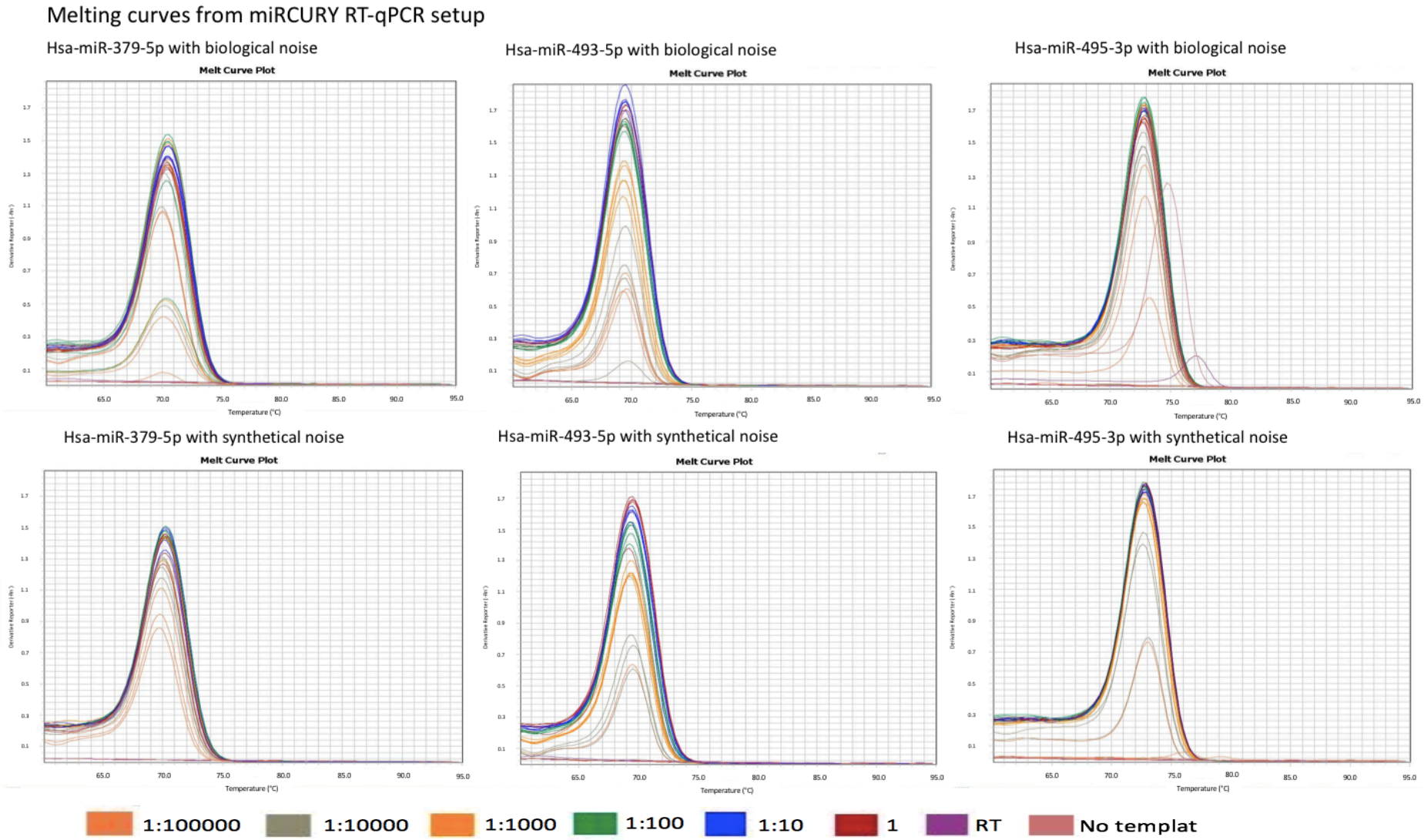

Figure 20: *The melting curve for miRNAs represented by the synthetic miRNA pool, hsa-miR-379-5p, hsa-miR-493-5p and hsa-miR-495-3p, with biological and synthetical noise for all samples dilutions and the two negative controls, RT-reagents template control (RT) and no template control.*

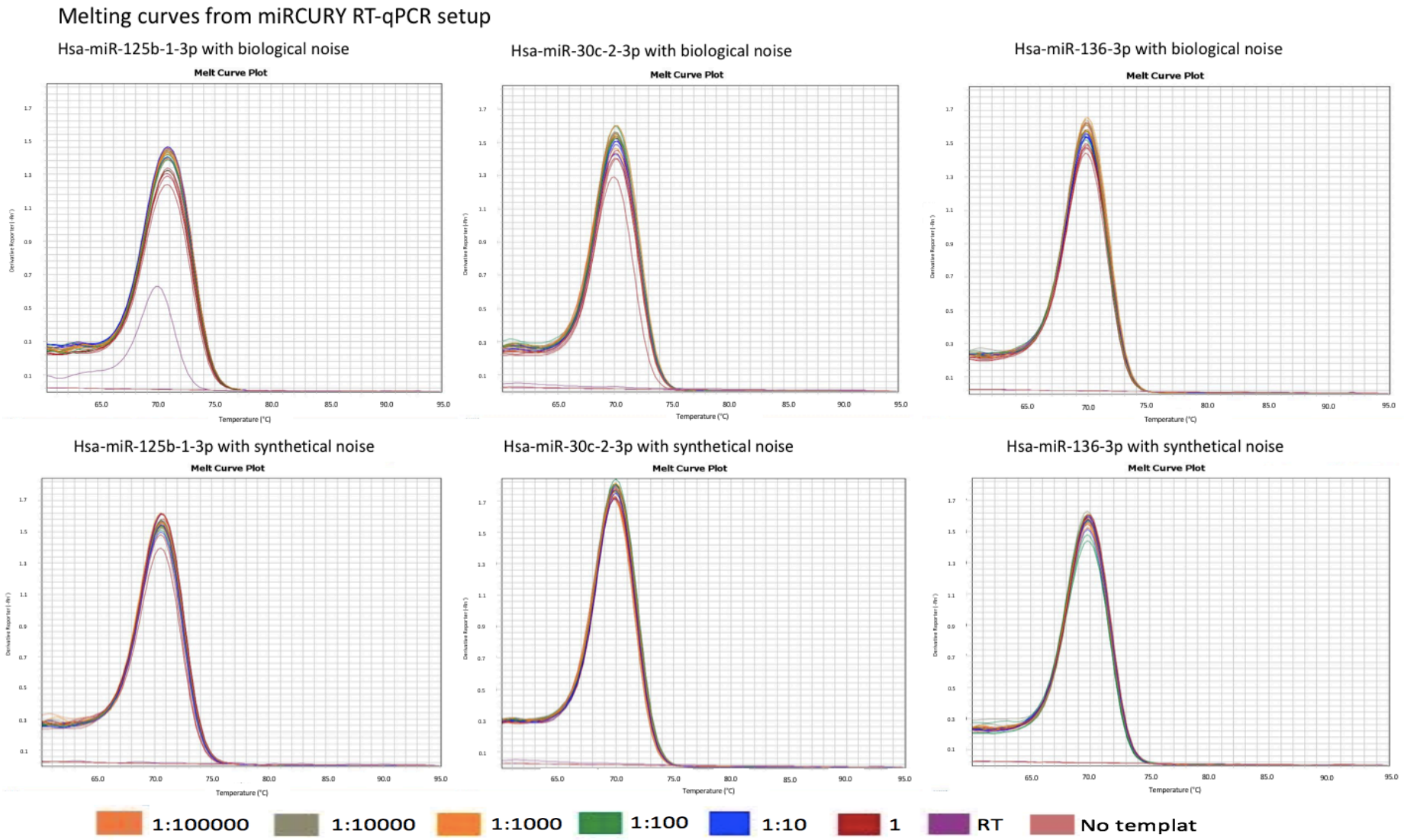

Figure 21: *The melting curve for miRNAs represented by the single oligos, hsa-miR-125b-1-3p, hsa-miR-136-3p and hsa-miR-30c-2-3p, with biological and synthetical noise for all samples dilutions and the two negative controls, RT-reagents template control (RT) and no template control..*

The melting curve for the miRNAs represented by the synthetic miRNA pool, hsa-miR-379-5p, hsa-miR-493-5p and hsa-miR-495-3p with biological noise and synthetical noise, showed that the T_m for the template detected was the same for all sample dilutions even though the lowest dilutions showed lower detected florescent. However, two distinct peaks were seen for the negative controls for hsa-miR-495-3p with biological noise. The RT-reagents template control seemed to contain an amplified product with T_m 77.1 °C, while the no template control seemed to contain an amplified product with T_m 74.8 °C. These T_m were higher than observed for the target template in the reaction for hsa-miR-495-3p, which was 72.1°C.

The melting curves for miRNAs represented by the single oligos, hsa-miR-125b-1-3p, hsa-miR-136-3p and hsa-miR-30c-2-3p with biological and synthetical noise, showed that the T_m for the template detected was the same for all sample dilutions. The detected florescence varied more for sample dilutions with added biological noise. One peak at 69.9 °C was observed for the RT-reagents template control for hsa-miR-125b-1-3p with biological noise. This T_m was somewhat lower than that observed for the target template for hsa-miR-125b-1-3p, which was 70.8 °C.

5.2.6 Repeatability

The repeatability, and thereby the precision was evaluated by the standard deviation (SD) between the five technical replicates. If the replicates were similar, the SD of their C_{rt}-values would be low and precision would be high. The acceptable SD between the five replicates was ≤ 0.3 (chapter 4.4 Data analysis and statistics). If the SD was higher than 0.3, the replicate with the largest difference from the mean C_{rt}-value was removed. This was continued until the SD was ≤ 0.3, and the number of remaining replicates was registered (Figure 22).

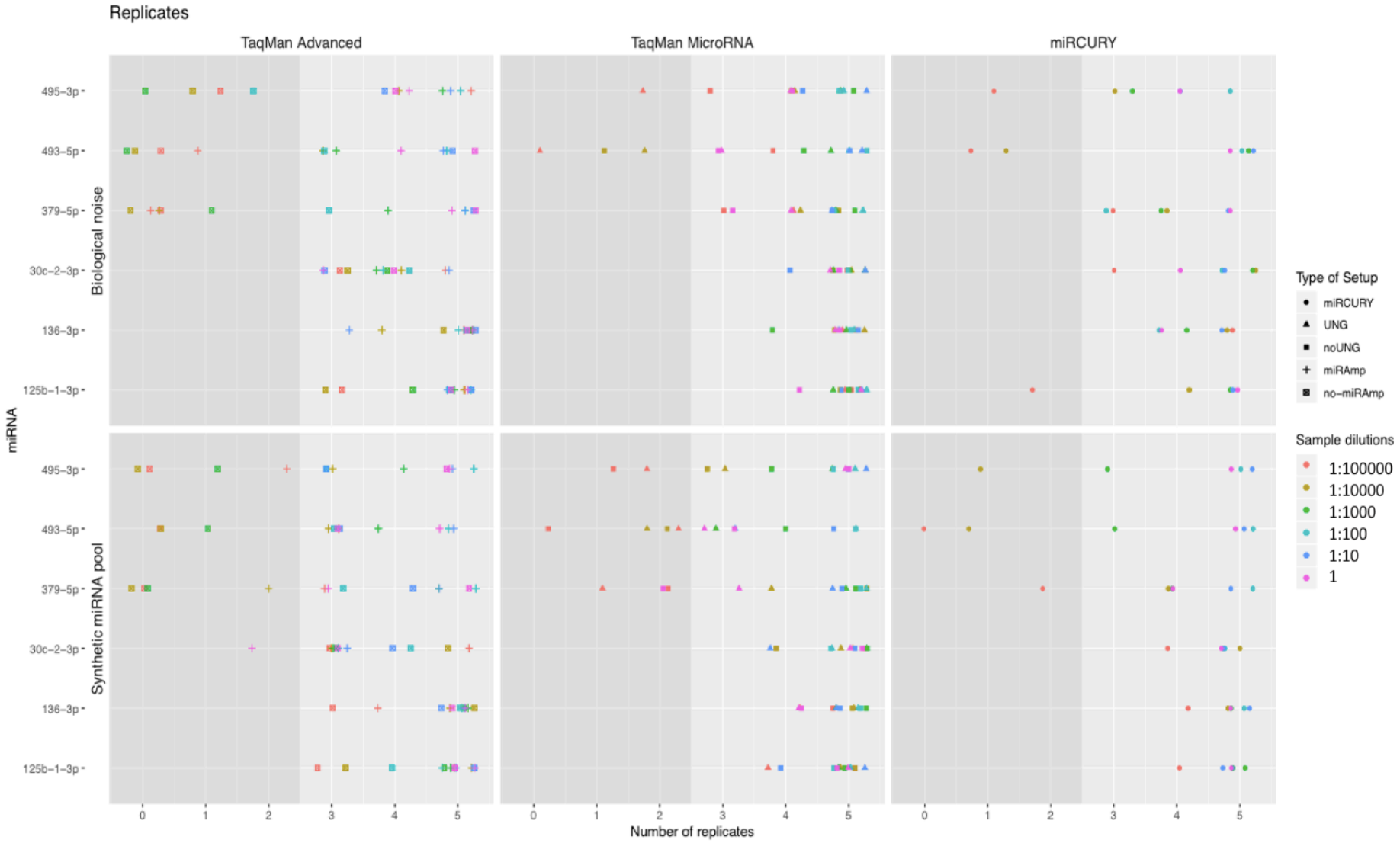

Figure 22: *The number of replicates for which the standard deviation (SD) was ≤ 0.3 for all miRNAs with biological and synthetical noise from the three different setups. The dark grey area represents the sample dilutions that did not have SD ≤ 0.3 for three or more replicates.*

Generally, high precision was observed, as most replicates obtained SD ≤ 0.3 with keeping at least three replicates for each sample dilutions. Most of the replicates with poorest precision were observed for the three lowest sample dilutions. No specific differences were seen for the samples with synthetical or biological noise added. The miRNAs represented by the synthetic miRNA pool, hsa-miR-495-3p, hsa-miR-493-5p and hsa-miR-379-5p, showed poorest precision.

The precision for samples with biological noise was highest for TaqMan MicroRNA RT-qPCR setup and lowest for TaqMan Advanced RT-qPCR setup. The precision for samples with synthetical noise was highest for miRCURY RT-qPCR setup and again lowest for TaqMan Advanced RT-qPCR setup. For TaqMan Advanced RT-qPCR setup, the poor precision was highly biased for samples without the miR-Amp reaction included. Master mix with or without UNG included for the TaqMan MicroRNA RT-qPCR setup did not seem to have any notable influence on the precision.

5.2.7 Comparison of C_{rt}-values

The C_{rt}-values of all miRNA with biological noise and synthetical noise for the three different setups were evaluated to obtain an overview of the detection range and the spread of the dilutions series (Figure 23). The accepted range for detection started at cycle 10, and the lowest C_{rt}-value where the negative controls showed amplification defined the accepted upper limit.

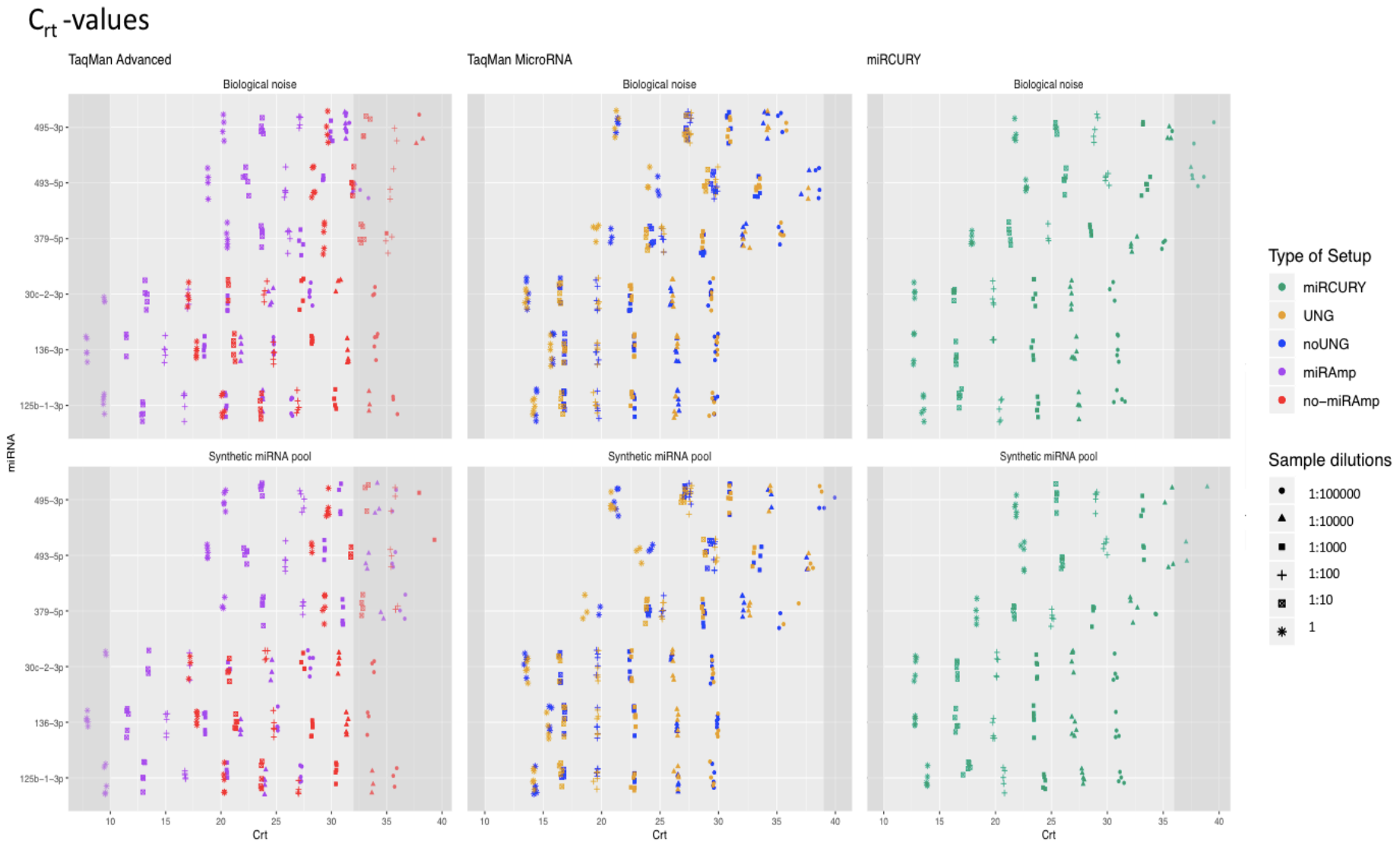

Figure 23: *The C_{rt} -values for all miRNAs with biological and synthetical noise for the three different setups. C_{rt} -values within the dark grey area are outside the accepted range and should not be taking into account.*

The C_{rt}-values did not show any clear difference between miRNAs with added biological noise or synthetical noise. The miRNAs represented by the synthetic miRNA pool, hsa-miR-495-3p, hsa-miR-493-5p and hsa-miR-379-5p, showed greatest variances in the replicates, particularly for the lowest sample dilutions. This was also registered for the results of repeatability (5.2.6 Repeatability), as well as in the standard curves (Appendix B). The standard curves showed that the lowest sample dilutions often ruined the linearity of the curves.

The C_{rt}-values showed distinct differences between samples without miR-Amp reaction and with miR-Amp reaction for TaqMan Advanced RT-qPCR setup. This was also observed in the standard curves (Appendix B), where curves generated for TaqMan Advanced RT-qPCR setup without miR-Amp reaction showed poorer linearity of the curves, than compared with TaqMan Advanced RT-qPCR setup with miR-Amp reaction. For TaqMan MicroRNA RT-qPCR setup, the C_{rt}-values showed no clear difference between UNG and no UNG included in the master mix. Sample dilutions with C_{rt}-values outside the accepted detection range of cycle 10 were only seen for the TaqMan Advanced RT-qPCR setup with miR-Amp. TaqMan Advanced RT-qPCR setup also had most sample dilutions outside the detection range where the negative controls showed amplification, mostly for samples without miR-Amp, which was also confirmed by the standard curves (Appendix B) with less detected sample dilutions for TaqMan Advanced RT-qPCR setup without the miR-Amp reaction.

The C_{rt}-values for the three setups cannot be compared directly due to different dilution steps after RT and the miR-Amp reaction for half of the samples from TaqMan Advanced RT-qPCR setup. To overcome this, the mean C_{rt}-values for 1:100, as chosen sample dilution, for all miRNAs were ranked from 1 to 6 for each of the different type of setups (Table 13). Ranking 1 represents the lowest C_{rt}-value, while ranking 6 represent the highest C_{rt}-value.

Table 13: *The rank of the mean C_{rt}-values for sample dilution 1:100, for all miRNAs with synthetical or biological noise for the different type of setups. Ranking 1 represents the lowest C_{rt}-value and ranking 6 represent the highest C_{rt}-value.*

Hsa-miR	miRCURY RT-qPCR Setup	TaqMan Advanced RT-qPCR Setup, no miR-Amp	TaqMan Advanced RT-qPCR Setup, with miR-Amp	TaqMan MicroRNA RT-qPCR Setup, no UNG	TaqMan MicroRNA RT-qPCR Setup, with UNG
With Biological noise					
125b-1-3p	3	3	2	3	1
136-3p	2	2	1	2	2
30c-2-3p	1	1	3	1	3
379-5p	4	4	5	4	4
493-5p	5	5	4	6	6
495-3p	6	6	6	5	5
With Synthetic miRNA pool					
125b-1-3p	3	3	2	1	1
136-3p	1	2	1	3	2
30c-2-3p	2	1	3	2	3
379-5p	4	6	6	4	4
493-5p	6	4	4	6	6
495-3p	5	5	5	5	5

The mean C_{rt}-values for the three miRNAs represented by single oligos, hsa-miR-125b-1-3p, hsa-miR-136-3p and hsa-miR-30c-2-3p, had always lower C_{rt}-values than the miRNAs represented by the synthetic miRNA pool, hsa-miR-379-5p, hsa-miR-493-5p and hsa-miR-495-3p.

All five of the different type of setups showed differences in the ranking of the mean C_{rt}-values. Results showed differences in mean C_{rt}-values between samples with added biological or synthetical noise for all type of setups, except TaqMan MicroRNA RT-qPCR setup with UNG. Differences were also seen in mean C_{rt}-values within the same setup, for samples with or without miR-Amp reaction for TaqMan Advanced RT-qPCR setup and samples with or without UNG included for TaqMan MicroRNA RT-qPCR setup.

5.2.8 Comparison of laboratory procedure and price

Another important consideration for the evaluation of different RT-qPCR setups are practical factors such as preparation in the laboratory, time (both for the entire process and hands on time), price per reaction and cost of the setups.

The estimated time was calculated only by the reaction-time and not by taking into account the time of any preparations. The price per reaction was calculated for use of one reaction for one target, and the cost efficiency was calculated by accounting for the maximum number of reactions that one RT could generate (Table 14).

Table 14: *The estimated time in laboratory calculated by time of reactions, calculated price per reaction for use of one reaction for one target in Norwegian kroner (NOK), and the cost efficiency for maximum reactions from one RT-reaction in Norwegian kroner (NOK).*

	Estimated time	**Price per reaction (NOK)**	**Cost efficiency (NOK)**
miRCURY RT-qPCR setup	3 hours and 30 minutes	64.9	14.2
TaqMan Advanced RT-qPCR setup	3 hours	56.7	16.4
TaqMan MicroRNA RT-qPCR setup *** For master mix with UNG**	2 hours	55.8 56.6*	29.3 30.3*

The estimated time was the longest for miRCURY RT-qPCR setup, in addition the price per reaction was the highest, but the cost efficiency was the lowest. The TaqMan MicroRNA RT-qPCR setup had the shortest estimated time and the lowest price per reaction, but highest cost efficiency.

The laboratory procedure was evaluated by personal experience and observations of the preparation in laboratory. None of the setups had any bias due to previously experience. One observation was the inconvenience of separate reactions for the RT-reaction for TaqMan Advanced RT setup. The inconvenience was caused by longer preparation time and multiple pipetting steps, causing the longest hands on time of the different setups. Another notedly observation was the need for more reagents and dead volume for the miRCURY qPCR-reactions setup. The protocol stated that one should account for 10 % greater volume than required, but experience showed that about 40 % greater volume of the reactions mix was

sufficient. This was due to bobbles in the reaction mix which caused problems during pipetting. A longer preparation time for TaqMan MicroRNA RT-reactions was also observed. This was caused by the need for preparation of more reactions as the RT was specific to each target.

5.2.9 Overall performance scores

To summarize the result from the systematic evaluation, the different RT-qPCR setups were scored from 5 (best) to 1 (poorest) for the different evaluated parameters (Figure 24).

The precision score was based on the number of sample dilutions with SD > 0.3 for all miRNA-assays with both biological and synthetical noise. The efficiency score was based on the lowest mean difference from 100 % efficiency for all miRNA-assays with both biological and synthetical noise. The feasibility was scored based on the personal experience and observations of the preparation in laboratory, by taking into account the time (both for the entire process and hands on time), number of pipetting steps and separate reactions, and by the practicability of the protocols. The false positives score was based on the number of replicates that had shown amplification for both negative controls analyzed with all miRNA-assay for both biological and synthetical noise setup. The price score was based on lowest price per reaction, and the cost efficiency was based on lowest price for calculated cost efficiency. The calculated detection score was based on the lowest calculated detection range. For TaqMan Advanced RT-qPCR setup only the calculated detection for the samples without the miR-Amp reaction was calculated. The observed detection score was based on linearity and correlation of the sample dilutions for the standard curves (Appendix B).

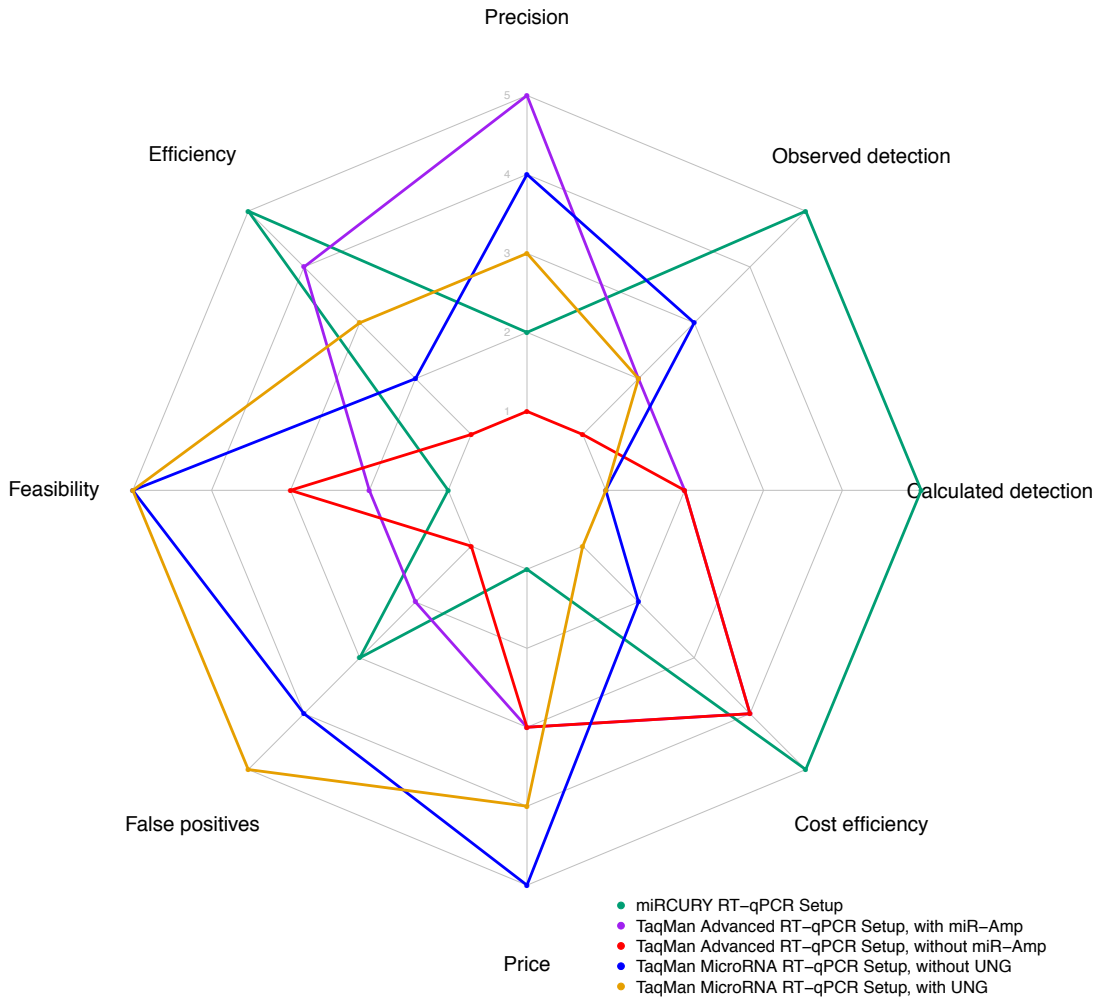

Figure 24: *The score for the different type of setups based on precision, efficiency, feasibility, false positives, price, cost efficiency, calculated detection and observed detection. The best score is indicated by 5 and the poorest score by 1.*

The miRCURY RT-qPCR setup showed best results with the highest score for efficiency, cost efficiency and calculated and observed detection. The TaqMan Advanced RT-qPCR setup without the miR-Amp reaction showed poorest results with the lowest score for precision, efficiency, false positives and observed detection. For the TaqMan MicroRNA RT-qPCR setup with and without UNG included in the master mix, the results showed slight difference. The precision, price, cost efficiency and observed detection score were higher for the TaqMan MicroRNA RT-qPCR setup without UNG, however the efficiency and false positives were lower than compared to TaqMan MicroRNA RT-qPCR setup with UNG included in the master mix.

6 Discussion

In this study the performance of miRCURY RT-qPCR setup, TaqMan Advanced RT-qPCR setup and TaqMan MicroRNA RT-qPCR setup for detecting miRNAs were evaluated. For the TaqMan Advanced RT-qPCR setup it was also tested if the preamplification reaction, miR-Amp, was necessary to achieve reliable results. Additionally, for the TaqMan MicroRNA setup, two different master mixes were tested, one with and one without uracil-N glycosylase (UNG), an enzyme which prevents contamination caused by carryover. To conduct this, synthetic material from a synthetic miRNA pool and single oligos represented six miRNAs. The different template was also analyzed together with biological noise and together with synthetical noise established from the synthetic miRNA pool.

Previous studies have shown that different platforms for detection of miRNAs show varying results (Git et al., 2010; Leshkowitz, Horn-Saban, Parmet, & Feldmesser, 2013; Wang et al., 2011), this have also been observed for detection by use of different RT-qPCR technologies (Mestdagh et al., 2014; Redshaw et al., 2013). The observations of varying results by use of different RT-qPCR technologies for detection of miRNAs have also been supported by the work in this study.

6.1 Reaction efficiencies

In this study, the majority of the template mixtures for the different setups had measured reaction efficiency within the acceptable range of 100 ± 10 %, and the miRCURY RT-qPCR setup showed least deviation in the reaction efficiency. The efficiency measures are an important indicator of the amplification in the qPCR-reaction and are calculated by using the standard curves. When the template in the reaction doubles after each thermal cycle during exponential amplification, the reaction will have an efficiency of 100 %. However, a variety of factors may influence the amplification.

Most of the samples that did not have an efficiency within the acceptable range, had efficiency measures higher than 110 %. Efficiency higher than 100 % may indicate presence of PCR-inhibitors (Cepin, 2017). To test if inhibitors are present, samples should be diluted before rerunning the reactions. In this study, if PCR-inhibitors were presents, it may have been enhanced by excessive amounts of template, as the miRCURY RT-qPCR setup included

the highest dilution of cDNA after RT and also resulted in lower efficiency measures, that were within the acceptable range.

Least deviation in efficiency measures for the miRCURY RT-qPCR setup may also be reasoned by the fact that these components were used to determine the dilutions series for conducting the systematic evaluation. As the miRCURY RT-qPCR setup was used for this, the detection range selected for the evaluation might have been set at a lower range than if the other kits had been used. The calculated detection range, both for TaqMan Advanced and TaqMan MicroRNA RT-qPCR setup, indicates that these setups would probably have performed better for a dilution series with higher concentrations. However, the detection range for TaqMan Advanced RT-qPCR setup including the preamplification reaction, miR-Amp, was not calculated as the copy number of cDNA in the starting material was unknown. It was, however, expected that TaqMan Advanced RT-qPCR setup with the miR-Amp reaction would perform better for low detection range, yet outlying points for the highly diluted samples observed in the standard curves, do not meet these expectations. Additionally, evaluating the performance of the different setups for low concentrations was also the most critical, because when detecting highly expressed miRNAs, the samples can easily be diluted before the qPCR-reaction. On the other hand, samples with lowly expressed miRNAs, are not easily up-concentrated, and up-concentration might also increase the amounts of PCR inhibitors.

It was also observed that adding biological noise generally lead to increased efficiency measures outside the acceptable range, this may indicate PCR-inhibitors in the pool of biological material used as biological noise. The PCR-inhibitors could be derived during RNA isolation of the biological material. The reagents from the isolation-step can cause interference in the RT-reaction, leading to inhibitors in the qPCR-reaction. Poor integrity values of RNA may not directly work as qPCR-inhibitors, however it can make it hard to synthesis cDNA because of interference by short degraded RNA-sequences in the sample. Notably, the RNA had integrity values above 8.5 (data not shown) for all three samples pooled and added as biological noise for this study. This has been tested to be high enough integrity values for detection of miRNAs (Ibberson, Benes, Muckenthaler, & Castoldi, 2009). Interestingly, the miRNA represented by single oligos did not show notably increased efficiency measures when adding biological noise, this may be due to the ratio of target miRNAs and the added noise. The amount of each single oligos may have been so high that

the impact of added biological noise may not have been notable in these reactions. To test this hypothesis, higher amounts of biological noise should also have been tested. It would also be interesting to analyse the biological material alone, as all six miRNAs tested was expected to be present in this material. Nevertheless, C_{rt}-values did not show any clear differences for samples with added biological noise. However, this is most likely caused by the low expression of these miRNAs in the material added as biological noise.

High efficiency for the qPCR-reaction may also be caused by other factors like pipetting errors, inaccurate dilution series or unspecific products in the reactions (Cepin, 2017). Unspecific products, like primer-dimers, in the reactions cannot be excluded as the negative controls showed amplification signals for the latest cycles for some assays for all setups. Indication of unspecific products in some of the reactions, was also confirmed by the melting curves for miRCURY RT-qPCR setup. In accordance, the negative controls for TaqMan Advanced RT-qPCR setup most clearly indicated false positives or unspecific amplification as well as the efficiency results showed the highest deviations from optimal efficiency of 100 %. High efficiency due to pipetting errors can neither be excluded, and the TaqMan Advanced RT-reaction set up included more pipetting steps, compared to the other protocols, due to multiple reactions for RT. This can increase the chance of potential pipetting errors and carry-over material causing PCR-inhibition. Also, possible experimental bias of variations due to preamplification reactions, as the miR-Amp reaction for TaqMan Advanced RT-qPCR setup, has been found with other PCR-detection technologies (Sanders et al., 2011). In this current study, it seemed like TaqMan Advanced RT-qPCR setup with preamplification by the miR-Amp reaction resulted in lower average efficiency from optimal, compared to samples without the miR-Amp reaction.

Even though the TaqMan Advanced RT-qPCR setup showed the highest deviating efficiency measures, TaqMan MicroRNA RT-qPCR setup showed a higher number of measures outside the acceptable range. The most notable difference of the TaqMan MicroRNA RT-qPCR setup is the use of miRNA-specific stem-loop RT-primers. The miRNA-specific RT-primers gives a more specific cDNA-synthesis as the primers are designed specifically to the sequence of the target miRNA, including being more stable due to the double stranded sections (Chen et al., 2005). Still, it has been reported that presence of different 3′ isomiR species of a particular miRNA can be reverse transcribed leading to false positive results by use of stem-loop primers (Schamberger & Orbán, 2014). When UNG was included in the master mix for

samples from TaqMan MicroRNA RT-qPCR setup, slightly improved efficiency measures were observed compared to the samples without UNG included in the master mix. However, most of the samples were still above the acceptable range. UNG prevents contamination by carryover in the qPCR-reaction, and results in this study support that this may lead to reaction efficiency closer to optimal exponential amplification.

Secondary structures and GC-content may as well influence the efficiency (Singh, Govindarajan, Naik, & Kumar, 2000). The secondary structures for several miRNAs showed hairpin structures. Hairpin structures and high GC-content may cause problems when detecting miRNAs due to higher T_m. The suppression effects of hairpin structures are mostly caused by competitive inhibition of primers binding to the template (Fan, Wang, Komiyama, & Liang, 2019). Nevertheless, the miRNAs with predicted hairpin structures did not seem to explain any notable difference in the efficiency measures in this study. However, for the miRNAs represented by the synthetic miRNA pool it was expected to observe C_{rt}-values at the same cycle, since the synthetic miRNA pool was equimolar and hence the input was identical. Interestingly, all setups showed differences in the C_{rt}-values for the three miRNAs represented by the synthetic miRNA pool. The observation was most notable with higher C_{rt}-values for hsa-miR-379-5p for the miRCURY RT-qPCR setup. This means that something may have inhibited the amplification of hsa-miR-493-5p and hsa-miR-495-3p to a greater extent than for hsa-miR-379-5p. This observation was not expected, as the secondary structures for hsa-miR-493-5p and hsa-miR-495-3p showed an open structure and lower GC-content.

In the standard curves used to calculate the reaction efficiency, it was observed notable differences in the linearity and poorer correlation for the highly diluted samples. This was especially true for the miRNAs represented by the synthetic miRNA pool, hsa-miR-379-5p, hsa-miR-493-5p and hsa-miR-495-3p. Reaction efficiency closer to optimal could have been observed by removing the points hampering the linearity of the standard curves. However, if the standard curves did not show specific outliers, optimization of the reaction efficiency is not always possible as it also may be caused be poor enzyme-efficiency in the reaction. For comparison of differentially expressed miRNAs, it is therefore important to take into account the measured difference of reaction efficiency.

Similar to this study, Redshaw et al. (2013) compared two different RT-qPCR technologies, TaqMan miRNA assays provided by Life Technologies (now provided by Thermo Fisher Scientific) and miRCURY LNA Universal RT microRNA PCR assay provided by Exiqon (now provided by Qiagen). Results from that study observed similar efficiency measures for the two assays compared, but noted that miRCURY LNA Universal RT microRNA PCR assay resulted in more variable measurements (Redshaw et al., 2013). Result from this current study, however, indicated higher efficiency measures for the TaqMan MicroRNA RT-qPCR setup with use of similar TaqMan miRNA assays, than for the miRCURY RT-qPCR setup with use of similar miRCURY LNA Universal RT microRNA PCR assays. It is unknown whether, and which, components may differ in the kits tested by the previous and current study.

6.2 Differences in repeatability

The mirQC study by Mestdagh et al. (2014) demonstrated differences in performance of different methods for hybridization, RNA-sequencing and RT-qPCR for miRNA detection. They reported that the most variation was seen for the RT-qPCR platform based on reproducibility and specificity (Mestdagh et al., 2014).

In our study the repeatability was evaluated by the standard deviation of the technical replicates. Results showed poorest precision for the lowest dilutions. This can indicate that when miRNAs are lowly expressed the repeatability decreases. This may be problematic for detecting lowly expressed miRNAs as the capacity to distinguish small expression changes requires high precision (Mestdagh et al., 2014). Poor precision for the lowest dilutions was true for all setups, however, the number of sample dilutions with SD > 0.3 was notably higher for TaqMan Advanced RT-qPCR setup without the miR-Amp reaction. The TaqMan Advanced RT-qPCR setup with the miR-Amp reaction did show highest precision, however the difference in number of sample dilutions with SD > 0.3 for the other setups were small.

Redshaw et al. (2013) noted that TaqMan miRNA assays showed lower average standard deviation between replicates compared to miRCURY LNA Universal RT microRNA PCR assay, although the differences were not statistically significant (Redshaw et al., 2013). The repeatability of the five technical replicates in this study, may support this as it showed that miRCURY RT-qPCR setup had one and two more sample dilution with SD > 0.3, than

TaqMan MicroRNA RT-qPCR setup without and with UNG included in the master mix, respectively. However, both setups struggled with the two lowest samples dilutions for several miRNA assays.

As it was shown that the TaqMan Advanced RT-qPCR setup without the miR-Amp reaction resulted in lower precision for samples with both biological and synthetical noise, this indicates that low copy number of target miRNA decreases the repeatability. This show that TaqMan Advanced RT-qPCR setup without including the preamplification by miR-Amp, should not be used for detection of lowly expressed miRNAs, as this requires high precision.

6.3 Indications of false positives and unspecific amplification

In order to ensure specific detection of target miRNA without any false positives and unspecific amplification, the negative controls were expected to not show any amplification.

For the miRCURY RT-qPCR setup the melting curves are an advantage as the detection method may be less specific due to the use of SYBR green I, which intercalate between bases of all double-stranded DNA. The melting curve analysis revealed unspecific amplification for the negative controls for hsa-miR-495-3p and hsa-miR-125b-1-3p with biological noise. Similar results can also be seen by detected C_{rt}-values of the negative controls. In addition, as the miRCURY qPCR-primers were optimized with LNA molecules which increases the melting temperature (Kauppinen et al., 2005), an interesting further analysis would be to compare the measured T_m of the target by use of the melting curve analysis with the theoretical T_m including the incorporated LNA. However, this was not possible as the LNA primer sequences were unknown.

One possible reason for false positive reactions is primer-dimers. Primer-dimers are caused by primers in the reaction that bind to each other and then are detected as template. Primer-dimers will often have different T_m than the target-template in a samples, due to differences in the length. However, the T_m of the template in the reactions was only evaluated by the melting curves for miRCURY RT-qPCR setup. Primer-dimers cannot be excluded as reason for the unspecific amplifications in the negative controls for the other setups. However, as all assays used in this study were commercially fabricated by different providers, the sequences of the primers are unknown. This makes it difficult to predict the primers behavior and

calculate their T_m. If primer-dimers occur, they may decrease the detected C_{rt}-value also for samples containing template, making quantitation and comparison of C_{rt}-values for different targets in the same sample difficult.

All RT-qPCR setups showed amplification of the negative controls. The indications of false positive signal in the reactions were especially biased for two assays, hsa-miR-136-3p and hsa-miR-125-1-3p. However, one replicate for hsa-miR-495-3p for both negative controls was also seen for miRCURY RT-qPCR setup. The bias towards some assays can indicate that some primer sequences are more prone to create primer-dimers, but also that this is dependent on the chemistry of each setup. Even though all RT-qPCR setups detected signal from the negative controls, TaqMan Advanced RT-qPCR setup performed notably worse as it was the only setup to show signals for more than one of the three replicates. This was an indication that something in the reagents created false positives, both for the RT-reagents and qPCR-assays. This may be caused by contamination of template in the samples by pipetting errors, however it could also indicate formation of primer-dimers. Nevertheless, this should be kept in mind when detecting miRNA in biological samples.

Although the false positive signals were detected at late thermal cycles, this may cause problems when detecting miRNAs in biological material where the expression of target is unknown. For detection of biological material, samples with C_{rt}-values 5 cycles or closer to where negative controls show signal, should not be taking into account. This is to clearly distinguish target and possible false positives (Bustin et al., 2009). The observations in this study clearly show the importance of controlling for false positives by incorporating negative controls for every RT-qPCR reaction.

6.4 Practical factors

TaqMan MicroRNA RT-qPCR setup had the lowest price per reaction when use of one reaction for one target miRNA. Importantly, this does not represent the price per samples used in laboratory procedures for conducting miRNA detection. For testing true biological samples, often several miRNA targets and assays may be performed on the same sample. In addition, three or more replicates are advantageous for statistical analyzes. By using TaqMan MicroRNA RT-qPCR setup, each miRNA target requires a separate RT-reaction due to the miRNA specific stem-loop primers. This will increase the cost, as well as the bias of the

different miRNA-target as they are not reverse transcribed in the same reaction. In most cases, the universal RT-reactions for TaqMan Advanced RT-qPCR setup and miRCURY RT-qPCR setup will be advantageous by the need of only one RT-reaction per sample, which thereafter can be used for detecting several miRNAs. This will again lower the overall cost and be more convenient for preparation in the laboratory.

Personal experience of the laboratory preparations noted that for the miRCURY RT-qPCR setup more reaction mix than claimed in the provider's protocol was required. This might again lead to higher costs than calculated theoretically. Nevertheless, the miRCURY RT-qPCR setup gives advantages by the wide range of input of total RNA and included the highest dilutions step after RT. This will result in higher volume of cDNA-template per RT-reaction. The TaqMan Advanced RT-qPCR setup also had some advantages, as it included the miR-Amp preamplification, and had the highest maximum input of template for the qPCR-reaction. This might result in higher possibility for detection of lowly expressed miRNA.

6.5 Challenges of RT-qPCR detection of miRNA

The preferred RT-qPCR technology for this study will be used for verifying miRNA-findings from small RNA sequencing of biological samples, and thereby potentially be used to establish a miRNA-profile for patients with rheumatoid arthritis. However, some general challenges for detection of miRNAs have been reported.

It has been shown that samples with low total RNA quality may result in the highest concentrations of miRNA. Becker, Hammerle-Fickinger, Riedmaier, and Pfaffl (2010) demonstrated that a significant rise in miRNA amount occurred with ongoing RNA degradation. This was caused by the formation of small RNA fragments by degradations of longer RNA, resulting in overestimation of the miRNA amount (Becker et al., 2010). The study pointed out the importance of high total RNA quality and the lack of universally valid guidelines for normalization of miRNA expression data due to this problem.

One general disadvantage of RT-qPCR detection of miRNA is the difficulty of normalization of miRNA expression data (Becker et al., 2010). Normalization adjust the data by removing non-biological variation across samples and thereby makes it easier to identify the biological differences. For gene expression experiment multiple reference genes are generally used for

data normalization (Vandesompele et al., 2002), however for miRNA profiling experiments suitable candidate reference miRNAs have proven hard to find (Chugh & Dittmer, 2012; Gutierrez et al., 2008). This, among other reasons, is due to the tissue and species differences of miRNAs and the differences in expression. Normalization should therefore be determined for each experiment separately, and other small non-coding RNA are often used for normalization (Gee et al., 2011). Another method of normalization of miRNA expression data suggest using the mean expression value of target miRNAs, and thereby select miRNAs/small RNA controls that resemble the mean expression value of targets (Mestdagh et al., 2009). However, universally guideline for normalization of miRNA expression data is still one of the biggest challenges for establishing reliable miRNA-profiles.

As mentioned, other studies have shown that different platforms for detection of miRNAs show varying results, but also that different technologies and/or providers used for the same platform show varying results. Git et al. (2010) compared microarray, RT-qPCR and NGS technologies for miRNA profiles, and found that the overlap for differentially expressed miRNAs was surprisingly low when comparing data. Also, Leshkowitz et al. (2013) reported bias of miRNA detection by using different technologies, and it was observed that the ability of miRNA detection was depended on miRNA modifications and sequence (Leshkowitz et al., 2013). This indicate challenges and bias due to different technologies also for different platforms and provides problems for detection of miRNAs.

As the preferred RT-qPCR setup from this study later will be used for verifying miRNA-findings from NGS, contradictory data may be a challenge. For this, reliable kits and protocols suitable for the expression level of target miRNAs are crucial.

7 Conclusion

This study has observed varying results by use of different RT-qPCR kits and protocols for detection and quantitation of miRNAs. The objective of the evaluation was to find a preferred RT-qPCR setup that later can be used for verifying miRNA-findings from NGS of lymphocytes from patients with RA. In this study the lower detection range for three different setups were evaluated, and result showed different preferred setups for different circumstances and different miRNA expression levels.

The study indicated that miRCURY RT-qPCR setup gave best results for verifying lowly expressed miRNAs. This was based on the least deviation in the reaction efficiency, low indication of false positives and unspecific amplification, and a wide range of input of total RNA. It was also indicated that TaqMan Advanced RT-qPCR setup without the preamplification reaction, miR-Amp, should not be used for detection and quantitation of lowly expressed miRNA. This was based on the setup's poor reaction efficiency, observed detection range and precision. TaqMan MicroRNA RT-qPCR setup indicated being advantageous when few miRNA-targets and replicates are required. This indication was due to the lowest price per reaction for one miRNA target and by the setup's feasibility. By including UNG in the master mix, the deviation of the reaction efficiency decreased.

References

Androvic, P., Valihrach, L., Elling, J., Sjoback, R., & Kubista, M. (2017). Two-tailed RT-qPCR: a novel method for highly accurate miRNA quantification. *Nucleic Acids Res, 45*(15), e144. doi:10.1093/nar/gkx588

Applied Biosystems, T. S. (2016). Crt, a relative threshold method for qPCR data analysis on the QuantStudio 12K Flex system with OpenArray technology.

Ballantyne, K., Van Oorschot, R., & Mitchell, R. (2008). Locked nucleic acids in PCR primers increase sensitivity and performance. *Genomics, 91*(3), 301-305.

Bartel, D. P. (2018). Metazoan MicroRNAs. *Cell, 173*(1), 20-51. doi:10.1016/j.cell.2018.03.006

Becker, C., Hammerle-Fickinger, A., Riedmaier, I., & Pfaffl, M. (2010). mRNA and microRNA quality control for RT-qPCR analysis. *Methods, 50*(4), 237-243.

Behm-Ansmant, I., Rehwinkel, J., Doerks, T., Stark, A., Bork, P., & Izaurralde, E. (2006). mRNA degradation by miRNAs and GW182 requires both CCR4: NOT deadenylase and DCP1: DCP2 decapping complexes. *Genes & development, 20*(14), 1885-1898.

Belver, L., de Yébenes, V. G., & Ramiro, A. R. (2010). MicroRNAs prevent the generation of autoreactive antibodies. *Immunity, 33*(5), 713-722.

Benes, V., Collier, P., Kordes, C., Stolte, J., Rausch, T., Muckentaler, M. U., . . . Castoldi, M. (2015). Identification of cytokine-induced modulation of microRNA expression and secretion as measured by a novel microRNA specific qPCR assay. *Scientific reports, 5*, 11590.

Benhamed, M., Herbig, U., Ye, T., Dejean, A., & Bischof, O. (2012). Senescence is an endogenous trigger for microRNA-directed transcriptional gene silencing in human cells. *NATURE CELL BIOLOGY, 14*(3), 266.

Bustin, S. A., Benes, V., Garson, J. A., Hellemans, J., Huggett, J., Kubista, M., . . . Shipley, G. L. (2009). The MIQE guidelines: minimum information for publication of quantitative real-time PCR experiments. *Clinical chemistry, 55*(4), 611-622.

Cepin, U. (2017). Understanding qPCR Efficiency and Why It Can Exceed 100%. Retrieved from https://biosistemika.com/blog/qpcr-efficiency-over-100/

Chen, C., Ridzon, D. A., Broomer, A. J., Zhou, Z., Lee, D. H., Nguyen, J. T., . . . Andersen, M. R. (2005). Real-time quantification of microRNAs by stem–loop RT–PCR. *Nucleic acids research, 33*(20), e179-e179.

Chugh, P., & Dittmer, D. P. (2012). Potential pitfalls in microRNA profiling. *Wiley Interdisciplinary Reviews: RNA, 3*(5), 601-616.

D'alessandra, Y., Devanna, P., Limana, F., Straino, S., Di Carlo, A., Brambilla, P. G., . . . De Simone, M. (2010). Circulating microRNAs are new and sensitive biomarkers of myocardial infarction. *European heart journal, 31*(22), 2765-2773.

de Planell-Saguer, M., & Rodicio, M. C. (2011). Analytical aspects of microRNA in diagnostics: a review. *Analytica chimica acta, 699*(2), 134-152.

De Rie, D., Abugessaisa, I., Alam, T., Arner, E., Arner, P., Ashoor, H., . . . Burroughs, A. M. (2017). An integrated expression atlas of miRNAs and their promoters in human and mouse. *Nature biotechnology, 35*(9), 872.

Denli, A. M., Tops, B. B., Plasterk, R. H., Ketting, R. F., & Hannon, G. J. (2004). Processing of primary microRNAs by the Microprocessor complex. *Nature, 432*(7014), 231.

Desvignes, T., Batzel, P., Berezikov, E., Eilbeck, K., Eppig, J. T., McAndrews, M. S., . . . Postlethwait, J. H. (2015). miRNA Nomenclature: A View Incorporating Genetic Origins, Biosynthetic Pathways, and Sequence Variants. *Trends Genet, 31*(11), 613-626. doi:10.1016/j.tig.2015.09.002

Duroux-Richard, I., Pers, Y.-M., Fabre, S., Ammari, M., Baeten, D., Cartron, G., . . . Apparailly, F. (2014). Circulating miRNA-125b is a potential biomarker predicting response to rituximab in rheumatoid arthritis. *Mediators of inflammation, 2014*.

Fan, H., Wang, J., Komiyama, M., & Liang, X. (2019). Effects of secondary structures of DNA templates on the quantification of qPCR. *Journal of Biomolecular Structure and Dynamics*, 1-8.

Fu, G., Brkić, J., Hayder, H., & Peng, C. (2013). MicroRNAs in human placental development and pregnancy complications. *International journal of molecular sciences, 14*(3), 5519-5544.

Gee, H., Buffa, F., Camps, C., Ramachandran, A., Leek, R., Taylor, M., . . . Homer, J. (2011). The small-nucleolar RNAs commonly used for microRNA normalisation correlate with tumour pathology and prognosis. *British journal of cancer, 104*(7), 1168.

Git, A., Dvinge, H., Salmon-Divon, M., Osborne, M., Kutter, C., Hadfield, J., . . . Caldas, C. (2010). Systematic comparison of microarray profiling, real-time PCR, and next-generation sequencing technologies for measuring differential microRNA expression. *RNA, 16*(5), 991-1006.

Griffiths-Jones, S., Grocock, R. J., van Dongen, S., Bateman, A., & Enright, A. J. (2006). miRBase: microRNA sequences, targets and gene nomenclature. *Nucleic Acids Res, 34*(Database issue), D140-144. doi:10.1093/nar/gkj112

Gutierrez, L., Mauriat, M., Guénin, S., Pelloux, J., Lefebvre, J. F., Louvet, R., . . . Bellini, C. (2008). The lack of a systematic validation of reference genes: a serious pitfall undervalued in reverse transcription-polymerase chain reaction (RT-PCR) analysis in plants. *Plant biotechnology journal, 6*(6), 609-618.

Hafner, M., Renwick, N., Brown, M., Mihailović, A., Holoch, D., Lin, C., . . . Ludwig, J. (2011). RNA-ligase-dependent biases in miRNA representation in deep-sequenced small RNA cDNA libraries. *RNA, 17*(9), 1697-1712.

Heid, C. A., Stevens, J., Livak, K. J., & Williams, P. M. (1996). Real time quantitative PCR. *Genome Res, 6*(10), 986-994.

Honda, S., & Kirino, Y. (2015). Dumbbell-PCR: a method to quantify specific small RNA variants with a single nucleotide resolution at terminal sequences. *Nucleic Acids Res, 43*(12), e77. doi:10.1093/nar/gkv218

Hussain, N., Zhu, W., Jiang, C., Xu, J., Wu, X., Geng, M., . . . Xu, P. (2018). Down-regulation of miR-10a-5p in synoviocytes contributes to TBX5-controlled joint inflammation. *Journal of cellular and molecular medicine, 22*(1), 241-250.

Hutvágner, G., McLachlan, J., Pasquinelli, A. E., Bálint, É., Tuschl, T., & Zamore, P. D. (2001). A cellular function for the RNA-interference enzyme Dicer in the maturation of the let-7 small temporal RNA. *science, 293*(5531), 834-838.

Ibberson, D., Benes, V., Muckenthaler, M. U., & Castoldi, M. (2009). RNA degradation compromises the reliability of microRNA expression profiling. *BMC biotechnology, 9*(1), 102.

James, A. M., Baker, M. B., Bao, G., & Searles, C. D. (2017). MicroRNA Detection Using a Double Molecular Beacon Approach: Distinguishing Between miRNA and Pre-miRNA. *Theranostics, 7*(3), 634-646. doi:10.7150/thno.16840

Jin, F., Hu, H., Xu, M., Zhan, S., Wang, Y., Zhang, H., & Chen, X. (2018). Serum microRNA profiles serve as novel biomarkers for autoimmune diseases. *Frontiers in immunology, 9*.

Jin, J., Vaud, S., Zhelkovsky, A. M., Posfai, J., & McReynolds, L. A. (2016). Sensitive and specific miRNA detection method using SplintR Ligase. *Nucleic Acids Res, 44*(13), e116. doi:10.1093/nar/gkw399

Kauppinen, S., Vester, B., & Wengel, J. (2005). Locked nucleic acid (LNA): High affinity targeting of RNA for diagnostics and therapeutics. *Drug Discovery Today: Technologies, 2*(3), 287-290.

Kozomara, A., & Griffiths-Jones, S. (2013). miRBase: annotating high confidence microRNAs using deep sequencing data. *Nucleic acids research, 42*(D1), D68-D73.

Lee, R. C., Feinbaum, R. L., & Ambros, V. (1993). The C. elegans heterochronic gene lin-4 encodes small RNAs with antisense complementarity to lin-14. *Cell, 75*(5), 843-854.

Lee, Y., Kim, M., Han, J., Yeom, K. H., Lee, S., Baek, S. H., & Kim, V. N. (2004). MicroRNA genes are transcribed by RNA polymerase II. *The EMBO journal, 23*(20), 4051-4060.

Leshkowitz, D., Horn-Saban, S., Parmet, Y., & Feldmesser, E. (2013). Differences in microRNA detection levels are technology and sequence dependent. *RNA, 19*(4), 527-538.

Liston, A., Lu, L.-F., O'Carroll, D., Tarakhovsky, A., & Rudensky, A. Y. (2008). Dicer-dependent microRNA pathway safeguards regulatory T cell function. *Journal of Experimental Medicine, 205*(9), 1993-2004.

Long, H., Wang, X., Chen, Y., Wang, L., Zhao, M., & Lu, Q. (2018). Dysregulation of microRNAs in autoimmune diseases: Pathogenesis, biomarkers and potential therapeutic targets. *Cancer Lett, 428*, 90-103. doi:10.1016/j.canlet.2018.04.016

Lorenz, R., Bernhart, S. H., Zu Siederdissen, C. H., Tafer, H., Flamm, C., Stadler, P. F., & Hofacker, I. L. (2011). ViennaRNA Package 2.0. *Algorithms for Molecular Biology, 6*(1), 26.

Ludwig, N., Leidinger, P., Becker, K., Backes, C., Fehlmann, T., Pallasch, C., . . . Meese, E. (2016). Distribution of miRNA expression across human tissues. *Nucleic acids research, 44*(8), 3865-3877.

Lund, E., Güttinger, S., Calado, A., Dahlberg, J. E., & Kutay, U. (2004). Nuclear export of microRNA precursors. *science, 303*(5654), 95-98.

Mestdagh, Hartmann, N., Baeriswyl, L., Andreasen, D., Bernard, N., Chen, C., . . . Vandesompele, J. (2014). Evaluation of quantitative miRNA expression platforms in the microRNA quality control (miRQC) study. *Nat Methods, 11*(8), 809-815. doi:10.1038/nmeth.3014

Mestdagh, P., Van Vlierberghe, P., De Weer, A., Muth, D., Westermann, F., Speleman, F., & Vandesompele, J. (2009). A novel and universal method for microRNA RT-qPCR data normalization. *Genome biology, 10*(6), R64.

Miao, L., Yao, H., Li, C., Pu, M., Yao, X., Yang, H., . . . Wang, Y. (2016). A dual inhibition: microRNA-552 suppresses both transcription and translation of cytochrome P450 2E1. *Biochim Biophys Acta, 1859*(4), 650-662. doi:10.1016/j.bbagrm.2016.02.016

Montecalvo, A., Larregina, A. T., Shufesky, W. J., Stolz, D. B., Sullivan, M. L., Karlsson, J. M., . . . Wang, Z. (2012). Mechanism of transfer of functional microRNAs between mouse dendritic cells via exosomes. *Blood, 119*(3), 756-766.

Moran-Moguel, M. C., Petarra-Del Rio, S., Mayorquin-Galvan, E. E., & Zavala-Cerna, M. G. (2018). Rheumatoid Arthritis and miRNAs: A Critical Review through a Functional View. *J Immunol Res, 2018*, 2474529. doi:10.1155/2018/2474529

Murata, K., Furu, M., Yoshitomi, H., Ishikawa, M., Shibuya, H., Hashimoto, M., . . . Mimori, T. (2013). Comprehensive microRNA analysis identifies miR-24 and miR-125a-5p as plasma biomarkers for rheumatoid arthritis. *PLoS One, 8*(7), e69118.

Nakamachi, Y., Kawano, S., Takenokuchi, M., Nishimura, K., Sakai, Y., Chin, T., . . . Kumagai, S. (2009). MicroRNA-124a is a key regulator of proliferation and monocyte chemoattractant protein 1 secretion in fibroblast-like synoviocytes from patients with rheumatoid arthritis. *Arthritis & Rheumatism, 60*(5), 1294-1304.

National Rheumatoid Arthritis Society. (2001, 2019). What is RA? Retrieved from https://www.nras.org.uk/what-is-ra-article#What%20is%20RA

Nolan, T., Hands, R. E., & Bustin, S. A. (2006). Quantification of mRNA using real-time RT-PCR. *Nat Protoc, 1*(3), 1559-1582. doi:10.1038/nprot.2006.236

O'Brien, J., Hayder, H., Zayed, Y., & Peng, C. (2018). Overview of MicroRNA Biogenesis, Mechanisms of Actions, and Circulation. *Front Endocrinol (Lausanne), 9*, 402. doi:10.3389/fendo.2018.00402

Okada, Y., Wu, D., Trynka, G., Raj, T., Terao, C., Ikari, K., . . . Yoshida, S. (2014). Genetics of rheumatoid arthritis contributes to biology and drug discovery. *Nature, 506*(7488), 376.

Olena, A. F., & Patton, J. G. (2010). Genomic organization of microRNAs. *Journal of cellular physiology, 222*(3), 540-545.

Pasquinelli, A. E., Reinhart, B. J., Slack, F., Martindale, M. Q., Kuroda, M. I., Maller, B., . . . Ruvkun, G. (2000). Conservation of the sequence and temporal expression of let-7 heterochronic regulatory RNA. *Nature, 408*(6808), 86-89. doi:10.1038/35040556

Pritchard, C. C., Cheng, H. H., & Tewari, M. (2012). MicroRNA profiling: approaches and considerations. *Nature Reviews Genetics, 13*(5), 358.

Redshaw, N., Wilkes, T., Whale, A., Cowen, S., Huggett, J., & Foy, C. A. (2013). A comparison of miRNA isolation and RT-qPCR technologies and their effects on quantification accuracy and repeatability. *Biotechniques, 54*(3), 155-164. doi:10.2144/000114002

Rodriguez, A., Griffiths-Jones, S., Ashurst, J. L., & Bradley, A. (2004). Identification of mammalian microRNA host genes and transcription units. *Genome research, 14*(10a), 1902-1910.

Ruby, J. G., Jan, C. H., & Bartel, D. P. (2007). Intronic microRNA precursors that bypass Drosha processing. *Nature, 448*(7149), 83.

Sanders, R., Huggett, J. F., Bushell, C. A., Cowen, S., Scott, D. J., & Foy, C. A. (2011). Evaluation of digital PCR for absolute DNA quantification. *Analytical chemistry, 83*(17), 6474-6484.

Schamberger, A., & Orbán, T. I. (2014). 3′ IsomiR species and DNA contamination influence reliable quantification of microRNAs by stem-loop quantitative PCR. *PLoS One, 9*(8), e106315.

Singh, S. K., Koshkin, A. A., Wengel, J., & Nielsen, P. (1998). LNA (locked nucleic acids): synthesis and high-affinity nucleic acid recognition. *Chemical communications*(4), 455-456.

Singh, V. K., Govindarajan, R., Naik, S., & Kumar, A. (2000). The effect of hairpin structure on PCR amplification efficiency. *Mol Biol Today, 1*(3), 67-69.

Ståhlberg, A., Kubista, M., & Pfaffl, M. (2004). Comparison of reverse transcriptases in gene expression analysis. *Clinical chemistry, 50*(9), 1678-1680.

Tanzer, A., & Stadler, P. F. (2004). Molecular evolution of a microRNA cluster. *Journal of molecular biology, 339*(2), 327-335.

Vandesompele, J., De Preter, K., Pattyn, F., Poppe, B., Van Roy, N., De Paepe, A., & Speleman, F. (2002). Accurate normalization of real-time quantitative RT-PCR data by geometric averaging of multiple internal control genes. *Genome biology, 3*(7), research0034. 0031.

Wang, B., Howel, P., Bruheim, S., Ju, J., Owen, L. B., Fodstad, O., & Xi, Y. (2011). Systematic evaluation of three microRNA profiling platforms: microarray, beads array, and quantitative real-time PCR array. *PLoS One, 6*(2), e17167.

Weber, J. A., Baxter, D. H., Zhang, S., Huang, D. Y., Huang, K. H., Lee, M. J., . . . Wang, K. (2010). The microRNA spectrum in 12 body fluids. *Clinical chemistry, 56*(11), 1733-1741.

Wightman, B., Ha, I., & Ruvkun, G. (1993). Posttranscriptional regulation of the heterochronic gene lin-14 by lin-4 mediates temporal pattern formation in C. elegans. *Cell, 75*(5), 855-862.

Yang, J.-S., Maurin, T., Robine, N., Rasmussen, K. D., Jeffrey, K. L., Chandwani, R., . . . Lai, E. C. (2010). Conserved vertebrate mir-451 provides a platform for Dicer-independent, Ago2-mediated microRNA biogenesis. *Proceedings of the National Academy of Sciences, 107*(34), 15163-15168.

youn Cha, S., ho Choi, Y., Hwang, S., Jeong, J.-Y., & An, H. J. (2017). Clinical impact of microRNAs associated with cancer stem cells as a prognostic factor in ovarian carcinoma. *Journal of Cancer, 8*(17), 3538.

Yuan, J. S., Reed, A., Chen, F., & Stewart, C. N. (2006). Statistical analysis of real-time PCR data. *BMC bioinformatics, 7*(1), 85.

Zhou, X., Jeker, L. T., Fife, B. T., Zhu, S., Anderson, M. S., McManus, M. T., & Bluestone, J. A. (2008). Selective miRNA disruption in T reg cells leads to uncontrolled autoimmunity. *Journal of Experimental Medicine, 205*(9), 1983-1991.

Appendix A - Details of the material

***Table 1**: The components used for miRCURY RT-qPCR setup.*

	Contents			Catalog no.	LOT no.	Supplier
Reverse transcription	miRCURY LNA RT kit	5x miRCURY RT reaction Buffer	128 µl	339340	76001261	Qiagen
		10x miRCURY RT enxyme mix	64 µl			
		Nuclease-free water	1,5 ml			
		UniSp6 RNA Spike-in Template	12 fmol			
Quantitative PCR	miRCURY LNA SYBR Green PCR kit	2x miRCURY SYBER green PCR master mix	1 ml/3 x 1ml	339346	75411739-26	Qiagen
		ROX Reference dye	250 µl / 1ml			
		Nuclease-free water	2x 1,5 ml			
Primers and probes	miRCURY LNA miRNA PCR assay	miRCURY LNA miRNA PCR primer mix		339306		Qiagen
			Hsa-miR-495-3p	YP00206015	201709110165-1	
			Hsa-miR-125b-1-3	YP00204400	201706010209-1	
			Hsa-miR-493-5p	YP00204166	201709110758-1	
			Hsa-miR-136-3p	YP00205503	201705190319-1	
			Hsa-miR-30c-2-3p	YP00205632	201705050404-1	
			Hsa-miR-379-5p	YP00205659	201705050329-1	

Table 2: *The components used for TaqMan Advanced RT-qPCR setup.*

		Contents	Catalog no.	LOT no.	Supplier
Reverse transcription	TaqMan Advanced miRNA cDNA Synthesis kit	10x Poly(A) Buffer ATP, 10 mM Poly(A) Enzyme, 5 U/ µl 5x DNA Ligase Buffer RNA Ligase, 10 U/ µl 50% PEG 8000 25x Ligation Adaptor 10x RT Enzyme Mix 5x RT Buffer 20x Universal RT Primer dNTP mix, 100 mM 20x miR-Amp Primer Mix 2x miR-Amp Master Mix	A28007	1884340	Thermo Fisher Scientific
Quantitative PCR	TaqMan Fast Advanced Master Mix	1 x 5 ml	4444557	1711143	Thermo Fisher Scientific
Primers and probes	TaqMan Advanced MicroRNA Assays	Hsa-miR-493-5p Hsa-miR-136-3p Hsa-miR-30c-2-3p Hsa-miR-379-5p Hsa-miR-125b-1-3p Hsa-miR-495-3p	A25576 478943_mir 477902_mir 479401_mir 478077_mir 478665_mir 478136_mir	P161216-015 C07 P170514-000 D09 P170802-019 G09 P180420-011 A07 P180429-000 B02 P180725-002 E12	Thermo Fisher Scientific

***Table 3**: The components used for TaqMan MicroRNA RT-qPCR setup.*

	Contents			Catalog no.	LOT no.	Supplier
Reverse transcription with primers and probes	TaqMan MicroRNA Reverse Transcription kit	10X RT buffer		4366596	00518808	Thermo Fisher Scientific
		dNTP mix w/dTTp, 100mM				
		RNase inhibitor, 20 U/µL				
		MultiScribe™ RT enzyme, 50 U/µL				
		5x RT primer				
			Hsa-miR-493-5p		P170627-001 G11	
			Mmu-miR-379-5p		P180212-011 G12	
			Hsa-miR-136-3p		P180213-002 D08	
			Hsa-miR-125b-1-3p		P180213-002 F05	
			Hsa-miR-30c-2-3p		P180224-002 G02	
			Mmu-miR-495-3p		P180503-006 C11	
Quantitative PCR	TaqMan Universal PCR Master Mix II, No UNG	1 x 5 ml		4440040	1703067	Thermo Fisher Scientific
Quantitative PCR	TaqMan Universal PCR Master Mix II, With UNG	1 x 5 ml		4440038	00670726	Thermo Fisher Scientific
Primers and probes	TaqMan MicroRNA Assays			4427975		Thermo Fisher Scientific
		Hsa-miR-493		001040	P170627-001 G11	
		Mmu-miR-379		001138	P180212-011 G12	
		Hsa-miR-136*		002100	P180213-002 D08	
		Hsa-miR-125b-1*		002378	P180213-002 F05	
		Hsa-miR-30c-2*		002110	P180224-002 G02	
		Mmu-miR-495		001663	P180503-006 C11	

Appendix B - Standard curves

Hsa-miR-125b-1-3p with synthetic miRNA pool

TaqMan Advanced setup

Without miR-Amp reaction:

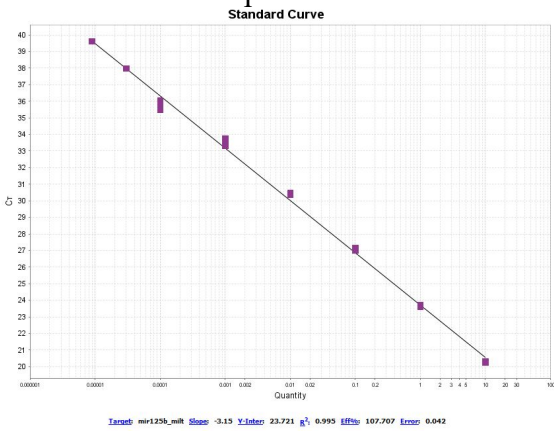

With miR-Amp reaction:

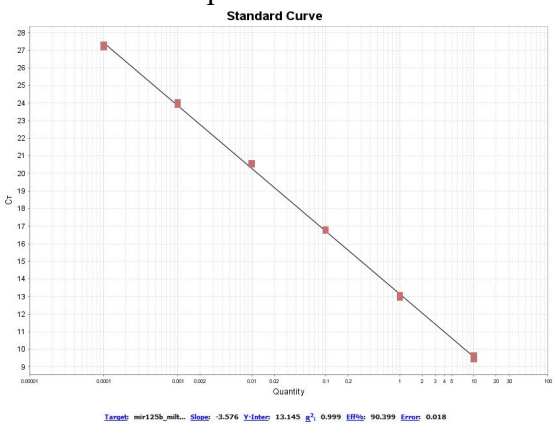

TaqMan MicroRNA setup

With UNG in master mix:

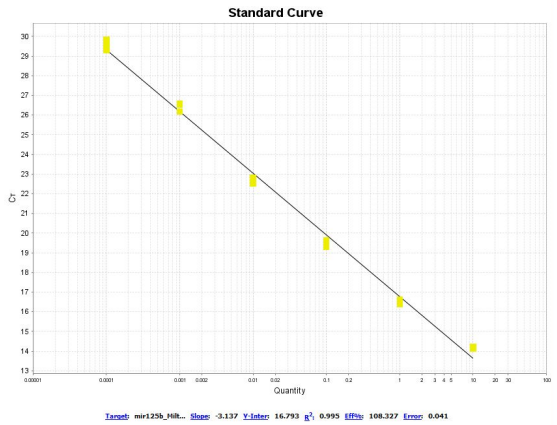

Without UNG in master mix:

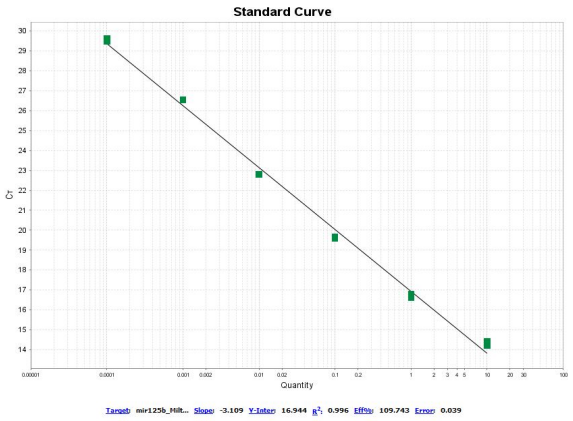

miRCURY setup

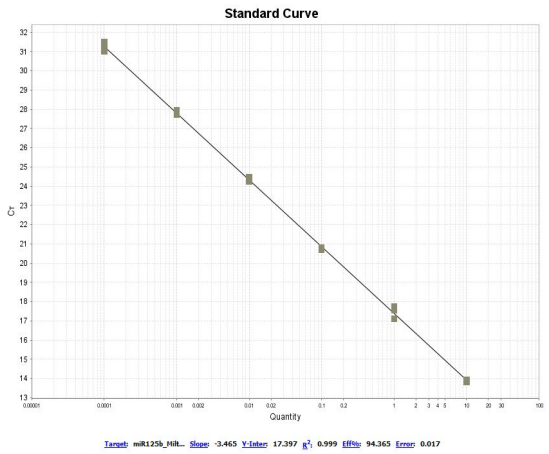

Figure 1: *The standard curves for hsa-miR-125b-1-3p with synthetic miRNA pool for the different type of setups.*

Hsa-miR-125b-1-3p with biological noise

TaqMan Advanced setup

Without miR-Amp reaction:

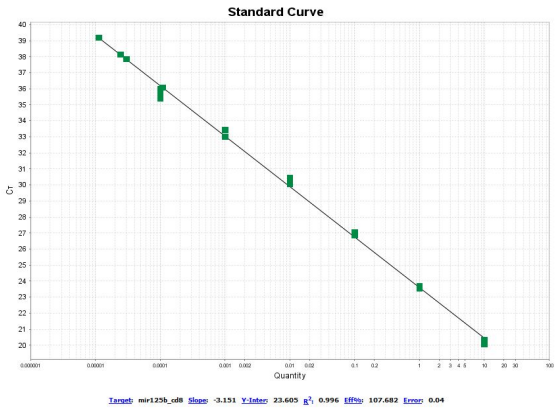

With miR-Amp reaction:

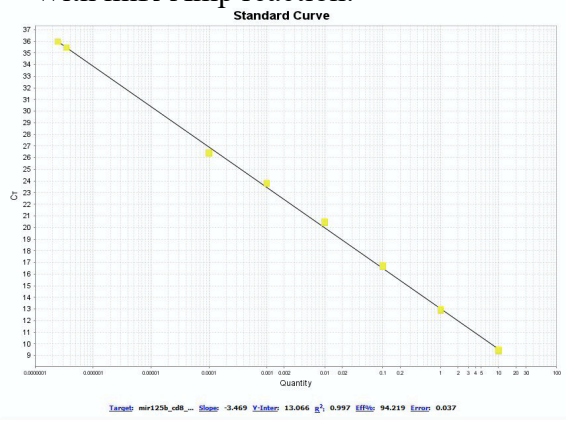

TaqMan MicroRNA setup

With UNG in master mix:

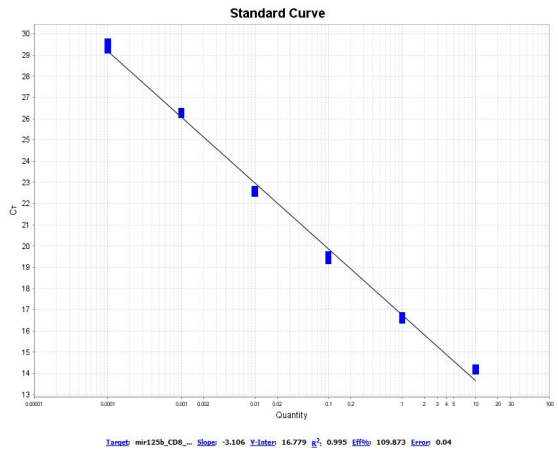

Without UNG in master mix:

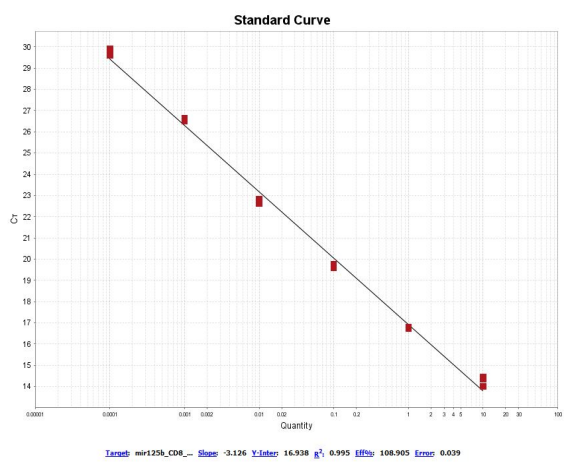

miRCURY setup

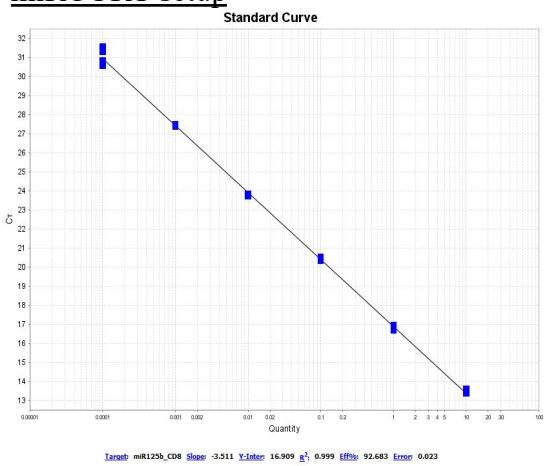

Figure 2: *The standard curves for hsa-miR-125b-1-3p with biological noise for the different type of setups.*

Hsa-miR-30c-2-3p with synthetic miRNA pool

TaqMan Advanced setup

Without miR-Amp reaction:

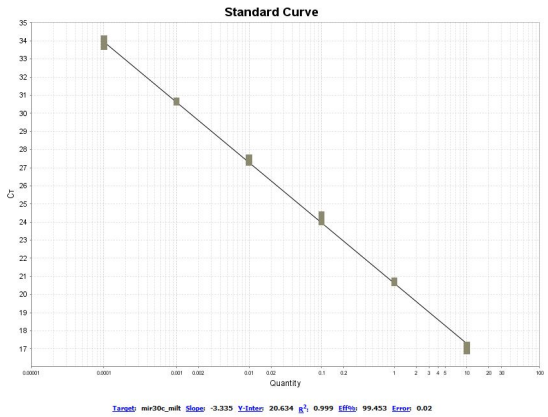

With miR-Amp reaction:

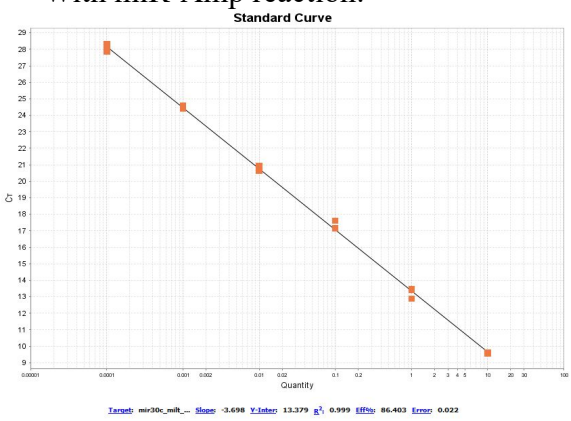

TaqMan MicroRNA setup

With UNG in master mix:

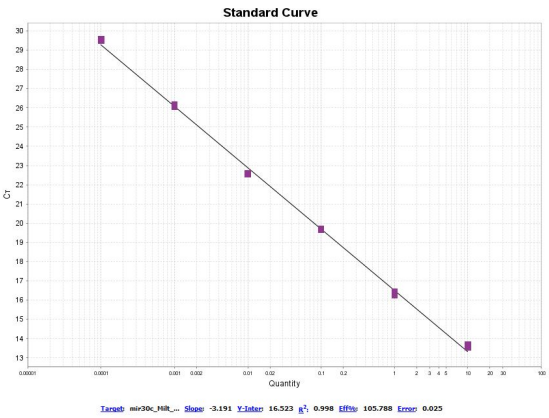

Without UNG in master mix:

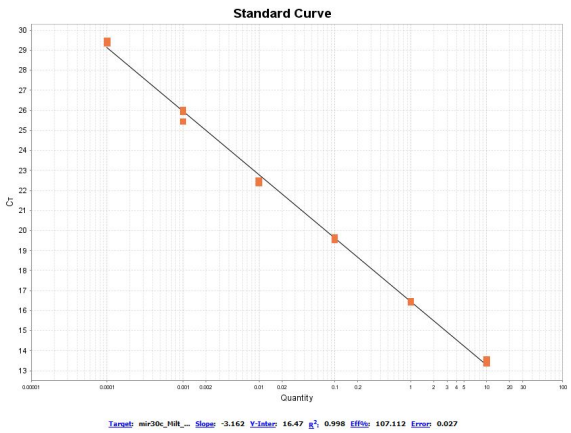

miRCURY setup

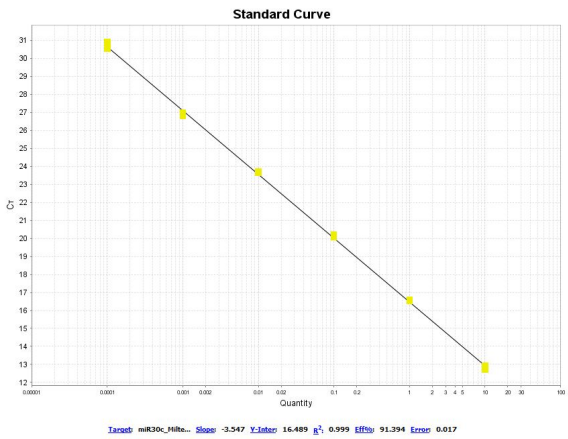

Figure 3: *The standard curves for hsa-miR-30c-2-3p with synthetic miRNA pool for the different type of setups.*

Hsa-miR-30c-2-3p with biological noise

TaqMan Advanced setup

Without miR-Amp reaction:

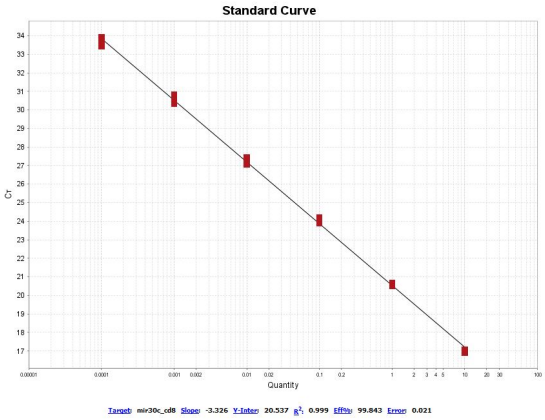

With miR-Amp reaction:

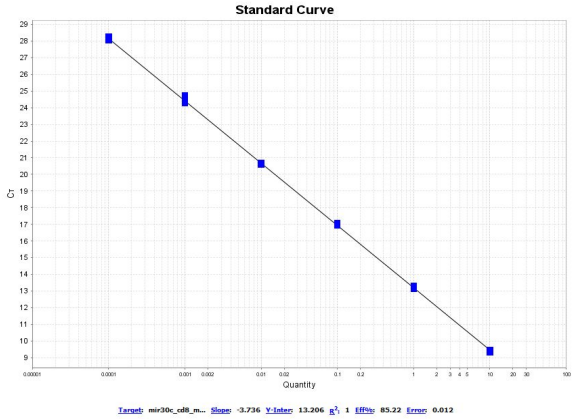

TaqMan MicroRNA setup

With UNG in master mix:

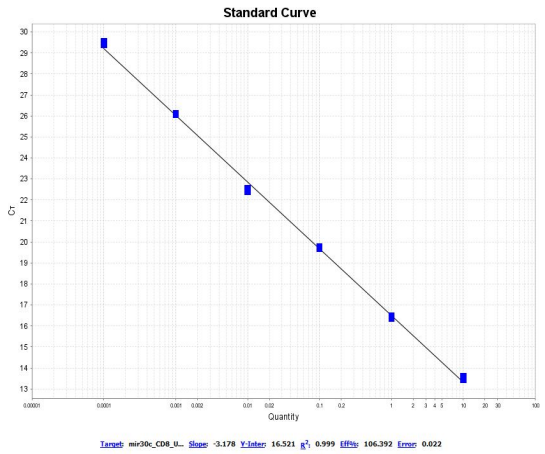

Without UNG in master mix:

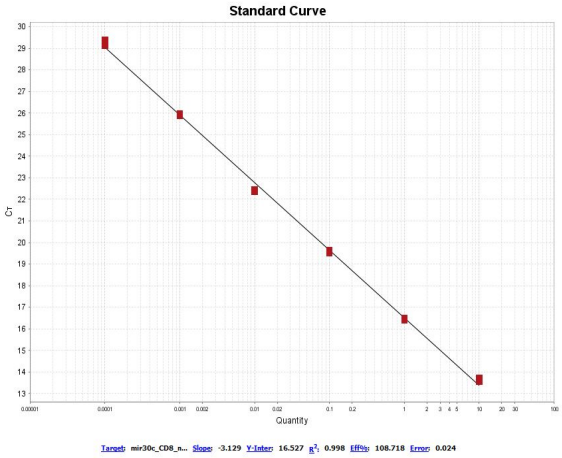

miRCURY setup

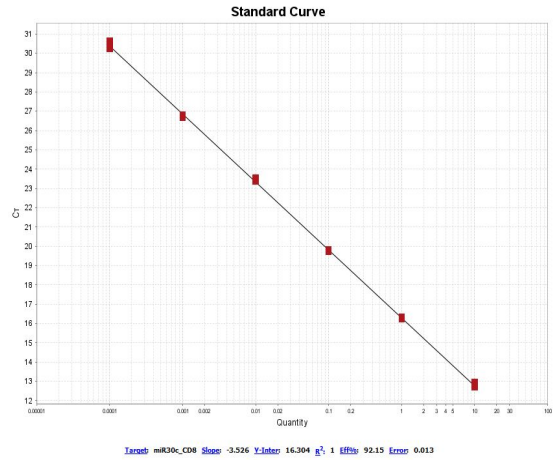

Figure 4: *The standard curves for hsa-miR-30c-2-3p with biological noise for the different type of setups.*

Hsa-miR-136-3p with synthetic miRNA pool

TaqMan Advanced setup

Without miR-Amp reaction:

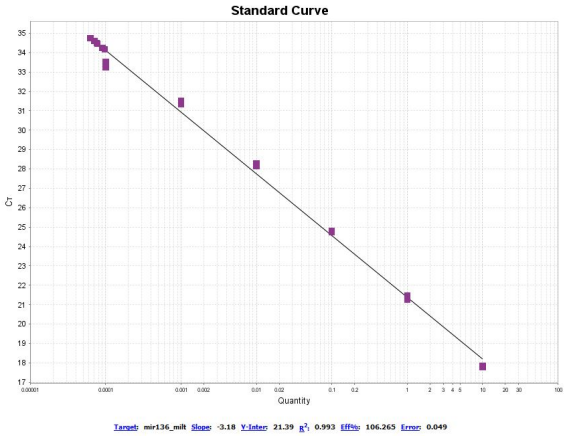

With miR-Amp reaction:

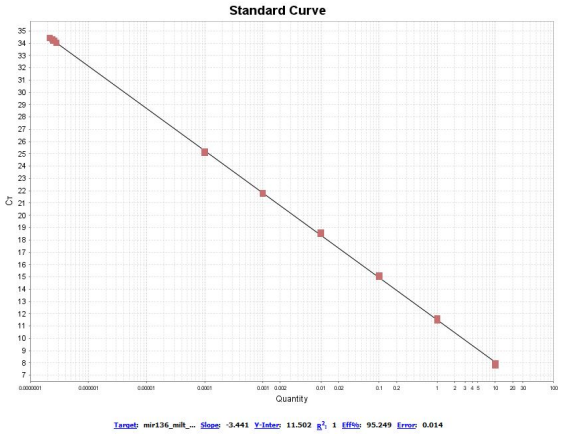

TaqMan MicroRNA setup

With UNG in master mix:

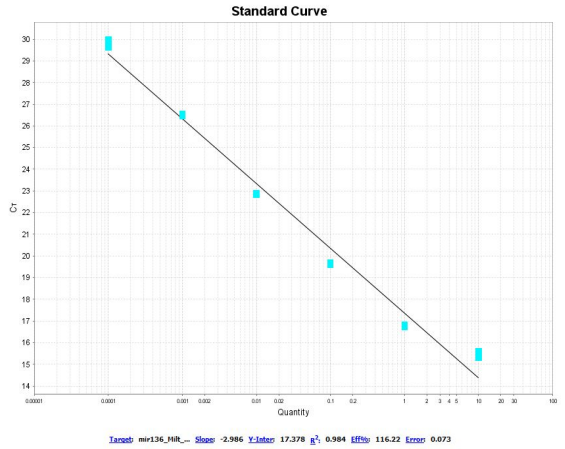

Without UNG in master mix:

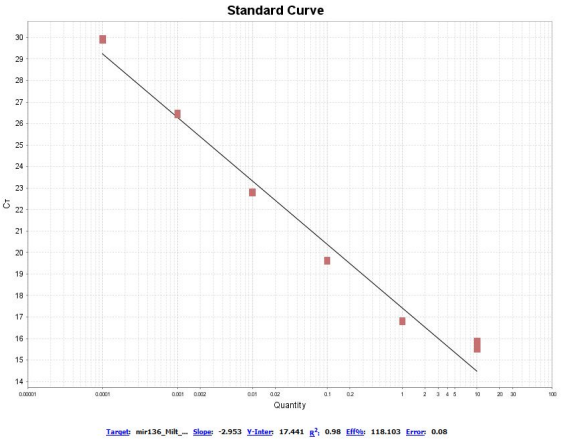

miRCURY setup

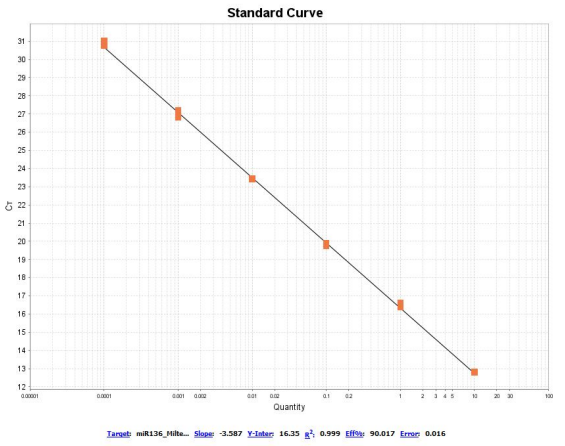

Figure 5: *The standard curves for hsa-miR-136-3p with synthetic miRNA pool for the different type of setups.*

Hsa-miR-136-3p with biological noise

TaqMan Advanced setup

Without miR-Amp reaction:

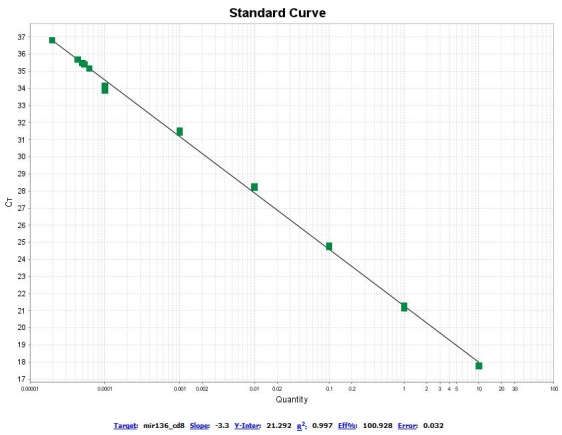

With miR-Amp reaction:

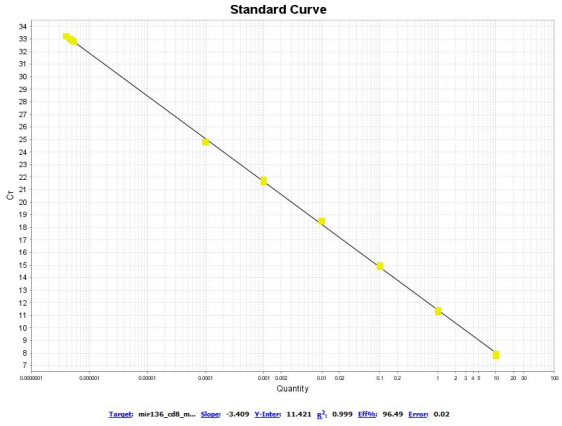

TaqMan MicroRNA setup

With UNG in master mix:

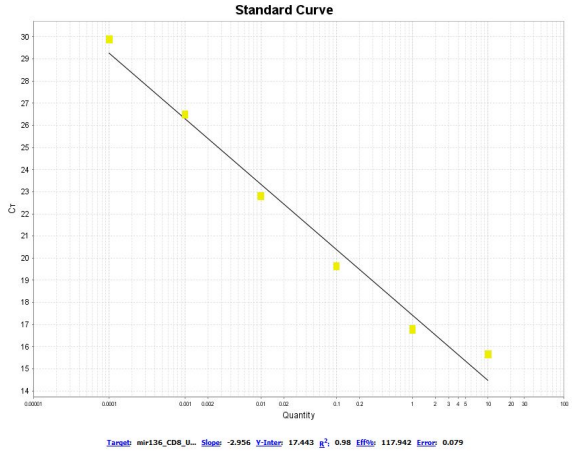

Without UNG in master mix:

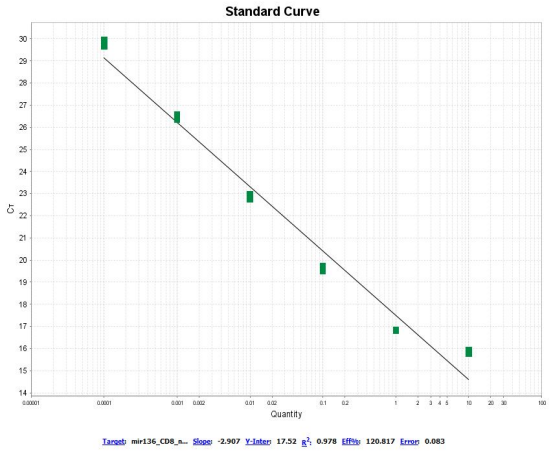

miRCURY setup

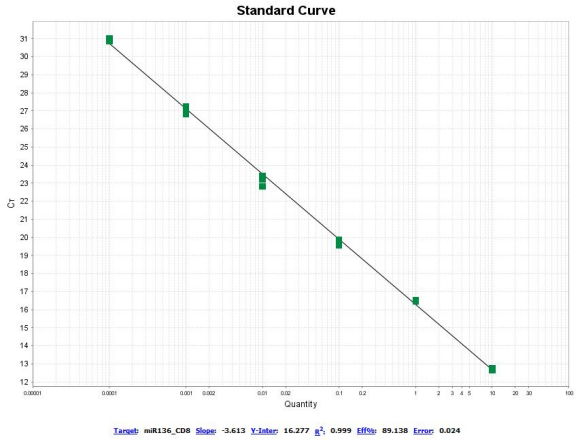

Figure 6: *The standard curves for hsa-miR-136-3p with biological noise for the different type of setups.*

Hsa-miR-379-5p with synthetic miRNA pool

TaqMan Advanced setup

Without miR-Amp reaction:

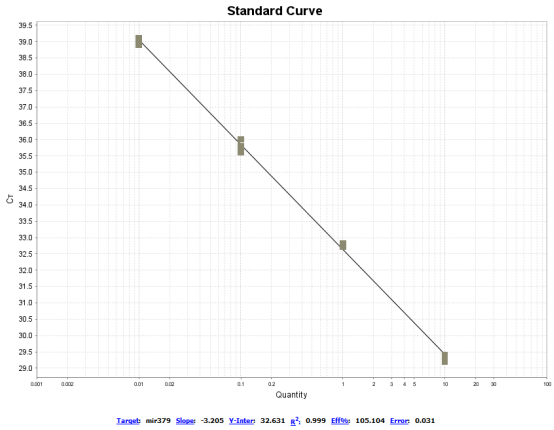

With miR-Amp reaction:

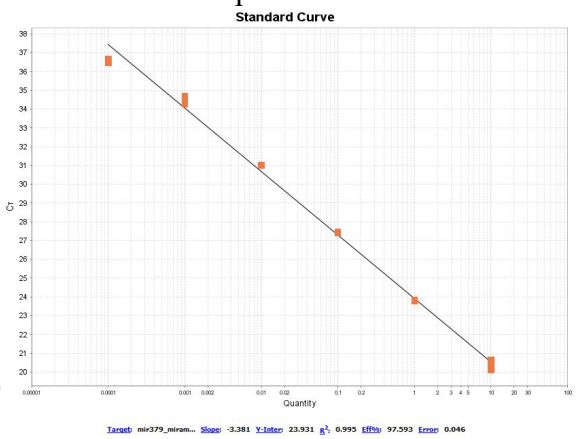

TaqMan MicroRNA setup

With UNG in master mix:

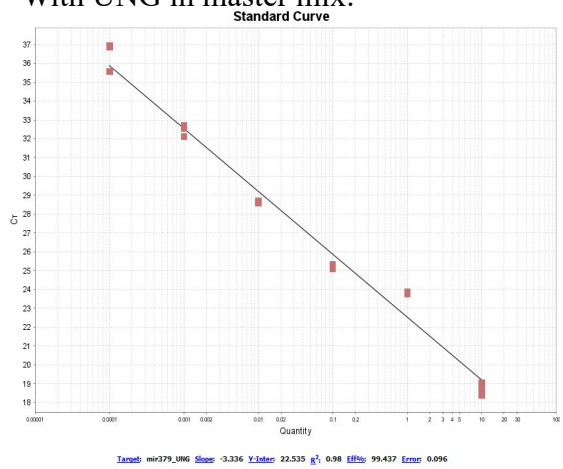

Without UNG in master mix:

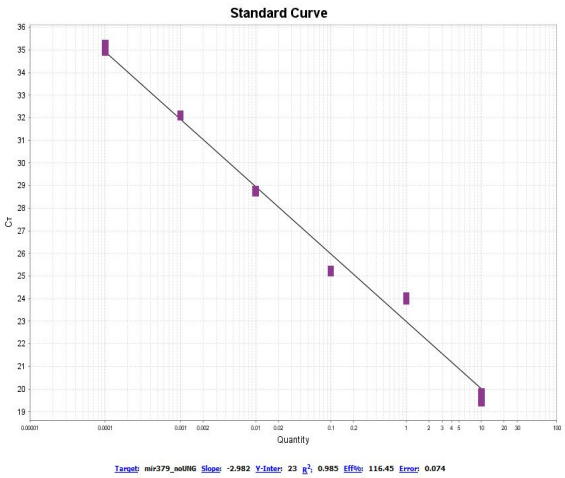

miRCURY setup

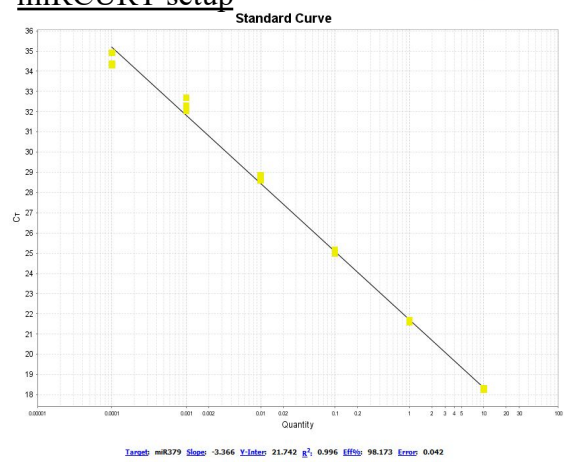

Figure 7: *The standard curves for hsa-miR-379-5p with synthetic miRNA pool for the different type of setups.*

Hsa-miR-379-5p with biological noise

TaqMan Advanced setup

Without miR-Amp reaction:

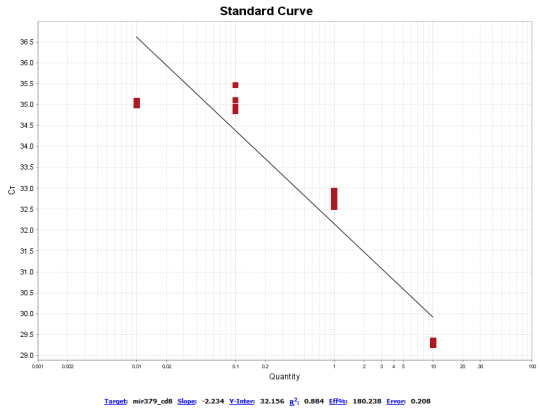

With miR-Amp reaction:

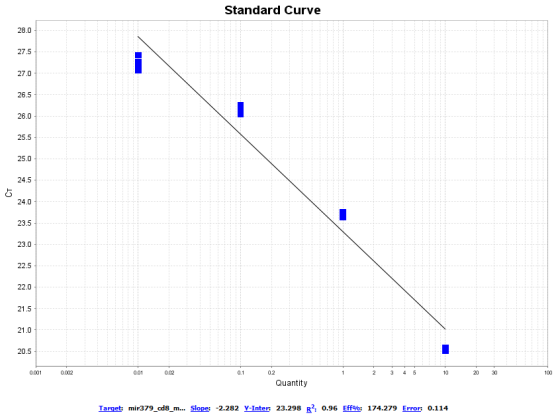

TaqMan MicroRNA setup

With UNG in master mix:

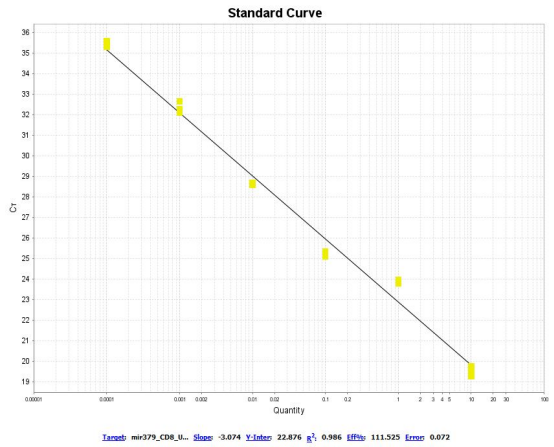

Without UNG in master mix:

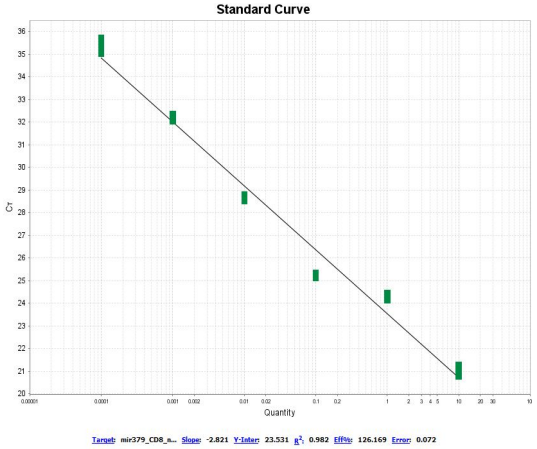

miRCURY setup

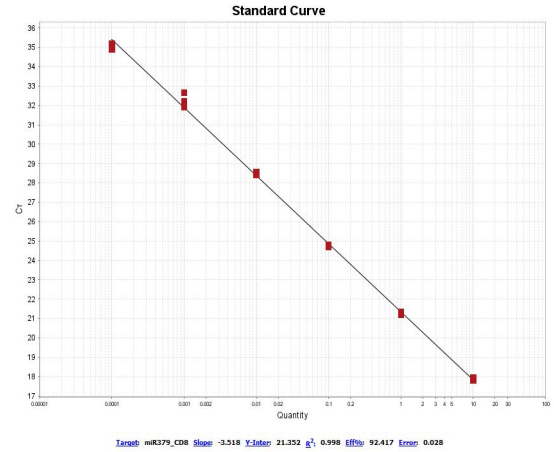

Figure 8: *The standard curves for hsa-miR-379-5p with biological noise for the different type of setups.*

Hsa-miR-493-5p with synthetic miRNA pool

TaqMan Advanced setup

Without miR-Amp reaction:

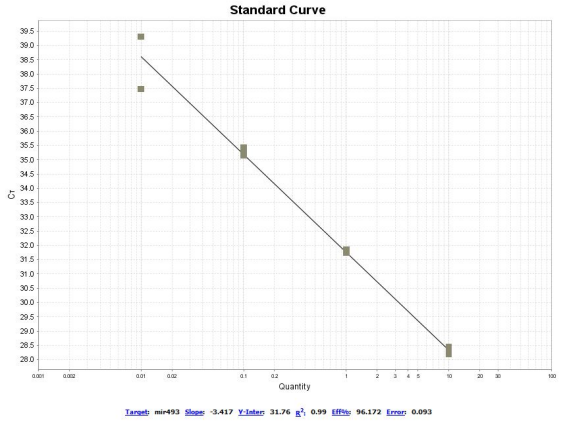

With miR-Amp reaction:

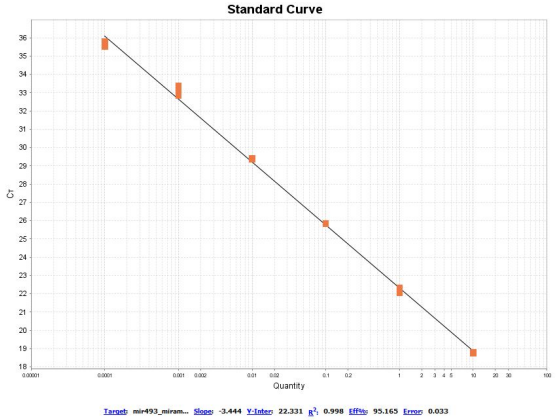

TaqMan MicroRNA setup

With UNG in master mix:

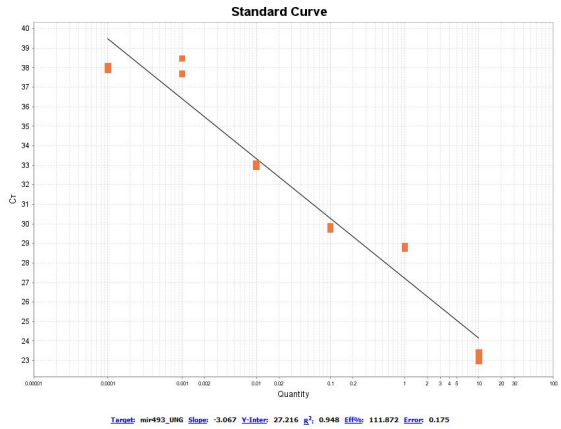

Without UNG in master mix:

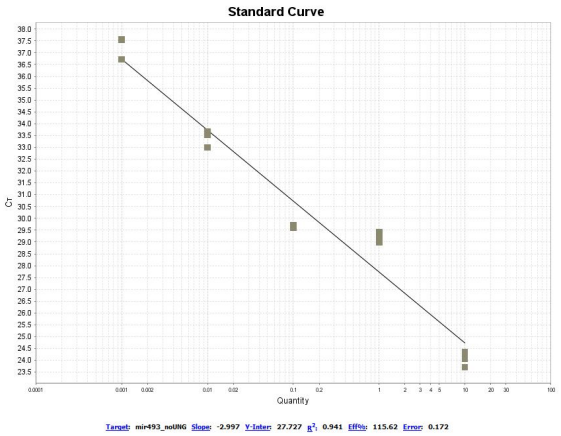

miRCURY setup

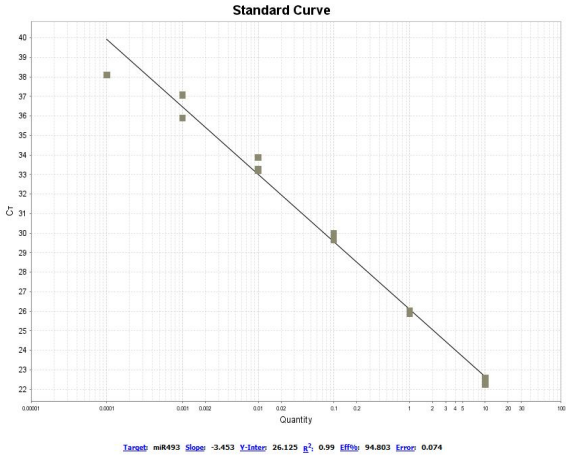

Figure 9: *The standard curves for hsa-miR-493-5p with synthetic miRNA pool for the different type of setups.*

Hsa-miR-493-5p with biological noise

TaqMan Advanced setup

Without miR-Amp reaction:

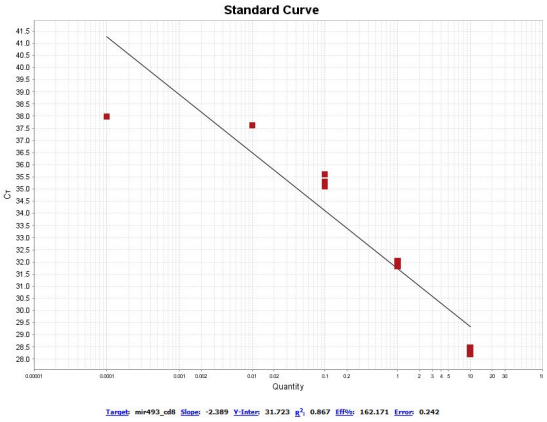

With miR-Amp reaction:

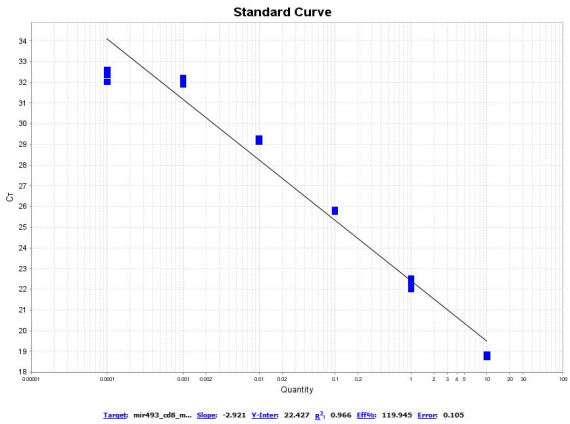

TaqMan MicroRNA setup

With UNG in master mix:

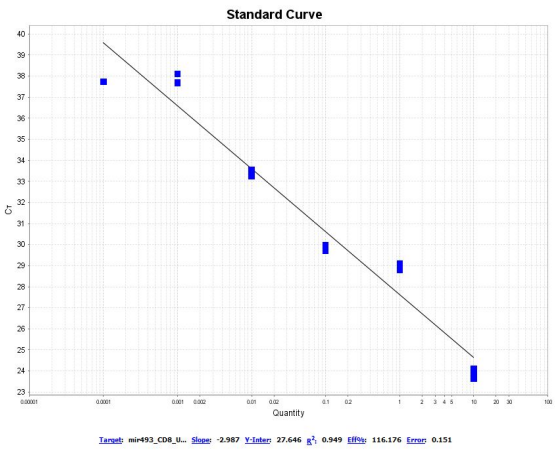

Without UNG in master mix:

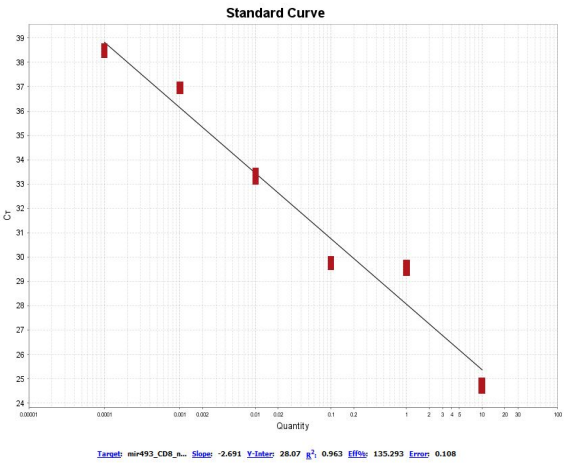

miRCURY setup

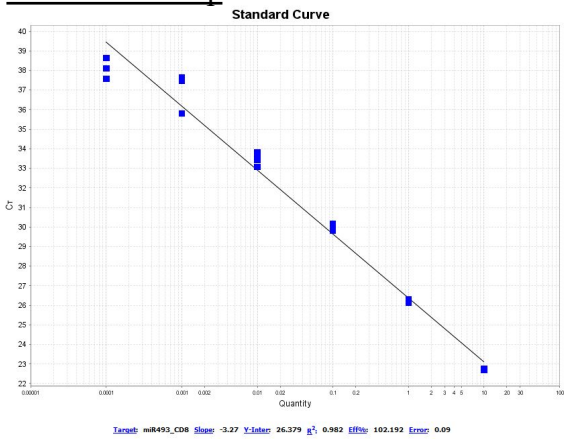

Figure 10: *The standard curves for hsa-miR-493-5p with biological noise for the different type of setups.*

Hsa-miR-495-3p with synthetic miRNA pool

TaqMan Advanced setup

Without miR-Amp reaction:

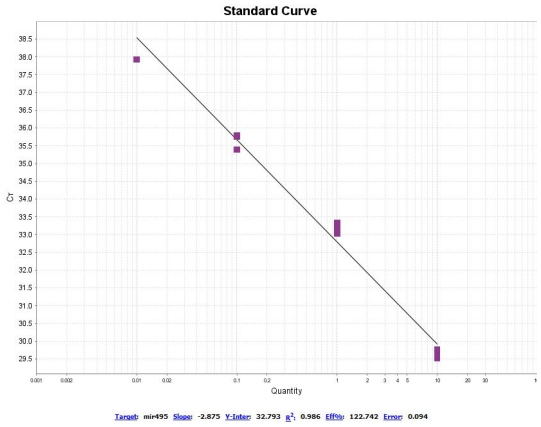

With miR-Amp reaction:

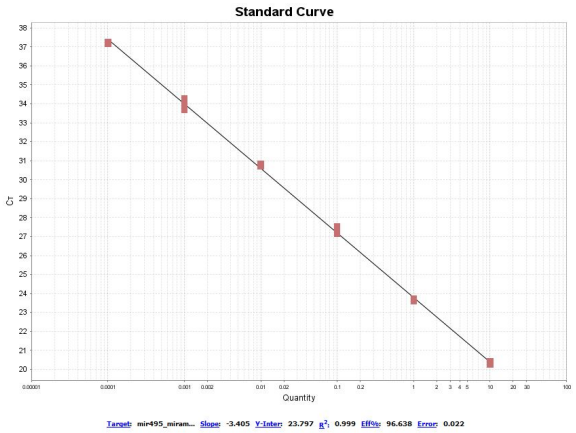

TaqMan MicroRNA setup

With UNG in master mix:

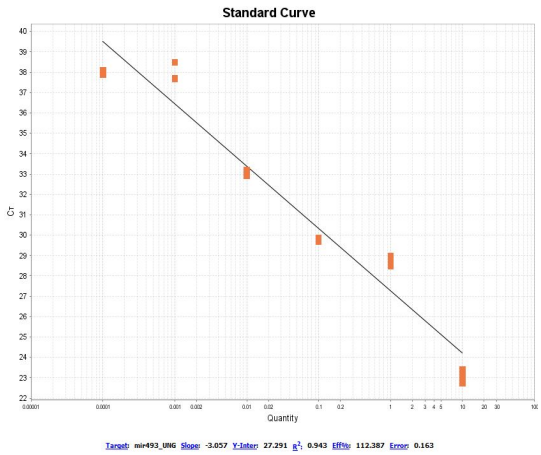

Without UNG in master mix:

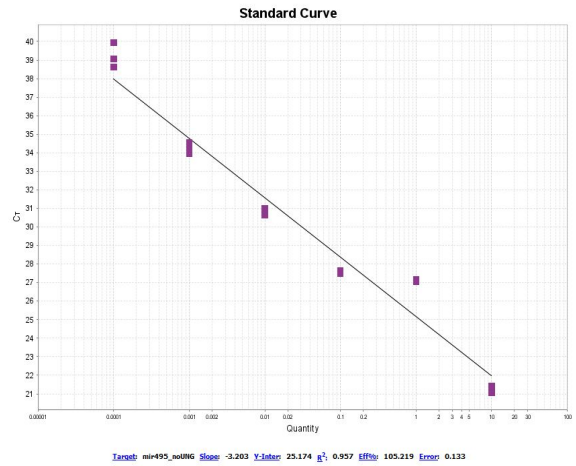

miRCURY setup

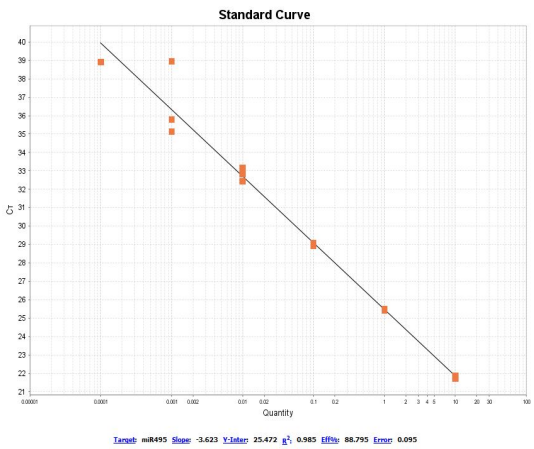

Figure 11: *The standard curves for hsa-miR-495-3p with synthetic miRNA pool for the different type of setups.*

Hsa-miR-495-3p with biological noise

TaqMan Advanced setup

Without miR-Amp reaction:

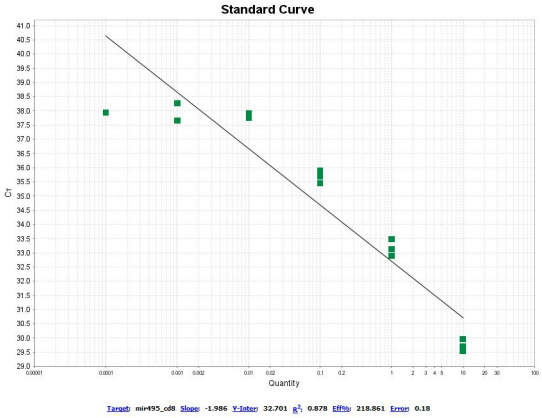

With miR-Amp reaction:

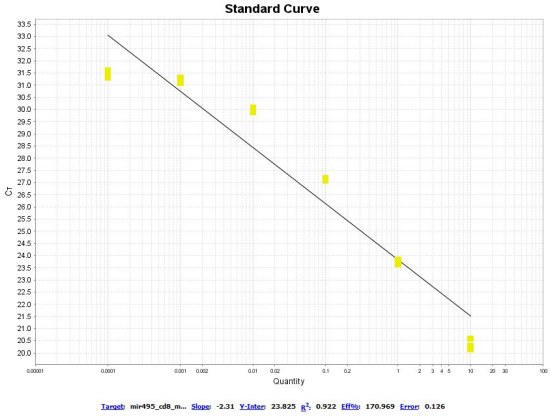

TaqMan MicroRNA setup

With UNG in master mix:

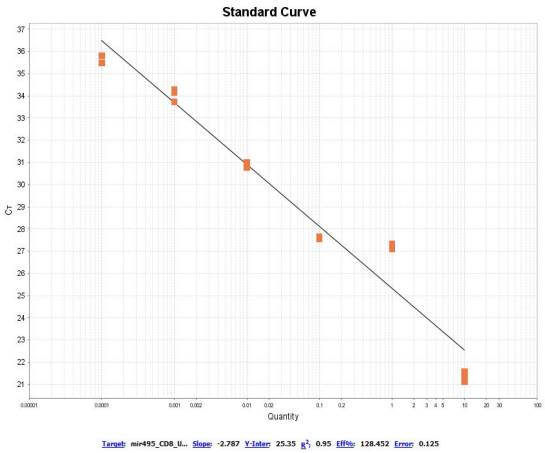

Without UNG in master mix:

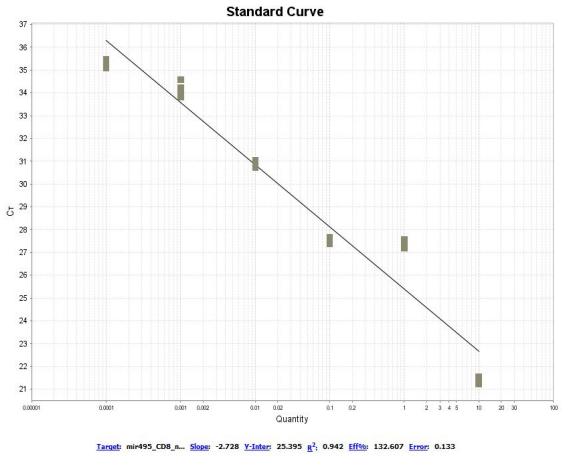

miRCURY setup

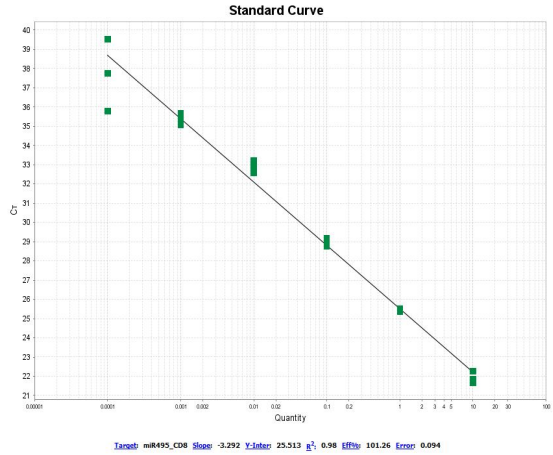

Figure 12: *The standard curves for hsa-miR-495-3p with biological noise for the different type of setups.*

Norges miljø- og biovitenskapelige universitet
Noregs miljø- og biovitskapelege universitet
Norwegian University of Life Sciences

Postboks 5003
NO-1432 Ås
Norway